1970

Use of the turbulence kinetic energy equation in prediction of nonequilibrium turbulent boundary layers

William Madison Byrne Jr.

Department: Mechanical and Aerospace Engineering

USE OF THE TURBULENCE KINETIC ENERGY EQUATION IN PREDICTION OF NONEQUILIBRIUM TURBULENT BOUNDARY LAYERS

by

WILLIAM MADISON BYRNE, JR., 1938-

A DISSERTATION

Presented to the faculty of the Graduate School of the

UNIVERSITY OF MISSOURI - ROLLA

In Partial Fulfillment of the Requirements for the Degree

DOCTOR OF PHILOSOPHY

in

MECHANICAL ENGINEERING

1970

Shen C. Lee
Advisor

R. B. Pitts

T. S. Chen

Ralph E. Lee

C. Y. Ho

ABSTRACT

A differential method is proposed for the prediction of a broad range of turbulent boundary layers of engineering and scientific interest. A digital computer program is presented which is applicable to boundary layers with positive, negative, and zero pressure gradient in the mainstream direction as well as boundary layers with suction, blowing or zero mass addition at the wall. The turbulence kinetic energy equation is solved simultaneously with the longitudinal momentum and continuity equations to provide an independent means for determining the effective viscosity which makes allowance for "history" effects in the flow. It is shown that the prediction method may be easily extended to cover the energy and species equations when the need arises to predict boundary layers with thermal gradients and/or those comprised of a mixture of gases. Mathematical models have been found which adequately close the system of governing equations as evident by the successful prediction of the behavior of a wide range of equilibrium and non-equilibrium turbulent boundary layers.

ACKNOWLEDGEMENTS

The writer would like to express his sincere appreciation to Professor Shen C. Lee for his assistance and encouragement during the research represented by this thesis as well as the preparation of the thesis itself. Dr. Lee's confidence, enthusiasm, and perseverance were particularly valuable during those times when seemingly insurmountable obstacles appeared to block the path to completion of the research. The writer would also like to thank Dr. R. B. Oetting, Chairman of the writer's Advisory Committee for his guidance in the course of study, attention to details required by the Graduate School, and constructive criticism and guidance during the preparation of this thesis. The writer would also like to thank the remainder of his Advisory Committee for their timely suggestions and guidance during the course of study and research.

The writer would like to express appreciation to the National Science Foundation, the National Aeronautics and Space Administration and the Department of Mechanical and Aerospace Engineering for financial assistance which made the acceptance of this challenge possible.

The author was fortunate to be able to secure the services of three competent people for the preparation of this manuscript. The cooperation of Mrs. Coralee Page and Mrs. Ann Burton who combined their efforts to produce the excellent typing is greatly appreciated along with the help provided by Mr. Steve Twitty during preparation of the illustrations.

Finally, and by no means least, the writer would also like to express his deep appreciation to his wife Connie and his children Bonnie and Paul who suffered the most by doing without all but the barest necessities

while allowing the writer to pursue this extravagance. Without their sustained support at every turn it would not have been possible to continue this task.

TABLE OF CONTENTS

TABLE OF CONTENTS - Continued

LIST OF ILLUSTRATIONS

LIST OF ILLUSTRATIONS - Continued

LIST OF TABLES

NOMENCLATURE

a_1, a_2	empirical constants
c_j	volume density of fluid j
D_c	general diffusional coefficient
D_k	dissipation of turbulence kinetic energy
F	blowing parameter
$\bar{H}$	empirical function (eqn. 10)
h	static enthalpy
$\bar{h}$	stagnation enthalpy
h_j	chemical energy released by fluid j
k	turbulence kinetic energy
KE	kinetic energy
l_*	mixing length
m_I	mass flux at the wall (eqn. 31)
m_E	mass flux at the outer edge of the boundary layer (eqn. 31)
p	static pressure
R_e	general generation plus dissipation of φ
r	distance from centerline of axisymmetric body
r_E	radius at the outer edge of the boundary layer
r_I	radius at the wall
U	instantaneous velocity in the streamwise direction
u	mean velocity in the streamwise direction
u*	wall shear velocity (eqn. 39)
u'	fluctuating velocity component in the streamwise direction
u_∞	free stream velocity
v	mean velocity normal to the wall

NOMENCLATURE - Continued

v'	fluctuating velocity component normal to the wall
w'	fluctuating velocity component normal to u' and v'
x	distance in the streamwise direction
y	distance normal to the wall
y_1	distance to the edge of the boundary layer
α	exponent differentiating planar and axisymmetric flow (eqn. 19)
β	power law exponent for velocity profile
γ	intermittency factor
δ^*	boundary layer momentum thickness
ϵ	effective viscosity
μ	molecular viscosity
ν	kinematic viscosity
ρ	density
ρ'	fluctuating density
σ_{c_j}	exchange coefficient of fluid j
σ_k	exchange coefficient of turbulence kinetic energy
σ_h	exchange coefficient of enthalpy
τ	shear stress
τ_m	maximum shear stress
τ_w	wall shear stress
φ	general dependent fluid property (u, k, h, c_j)
Ψ	stream function
Ψ_I	the wall at a given x location
Ψ_E	the outer edge of the boundary layer at a given x location
ω	nondimensional cross stream distance

NOMENCLATURE - Continued

Ω	a universal function (eqn. 10)

I. INTRODUCTION

The behavior of turbulent boundary layers is of great importance in many situations. Turbulent boundary layers in the presence of a pressure gradient and heat and mass transfer occur in meteorological, hydrological, and engineering design applications. Accurate prediction of the behavior of these boundary layers is the first step in understanding the structure of the turbulent flow field. Once the structure is well understood, control of these boundary layers can be more reliably accomplished so that engineering goals can be met.

The polluted air flowing over a city can be considered as an outsized turbulent boundary layer. If the coupling between thermal gradients, velocity gradients and concentration gradients as well as the basic conservation of these quantities were better understood, pollutant control could be made more effective. Similarly, accurate prediction of the spread of thermal and particulate pollutants in flowing streams coupled with an understanding of the ecological effects could lead to more reasonable policies for the disposal of such wastes. The fluid mechanical aspects of this problem can also be approached by consideration of the turbulent mixing between the polluted and clean streams.

Turbulent boundary layers are much more common in engineering applications than any other kind of boundary layer. Turbulent boundary layers play an important role in the operation of jet propulsion systems for instance. The turbulent boundary layer in an engine inlet system must be controlled to provide efficient inlet operation. This usually means the prevention of boundary layer separation by proper diffuser

design which may include bleeding off part of the boundary layer through the surface of the diffuser. On the other hand, in the combustor it is desirable to maintain as high a working fluid temperature as possible to maximize thermodynamic cycle efficiency. The walls of the combustion chamber and the surfaces of the turbine (in the case of a turbojet) are often protected by transpiration of cooler air through the exposed surfaces. Another example of the importance of understanding turbulent boundary layers is the protection of high speed flight vehicles from aerodynamic heating caused by the relative kinetic energy of the air. Protection is usually afforded by modification of the boundary layer structure by mass injection at the wall either by transpiration or ablation. The hybrid rocket motor is a dramatic example of the importance of understanding a turbulent boundary layer. Although the hybrid motor is a mixture of solid and liquid types, progress on the efficient operation of hybrid rocket systems was slow until it was realized that the combustion is strongly dependent on the boundary layer structure in the motor and, therefore, actually unrelated to the design techniques used in solid and liquid systems.

The design of many devices dependent on the behavior of turbulent boundary layers is often accomplished by relying heavily on empiricism and experience. The structure of turbulent boundary layers is not well understood and historically methods have been devised to handle a narrow range of conditions since the development of a more general method could not be justified. Extrapolation to new operating conditions has thus been risky.

Figure 1 is a schematic drawing of the phenomena of interest. When a body is immersed in a flowing fluid, a boundary layer is created in which the fluid properties differ from those of the free stream. At some distance along the body, the boundary layer will change from a laminar flow in which the velocity is steady to a turbulent flow in which the velocity at any location fluctuates with time. It is common for turbulent boundary layers of engineering interest to grow under the influence of free stream conditions in which the static pressure is either increasing or decreasing in the direction of the flow. It is also common for boundary layers to be controlled by either mass addition or removal at the wall. The shear stress and heat transfer at the wall will depend on the pressure gradient impressed by the external flow field and the mass transfer at the wall.

The objective of this research then has been to develop a suitable engineering tool for the prediction of the behavior of turbulent boundary layers with as large a range of application capability as possible. This tool was to be flexible enough to permit eventual application to boundary layers with heat transfer, concentration gradients (including mass injection or removal at the surface), and combustion so that it could be expanded to a broader range of application in the future. Empirical information required and mathematical models used had to be inserted in such a way that they could be easily changed as more is learned about the structure of turbulent flow so that the tool would not become obsolete, but could easily be modified to take advantage of more accurate understanding of the phenomena.

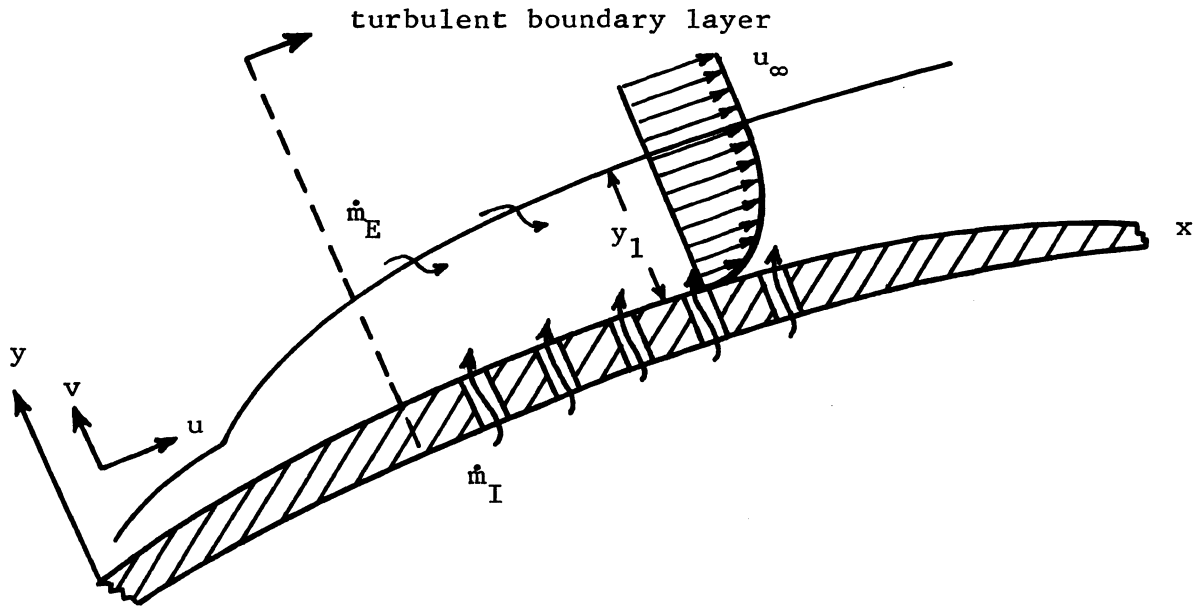

Figure 1. The Turbulent Boundary Layer

II. REVIEW OF PREVIOUS PREDICTION METHODS

There are basically two groups of prediction theories; the integral methods and the differential methods (sometimes called field methods). These groups get their names from the form of the governing equations used.

A. Integral Methods

One of the first to use the integral method for the study of turbulent boundary layers was T. von Karman.[1] By integrating the streamwise mean momentum equation across the boundary layer, the effects of the shear stress can be considered in a global way so that information concerning the local shear stress is lost and need not be known. However, relations between the displacement thickness, the momentum thickness and the wall shear must be assumed. The philosophy of this approach is that given enough experimental data one could arrive at empirical relations between these three quantities. Von Doenhoff and Tetervin[2] have used this approach more recently.

Efforts to minimize empiricism with the integral approach have been made by considering additional equations. One approach has been to create a mean energy integral equation by multiplying the streamwise momentum equation by the streamwise velocity and integrating across the boundary layer. Before integration, the momentum and mean energy equations do not offer independent information. The integration process causes different information to be lost by each equation so that the integral equations provide independent information. Zwarts[3] makes use of the mean energy integral equation by making a local assumption about the

Reynolds stress distribution while Alber,[4] Rotta,[5] and Escudier and Nicoll[6] make global assumptions about the relationship between the resulting dissipation integral of the mean energy integral equation and properties of the mean field. Head[7] has used an entrainment equation as an auxiliary equation to be solved in addition to the momentum integral equation. The entrainment equation is derived from the concept that turbulent boundary layers grow by entraining laminar fluid into the turbulent boundary layer. He then used a postulated relationship between the entrainment rate and the turbulence.

A "moment of momentum" integral equation can be formed by multiplying the momentum equation by a suitable function. Abbot and Deiwert[8] have used this method. The resulting equation contains an integral of the turbulent stress over the layer and an assumption about this term is required.

Additional integral equations can be generated by integrating only over a segment of the boundary layer. These "strip" methods require knowledge of the turbulent shear stress at intermediate points within the layer and assumptions must be made to permit evaluation of these terms.

Except for the momentum integral equation, all of these integral equations involve the turbulent stress. The assumptions required to evaluate these terms amount to implicit consideration of the turbulence. Hirst and Reynolds[9] formed a turbulence energy integral by integrating the turbulence kinetic energy equation across the boundary layer and relating the production and dissipation of turbulence kinetic energy within

the boundary layer to a combination of the turbulence and mean field velocity scales.

The advantages of the integral methods lie in the global way in which turbulence effects can be handled and the ability to avoid solving the partial differential equations. However, these methods require a large amount of empirical information. As discussed by Spalding[10], the extension of the integral methods to more complex situations demands a greater amount of empirical information.than can be provided. Thus, a massive experimental research program must precede extension of these methods to larger ranges of applicability involving fluid density variations or mass transfer at the wall for example. The prediction method sought in this research should develop detailed dependent variable profiles which react to changes in boundary conditions and disturbances in these profiles to allow a better understanding of the structure of turbulent flow. Since integral methods can not provide this information, they were not considered to be relevant to the present research objectives and are not included in the remainder of this thesis.

B. Differential Methods

Various differential methods are based on the numerical solution of finite element approximations to the governing partial differential equations. The equations to be solved may be parabolic or hyperbolic in form depending on the mathematical model used to evaluate the Reynold's shear stress terms. If a gradient diffusion model is used, the boundary layer equations are parabolic and may be solved by marching downstream with a rectangular net. If the Reynold's shear stresses are modeled in such a way that they are not of the gradient diffusion type but are independently

calculated, then the governing equations are hyperbolic in form and can be solved using the method of characteristics. In general, some sort of transformation is made to simplify the form of the equations before computations are made. Most methods have restricted the computational field to the "active" boundary layer (where significant gradients exist) and thereby increased their computational efficiency by not carrying on calculations where no change is taking place. Virtually all of the differential methods using an effective viscosity, as introduced by Boussinesq[11], may be modified to accept any model for effective viscosity that one chooses to investigate.

A basic division exists among the various investigators concerning the closure of the system of equations (i.e., how the Reynold's shear stress terms are to be modeled). The mixing length approach has been used by many because of its relative simplicity and demonstrated value in the solution of engineering problems. It has been argued by others that there is strong evidence that the shear stresses are closely related to the turbulence kinetic energy. The mixing-length approach suffers from the fact that it sometimes fails to give accurate predictions when extended to situations where sufficient empirical information is not known beforehand (i.e., the effective mixing-length is not known). Proponents of models which link the shear stresses with the turbulence kinetic energy hypothesize that this occurs because the mixing-length approach, in which the shear stresses are related directly only to local conditions, can not adequately account for the history of the flow. It is argued that the history of the flow can be adequately taken into account and more of the physics of the flow brought into play when the turbulence kinetic energy equation is

employed. They state that the shear stresses are closely related to the turbulence kinetic energy which is of course not governed by the local mean velocity profile but has its own history dependent on the upstream balance of the turbulence kinetic energy equation.

Having thus completed a brief sketch of the similarities and differences between the approaches used by previous investigators, the remainder of this section gives a description of some of the major differences in detail and tells why the chosen approach has been used. First, the precedence for the mixing-length concepts are reviewed*. Then, two examples of mixing-length models are discussed in which the effective viscosity is assumed to be dependent solely on the mean velocity profile. Three other methods are also discussed in which the Reynold's shear stress terms are related to the turbulent kinetic energy equation through different proposed models.

Prandtl[12] originally introduced the "mixing-length" hypothesis in which the effective turbulent viscosity may be written as the product of the square of the mixing-length and the cross stream derivative of the mean velocity. In working with free turbulent mixing Prandtl assumed: (1) the mixing-length is constant in a cross section of the mixing zone in a free turbulent flow and (2) the mixing length is proportional to the width of the mixing zone. Prandtl arrived at the mixing-length hypothesis after experimentally observing several free turbulent mixing situations. He concluded that a lump of fluid carries with it a constant amount of

---

* Mixing length concepts are equally applicable to the integral methods discussed earlier but this review is presented in this section for convenience.

momentum, as it moves in the cross stream direction, which is not disturbed by the movement until it arrives at its destination. Prandtl later found that this original theory disagreed with measured distributions particularly at locations where the cross stream derivative of the mean velocity was zero. Prandtl[13] then amended his original theory to include an additional term for evaluating the effective viscosity. This additional term contained the second derivative of the mean velocity in the cross stream direction as well as an additional length parameter. A fundamental objection to this momentum transport theory has been made by Hinze[14]. As the "lump" of fluid moves in the cross stream direction, it will be subjected to pressure fluctuations and therefore the momentum of the lump can not remain constant during this passage.

Von Karman[15] made a different assumption concerning the value of the mixing length. He assumed that it is determined by the local flow conditions and that it may be described in terms of quantities determined by these local conditions. His equation for mixing length contains the first and second derivatives of the mean velocity in the cross stream direction. The von Karman theory also results in some unreasonable predictions at certain points in the boundary layer. In particular, it is possible for the effective viscosity to become infinite when $\partial^2 u/\partial y^2 = 0$ and $\partial u/\partial y \neq 0$ since von Karman defines the mixing length by,

$$l_* \propto \frac{\partial u/\partial y}{\partial^2 u/\partial y^2}$$

Van Driest[16] made a significant contribution to the mixing-length theories more recently when he considered the turbulent flow near a wall. He assumed that the mixing length (1) is constant in the outer part of the boundary layer, (2) is proportional to the distance from the wall in the center region of the boundary layer, and (3) decays exponentially very near the wall.

The mixing-length theory exhibits some serious weaknesses but has found wide acceptance because of its simplicity and probably more basically because it can be made to work. As Bradshaw[17] points out, it strictly applies only to equilibrium boundary layers and can not be expected to work in the case of a non-equilibrium boundary layer since the approach does not consider the history of the boundary layer. The first two differential methods described below are examples of more recent application of the mixing-length concept.

Patankar and Spalding[18] use a mixing-length hypothesis based on the method first proposed by van Driest[16] to compute the effective viscosity of the flow. They do not solve the turbulence kinetic energy equation or draw a correlation between shear stress and turbulence kinetic energy. The effective viscosity is defined as,

$$\epsilon = \rho l_*^2 \left|\frac{\partial u}{\partial y}\right| \qquad (1)$$

where: ρ = the fluid density

l_* = the mixing-length

$\left|\frac{\partial u}{\partial y}\right|$ = the absolute magnitude of the streamwise velocity in a direction normal to the streamlines

The shear then becomes,

$$\tau = \rho l_*^2 \frac{\partial u}{\partial y} \frac{\partial u}{\partial y} \tag{2}$$

The mixing length is a continuous empirical function of distance from the wall (y) of the form,

$$l_* = .435\ y \left\{1 - \exp\left(-y\sqrt{\tau\ \rho}/25.3\mu\right)\right\} \text{for } y/y_1 \leq .207 \tag{3}$$

where μ is the molecular viscosity and y_1 is the farthest distance from the wall at which the local mean velocity differs from the inviscid velocity by only one percent. In the outer part of the boundary layer the mixing-length is determined by,

$$l_* = .09\ y_1 \text{ for } y/y_1 > .207 \tag{4}$$

The exponential term is active only very near the wall and represents the damping of the eddy motion of the fluid due to the presence of the wall. Patankar and Spalding used the local value of shear stress in the exponential term. Van Driest had used the wall shear stress instead, but he was concerned with boundary layers in which the shear stress gradient at the wall was zero whereas Patankar and Spalding have generalized the expression to include other cases (i.e., those of pressure gradient and mass transfer at the wall). One unique feature of this method which should be mentioned is that it makes use of the fact that the partial differential equations can be reduced to ordinary differential equations near the wall since the longitudinal velocity becomes small and hence the gradient of longitudinal velocity in the longitudinal direction term can be neglected. They then proceed to numerically solve these ordinary

differential equations with parametric variations and express these solutions algebraically in terms of the finite difference notation. This feature has the added bonus of allowing the calculations to proceed in the boundary layer region of relatively lower gradients and conserves computation time. The calculations proceed in typical parabolic fashion except that two "slip" nodes are added near each boundary to take advantage of the ordinary differential equation solutions mentioned above.

Smith and Cebeci[19] used a physical hypothesis very similar to that of Patankar and Spalding to compute the effective viscosity. They also break the effective viscosity model down into two regions, but switch from one model to the other where the two functions produce identical effective viscosities. This approach is necessary to give a continuous model because of the model used in the region away from the wall. Near the wall they compute the mixing length from

$$l_* = .4\, y \left\{1 - \exp\left(-y\sqrt{\tau_w \rho}\,/26\mu\right)\right\} \tag{5}$$

The effective viscosity is then computed using equation 1. Once again the influence of van Driest's hypothesis is evident. There are slight differences in the empirical constants between this model and that of Patankar and Spalding. In this case the wall shear has been used in the exponential term. In the outer region of the boundary layer they compute the effective viscosity from,

$$\epsilon = .0168\, \rho u_\infty \delta^* \gamma \tag{6}$$

where δ^* is the momentum thickness and the intermittency factor

γ is defined as

$$\gamma = \frac{1}{2}\left\{1 - \text{erf}\left(5\left[y/y_1 - .78\right]\right)\right\} \tag{7}$$

The empirical intermittency factor is simply a curve fit of the intermittency data measured by Kebanoff for flow along an impermeable flat plate. In a more recent publication[20], the authors change the mixing length expression for the inner region to,

$$l_* = .4\, y \left\{1 - \exp \frac{-y\rho}{26\mu}\left[\frac{\tau_w}{\rho} + \frac{dp}{dx}\,\frac{y}{y_1}\right]^{.5}\right\} \tag{8}$$

in an effort to account for pressure gradients.

Nee and Kovasznay[21] use an auxiliary governing equation closely related to the turbulence kinetic energy equation to close the system of equations. They assume that the effective viscosity obeys a rate equation of the form,

$$u\frac{\partial \epsilon}{\partial x} + v\frac{\partial \epsilon}{\partial y} = \frac{\partial}{\partial y}\left(\epsilon \frac{\partial \epsilon}{\partial y}\right) + A\,(\epsilon - \mu)\frac{\partial u}{\partial y} - B\,\frac{\epsilon(\epsilon - \mu)}{y_1^2}$$

$$- C\frac{\epsilon(\epsilon - \mu)}{U_\infty^2}\,\frac{dU_\infty}{dx}\,\frac{\partial u}{\partial y} \tag{9}$$

where $A = 0.1$, $B = 1.0$ and $C = 1.0$. The "universal constants" A, B and C were obtained empirically. In this case the effective viscosity is not entirely dependent on the local average velocity profile and since this additional rate equation must be solved simultaneously with the momentum equation, it is possible for flow history effects to influence the solution.

Glushko[22] solves the continuity, longitudinal momentum and turbulence kinetic energy equations simultaneously. He relates the

turbulent shear stress to the local value of turbulence kinetic energy by means of

$$\tau = \alpha\rho \bar{H}(r) \sqrt{k} \quad \Omega \frac{\partial u}{\partial y} \tag{10}$$

where α is a proportionality constant, $\bar{H}(r)$ is an empirical function related to the local value of turbulence kinetic energy (k), and Ω is taken as a "universal function" related to the distance from the wall. The $\bar{H}(r)$ function is defined as:

$$\bar{H}(r) = \begin{cases} \frac{r}{ro} & 0 < \frac{r}{ro} < .75 \\ \frac{r}{ro} - (\frac{r}{ro} - 0.75)^2 & .75 < \frac{r}{ro} < 1.25 \\ 1 & 1.25 < \frac{r}{ro} < \infty \end{cases} \tag{11}$$

where $r = \rho l_* \sqrt{k}/\mu$

$k = \frac{1}{2}(u'^2 + v'^2 + w'^2)$ (turbulence kinetic energy)

ro = constant

Glushko writes the turbulence kinetic energy equation as

$$\rho u \frac{\partial k}{\partial x} + \rho v \frac{\partial k}{\partial y} = -\rho\, u'v' \frac{\partial u}{\partial y} + \frac{\partial}{\partial y}\left\{\mu \frac{\partial k}{\partial y} - v'(\rho' + \rho k)\right\} - \epsilon_* \tag{12}$$

and defines the production term as,

$$-\rho\, u'v' \frac{\partial u}{\partial y} = \tau \frac{\partial u}{\partial y} = \alpha\, \rho\, \bar{H}(r) \sqrt{k} \quad \Omega \left(\frac{\partial u}{\partial y}\right)^2 \tag{13}$$

and the dissipation term as

$$\epsilon_* = \frac{\mu}{\rho l_*^2} C\left\{1 + \bar{H}(\kappa r)\, \alpha\, \kappa r\right\} k \tag{14}$$

$\bar{H}$ (kr) is the same function as $\bar{H}$ (r) except that r is replaced by kr . C is a constant. Glushko assumed that the total diffusion of turbulence kinetic energy was due to the gradient of k and assumed the diffusion term to be of the form,

$$\frac{\partial}{\partial y}\left\{\mu \frac{\partial k}{\partial y} - v' (\rho' + \rho k)\right\} = \frac{\partial}{\partial y}\left\{\mu \left[1 + \bar{H} (kr) \alpha k r\right] \frac{\partial k}{\partial y}\right\} \tag{15}$$

His basis for the various models assumed above was analysis of the measurements of Klebanoff. The generality of these assumed expressions for the production, dissipation, and diffusion of turbulence kinetic energy can only be determined by comparison of final results with data. Beckwith and Bushnell[23] tested modifications of Glushko's models to a wider range of boundary layers and concluded that "simple modifications to the turbulence scale function and to the turbulent fluctuation terms as modeled by Glushko result in accurate predictions of mean and fluctuating characteristics of turbulent and transitional boundary layers with arbitrary boundary conditions."

Bradshaw et al[24] convert the turbulent kinetic energy equation into a shear stress equation which then forms a hyperbolic system of equations with the momentum and continuity equations. This conversion requires three empirical functions relating the turbulent intensity, turbulent kinetic energy diffusion, and turbulent kinetic energy dissipation to the shear stress profile. Their converted equation becomes

$$u \frac{\partial}{\partial x}\left(\frac{\tau}{2a_1\rho}\right) + v \frac{\partial}{\partial y}\left(\frac{\tau}{2a_1\rho}\right) - \frac{\tau}{\rho}\frac{\partial u}{\partial y} + \left(\frac{\tau_m}{\rho}\right)^{\frac{1}{2}} \frac{\partial}{\partial y}\left(G\frac{\tau}{\rho}\right) + \frac{(\tau/\rho)^{\frac{3}{2}}}{L} \qquad (16)$$

where

$$a_1 = \tau/\rho\ \overline{q^2}$$

$$\overline{q^2} = u'^2 + v'^2 + w'^2$$

$$L = (\tau/\rho)^{3/2}\ /\epsilon'$$

$$G = \frac{\frac{\rho'v'}{\rho} + \frac{1}{2}q^2v'}{(\tau_m/\rho)^{1/2}\ \frac{\tau}{\rho}}$$

$$\epsilon' = \frac{\mu}{\rho}\left(\partial u'_i/\partial k'_j\right)^2 \qquad \begin{matrix} i = 1,2,3 \\ j = 1,2,3 \end{matrix} \qquad (17)$$

They assume that a_1, L, and G are functions which depend on the shape of the shear profile. L is the most important of the three functions because the dissipation of turbulence kinetic energy is much larger than the advection or diffusion over most of the boundary layer. The accuracy of predictions then depends on the adequacy of the functions a_1, L, and G. Based on the measurements of Klebanoff and two additional test cases generated by Bradshaw et al, they have chosen these functions as,

$$a_1 = .15$$

$$L = y_1 f_1(y/y_1)$$

$$G = (\tau_m/u_\infty^2)^{.5}\ f_2\ (y/y_1) \qquad (18)$$

where f_1 and f_2 are simply empirical functions and τ_m is the maximum shear in the profile which is evaluated at $y/y_1 = .25$ if a higher shear value does not occur at a greater distance from the wall.

C. Conclusions from the Review of the Prediction Schemes of Previous Investigators

The following conclusions were reached as a result of a review of the literature:

(1) There are a large number of prediction schemes which can be made to give reasonable predictions at least over a narrow range of conditions.

(2) Integral techniques are valuable from a historic standpoint and can be a valuable design tool once a large amount of empirical data is available at conditions close to those encountered in practice. Integral techniques are not likely to be of much help in the understanding of the structure of turbulent flow since they lose the detail of the boundary layer in application.

(3) A parabolic equation approach to the simulation of the differential equations of motion is preferable since it appears to allow easier extension to more complicated boundary layer situations.

(4) The method of Patankar and Spalding is one of the best computation schemes available since it takes advantage of the one dimensional character of the flow very near the wall and may be easily modified to accept more dependent variable equations when they are desired.

(5) Simultaneous solution of the turbulence kinetic energy equation and its use in predicting the shear stress is advisable since a definite correlation between the two has been established and it allows for the history of the flow to be considered.

III. APPROACH

The criteria used in searching for a boundary layer prediction technique to be used as an engineering tool were established as: (1) the method should have ample flexibility for extension to problems involving heat and mass transfer at the wall including the injection of a foreign gas and chemical reaction, (2) the method should be reasonably inexpensive in terms of computer time so that it can be used in engineering design, and (3) empiricism should be minimized to facilitate application to as broad a range of situations as possible. In other words, what one would like to have is an inexpensive method to analyze a wide range of complex turbulent boundary layer problems. The chosen approach then has been to apply modified versions of Bradshaw's models[24] using a modification of the calculation scheme of Patankar and Spalding[18] in which provisions are made to add the turbulence kinetic energy equation to be solved simultaneously with the momentum and continuity equations. A similar technique has been used by Lee and Harsha[25] for the prediction of free mixing flows. The turbulence kinetic energy equation is used to define the shear stress because it brings more of the physics of the flow into play and should therefore have a wider range of applicability than the mixing length theories. An effective viscosity formulation is used rather than the hyperbolic approach of Bradshaw since it appears that the parabolic equations are more easily extended to more complicated flow situations such as those with heat transfer, density fluctuations, chemical reactions, etc. The computation scheme of Patankar and Spalding was chosen since it conserves computer time to a high degree and could be easily modified to accept the

addition of the turbulence energy equation (as well as any additional dependent variable equation one might want to add later). The models used by Bradshaw to express the dissipation and diffusion have been modified to reduce the amount of empiricism.

The remainder of this section describes the governing equations, the transformation of these equations, the empirical models used to close the system of equations, the methods used to produce the "slip" boundary conditions at the wall, and provides a brief introduction to the computer program.

A. Governing Equations

The governing equations of the two dimensional compressible turbulent boundary layer are those of continuity, momentum, turbulence kinetic energy, total enthalpy, and species. These equations are simply stated here to enumerate the assumptions used and to provide a working explanation of the nomenclature. The reader interested in the derivation of these equations is referred to Appendix A where the derivations are explained in detail following the approach of Goldstein[26]. x and y are a set of orthogonal coordinates with the x-axis along the wall on which the boundary layer is developing. r is the perpendicular distance from the body axis in the case of axisymmetric flows (see Figure A-1).

The "steady" state continuity equation is an expression for the conservation of matter. It may be written as,

$$\frac{\partial}{\partial x}\left(r^{\alpha}\rho u\right) + \frac{\partial}{\partial y}\left(r^{\alpha}\rho v\right) = 0 \qquad (19)$$

where ρ is the mean fluid density and u and v are the mean velocities in the x and y directions, respectively. α is equal to zero in the case of planar flows and equal to one in the case of axisymmetric flows.

The longitudinal momentum equation (an expression for Newton's second law of motion) may be condensed from the Navier-Stokes equations using order of magnitude arguments by assuming that: (1) distances in the cross stream direction are small compared to longitudinal distances, (2) the mean velocity in the direction normal to the x-y plane is small, and (3) the velocity in the x direction is large compared to the velocity in the y direction. This leads to the conclusion that the velocity gradient normal to the wall is large compared to the velocity gradients along the wall. By neglecting normal stress terms (which will be relatively small except near separation), the longitudinal momentum equation can be written as,

$$\rho u \frac{\partial u}{\partial x} + \rho v \frac{\partial u}{\partial y} = - \frac{dp}{dx} + r^{-\alpha} \frac{\partial}{\partial y} \left(r^{\alpha} \epsilon \frac{\partial u}{\partial y} \right) \tag{20}$$

where dp/dx is the static pressure gradient in the flow direction. The static pressure gradient is imposed by the external inviscid flow. ϵ is the effective viscosity of the fluid as defined by,

$$\epsilon = \frac{\tau}{\partial u / \partial y} \tag{21}$$

where τ is the shear stress.

The turbulence kinetic energy equation is an expression for the conservation of turbulence energy. It is probably the least well known

of the governing equations. The instantaneous value of each fluctuating component in a turbulent flow is assumed to consist of a mean component and a fluctuating component. For example, the instantaneous longitudinal velocity (U) is conceived to be,

$$U = u + u'$$

where u represents the mean component of the velocity and u' represents the fluctuating component. A superscript $\overline{\quad}$ indicates time averaging as,

$$\bar{U} = \frac{1}{t_2 - t_1} \int_{t_1}^{t_2} U dt$$

By definition of u then,

$$\bar{U} = \overline{u + u'} = \overline{u}$$

The kinetic energy in the longitudinal direction then becomes,

$$KE \propto U^2 = (u + u')^2 = u^2 + 2uu' + u'^2$$

Time averaging of this component of the fluid kinetic energy then gives,

$$\overline{KE} \propto \overline{U^2} = \overline{u^2} + \overline{2uu'} + \overline{u'^2} = \overline{u^2} + \overline{u'^2}$$

Therefore, we see that for turbulent flows, the kinetic energy of the flow depends not only on the mean velocity but also on the fluctuating component of the velocity. Obvious extension of the above reasoning leads to a definition of turbulence kinetic energy as,

$$k = \frac{1}{2} (\overline{u'^2} + \overline{v'^2} + \overline{w'^2}) \qquad (22)$$

The turbulence kinetic energy equation as derived in Appendix A is,

$$\rho u \frac{\partial k}{\partial x} + \rho v \frac{\partial k}{\partial y} = r^{-\alpha} \frac{\partial}{\partial y} (r^{\alpha} \frac{\varepsilon}{\sigma_k} \frac{\partial k}{\partial y}) + \varepsilon (\frac{\partial u}{\partial y})^2 - Dk \qquad (23)$$

The terms on the left hand side of equation 23 represent the advection of turbulence kinetic energy due to the mean velocities of the flow. The first term on the right hand side of equation 23 represents the diffusion of turbulence energy due to the gradient in turbulence energy. ϵ/σ_k is the diffusion coefficient for turbulence kinetic energy. A model must be found or assumed for σ_k. σ_k has been assumed to be constant throughout the flow field in this research. The second term on the right hand side of equation 23 represents the generation of turbulence energy caused by mean velocity gradients while D_k represents the dissipation of turbulence energy by the molecular viscosity of the fluid.

If the boundary layer is composed of more than one fluid, a conservation of species equation may be written as,

$$\rho u \frac{\partial c_j}{\partial x} + \rho v \frac{\partial c_j}{\partial y} = r^{-\alpha} \frac{\partial}{\partial y} \left\{ r^{\alpha} \frac{\epsilon}{\sigma c_j} \frac{\partial c_j}{\partial y} \right\} + R_j \qquad (24)$$

where c_j is the volume density of fluid j, R_j is the volume rate of the net destruction of fluid j by means of chemical reaction, and $\epsilon/\sigma c_j$ is the diffusion coefficient of fluid j. The assumption has been made that the diffusion of fluid j in the cross stream direction is large compared to the longitudinal diffusion of fluid j due to the larger concentration gradients and momentum diffusion in the cross stream direction. When analyzing a boundary layer composed of a group of fluids, a species equation may be written for all but one constituent which is then handled implicitly by the continuity equation.

Application of the first law of thermodynamics with the typical boundary layer assumptions on the diffusional terms produces an equation for the

conservation of total enthalpy (see Appendix A).

$$\rho u \frac{\partial \bar{h}}{\partial x} + \rho v \frac{\partial \bar{h}}{\partial y} = r^{-\alpha} \frac{\partial}{\partial y} \left\{ \frac{r^{\alpha} \epsilon}{\sigma_h} \left(\frac{\partial \bar{h}}{\partial y} + \left[\frac{\sigma_h}{\sigma_k} - 1 \right] \frac{\partial k}{\partial y} \right. \right.$$
$$\left. \left. + \sum_{j=1}^{n} \left[\frac{\sigma_h}{\sigma_{c_j}} - 1 \right] \frac{\partial c_j}{\partial y} + \left[\sigma_n - 1 \right] \frac{\partial (u^2/2)}{\partial y} \right) \right\} \qquad (25)$$

where ϵ/σ_h is the diffusional coefficient for the stagnation enthalpy which is defined as

$$\bar{h} = h + \frac{u^2}{2} + k + \sum_{j=1}^{n} h_j c_j \qquad (26)$$

h_j is the energy released during chemical combination of fluid j. If there is no energy generation or dissipation due to chemical reaction, the summation terms on the right hand side of the last two equations become zero.

The governing equations are closed if one has a method for determining the effective viscosity and the various diffusional coefficients. It is this point where the firm physics of the fluid ends and the various forms of empiricism take over. The empirical models used in this study are described in subsection C of this section.

B. Coordinate Transformations and the Generalized Parabolic Equation

The governing equations are transformed twice before they are solved to reduce by one the explicit number of equations which must be solved and to allow the computational net to grow with the boundary layer so that only that part of the flow field in which significant transverse gradients exist is treated. All of the governing equations with the exception of the continuity equation are of the form,

$$\rho u \frac{\partial \varphi}{\partial x} + \rho v \frac{\partial \varphi}{\partial y} = r^{-\alpha} \frac{\partial}{\partial y} \left(r^{\alpha} D_c \frac{\partial \varphi}{\partial y} \right) + R_e \qquad (27)$$

where φ represents the dependent variable under consideration, D_c represents the diffusional coefficient and R_e represents the remainder of terms in the φ equation. This allows one to examine one of the governing equations and solve the remainder in a similar fashion. As will be seen, this is also the case after transforming the equations so that the typical parabolic equation "marching" solution may be carried out by simply solving as many dependent variable equations as are of interest at each succeeding longitudinal step. In contrast to the hyperbolic equation method of characteristics approach preferred by Bradshaw, the dependent variables are solved at the same location downstream since the solution need not proceed along characteristic lines which may be different for each set of equations solved. Because of the similar form of the various equations, the following coordinate transformation discussion is applied only to the longitudinal momentum equation for illustration.

The initial physical plane for which the governing equations have been derived is represented by a set of orthogonal x and y coordinates (see Figure 2-a). The x axis lies along the surface on which the boundary layer is developing while the y axis is perpendicular to the surface. The coordinate r is the perpendicular distance from the axis of symmetry in the case of axisymmetric flows. The y coordinate is first stretched by a von Mises transformation which also insures that the continuity equation is satisfied. Thus, $x,y \longrightarrow x,\Psi$

where $$\frac{\partial \Psi}{\partial x} = -r^{\alpha} \rho v, \qquad \frac{\partial \Psi}{\partial y} = -r^{\alpha} \rho u \tag{28}$$

and the resulting orthogonal computation net appears as in Figure 2-b. Application of this transformation to the longitudinal momentum equation

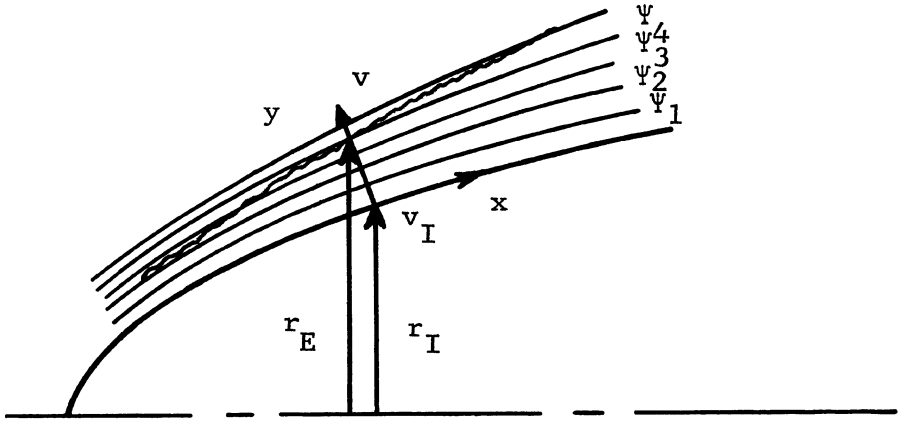

- a -

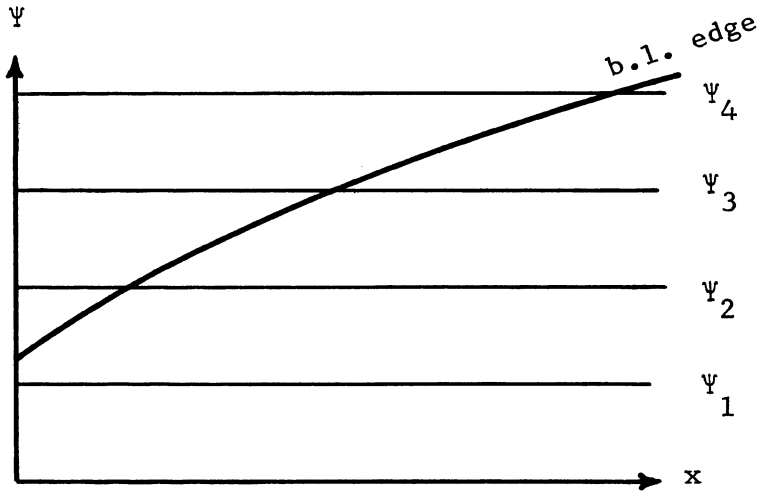

- b -

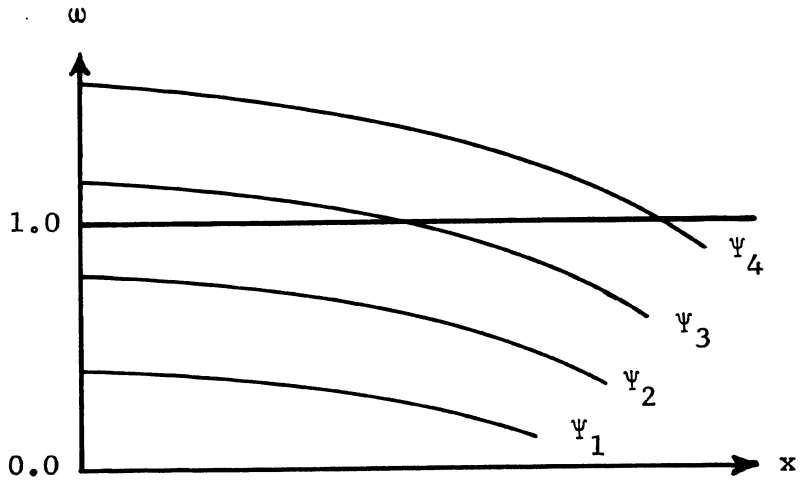

- c -

Figure 2. The Transformed Coordinates

produces (see Appendix B)

$$\frac{\partial u}{\partial x} = -\frac{1}{\rho u}\frac{dp}{dx} + \frac{\partial}{\partial \Psi}\left\{\rho u r^{2\alpha}\, \epsilon \frac{\partial u}{\partial \Psi}\right\} \tag{29}$$

The transverse coordinate is next nondimensionalized to limit the computational net to the "active" boundary layer (i.e., the part where significant gradients exist). Thus, $x, \Psi \longrightarrow x, \omega$

where $$\omega = \frac{\Psi - \Psi_I}{\Psi_E - \Psi_I} \tag{30}$$

Ψ_I = the wall at a given x location

Ψ_E = the outer edge of the "active" boundary layer at a given x location

and the resulting computational net appears in Figure 2-c. The longitudinal momentum equation then becomes (see Appendix B),

$$\frac{\partial u}{\partial x} + \left\{\frac{r_I^{\alpha}\dot{m}_I + \omega(\dot{m}_E r_E^{\alpha} - r_I^{\alpha}\dot{m}_I)}{\Psi_E - \Psi_I}\right. \frac{\partial u}{\partial \omega} = -\frac{1}{\rho u}\frac{dp}{dx} + \frac{\partial}{\partial \omega}$$
$$\left\{\frac{\epsilon \rho u r^{2\alpha}}{(\Psi_E - \Psi_I)^2}\frac{\partial u}{\partial \omega}\right\} \tag{31}$$

where $\dot{m}_I$ = $\rho_I v_I$ evaluated at the inner boundary of the computational net.

$\dot{m}_E$ = $\rho_E v_E$ evaluated at the outer boundary of the computational net.

Thus it is possible to carry out the computation in an orthogonal net which automatically conserves the computation time by excluding the inviscid flow field. This hinges on the ability to adequately predict the entrainment of fluid ($\dot{m}_I$ and $\dot{m}_E$) between longitudinal computation

steps. Although this at first appears to be a critical part of the scheme, in practice almost any manner of estimating the entrainment is suitable as long as it entrains enough flow to include all significant dependent variable transverse gradients. This point is very important when the method is expanded to include the energy equation since in some accelerated boundary layers, the thermal boundary layer may be much larger than the velocity boundary layer.

The above transformations reduce the governing equations to the common form,

$$\frac{\partial \varphi}{\partial x} + (a + b\omega)\frac{\partial \varphi}{\partial \omega} = \frac{\partial}{\partial \omega}\left(c \frac{\partial \varphi}{\partial \omega}\right) + d \qquad (32)$$

where φ = the dependent variable of interest (u, k, T, etc.)

$$a = m_I/(\Psi_E - \Psi_I) \qquad d = d(\varphi)$$

$$b = (m_E - m_I)/(\Psi_E - \Psi_I)$$

$$c = \frac{\varepsilon \rho u r^{2\alpha}}{(\Psi_E - \Psi_I)^2}$$

The longitudinal momentum equation (31) is non-linear because of the last term on the right hand side of the equation. The equation has been linearized for purposes of this analysis by evaluating "c" at the previous x location. Due to this linearization, it is possible for the intrinsic non-linear nature of the equation to manifest itself as an instability in the solution of the linearized equation even though a fully implicit finite difference scheme is used (see subsection E of this section). This phenomena, which was observed infrequently during this research, was controlled by simply reducing the integration step size when instability obviously occurred. Coupling between equations occurs in the diffusion

coefficient ("c") and source ("d") terms of the various equations. In the present analysis for instance, the effective viscosity and hence all of the diffusional coefficients are related to the turbulence kinetic energy. Therefore, all of the governing equations are coupled to the turbulence kinetic energy equation and the momentum equation since $c = c(k,u)$. Similarly, the turbulence kinetic energy equation is coupled to the longitudinal momentum equation because the generation of turbulence kinetic energy is a function of the mean velocity gradient; $d = d(u)$. The coupling has been broken by computing the effective viscosity from the turbulence kinetic energy at the previous x step. In this way iteration can be avoided and the momentum equation solved directly. The resulting mean velocity profile is then available for use during integration of the turbulence energy equation.

The finite difference scheme is based on a miniature integral concept which is fully implicit and removes the necessity for equal spacing of nodal points in the transverse direction. This is of some help since the computation may be started by using data input in physical coordinates directly without modifying it to achieve equally spaced nodes in the transformed cross stream coordinate.

C. Empirical Models

To solve equations 19, 20 and 23 simultaneously, it is necessary to have an empirical model relating the local turbulence kinetic energy to the local shear stress, to be able to compute the dissipation of turbulence kinetic energy, and to have an acceptable model for the diffusion of turbulence kinetic energy. If these empirical models are known adequately, these equations may be solved and predictions of the behavior of

the turbulent boundary layer made. Unfortunately, there is a paucity of information either analytical or experimental to guide the selection of these models as the large difference in models of this kind in the literature reveals. The models described below are based on the models of Bradshaw modified to reduce the amount of empiricism without changing the accuracy of the solutions obtained. The models of Bradshaw have been chosen over those of Glushko to avoid the larger amount of empiricism involved in Glushko's models.

The shear stress has been assumed to be related to the turbulence kinetic energy through the relation

$$\tau = .3\rho k \tag{33}$$

Correlations between measured values of shear stress and turbulence kinetic energy are presented for a variety of flow conditions in Figure 3. Although the rather simple relation given above is not entirely justified by the data correlation, no better trend could be found to hold in general. As can be seen in Figure 3b, the correlation definitely breaks down very near the wall and at the outer edge of the boundary layer. The discrepancy at the outer edge of the boundary layer is not of particular significance since the shear is very low here anyway and errors in the computation of the shear force here will not significantly affect the balance of the momentum equation. The discrepancy near the wall is significant however, since this is a region of high shear where the shear forces are of the same order of magnitude as the advection momentum forces. Initial attempts were made to follow the suggestion of Lee and Harsha[25] as they dealt with a similar problem in free turbulent mixing. Their approach

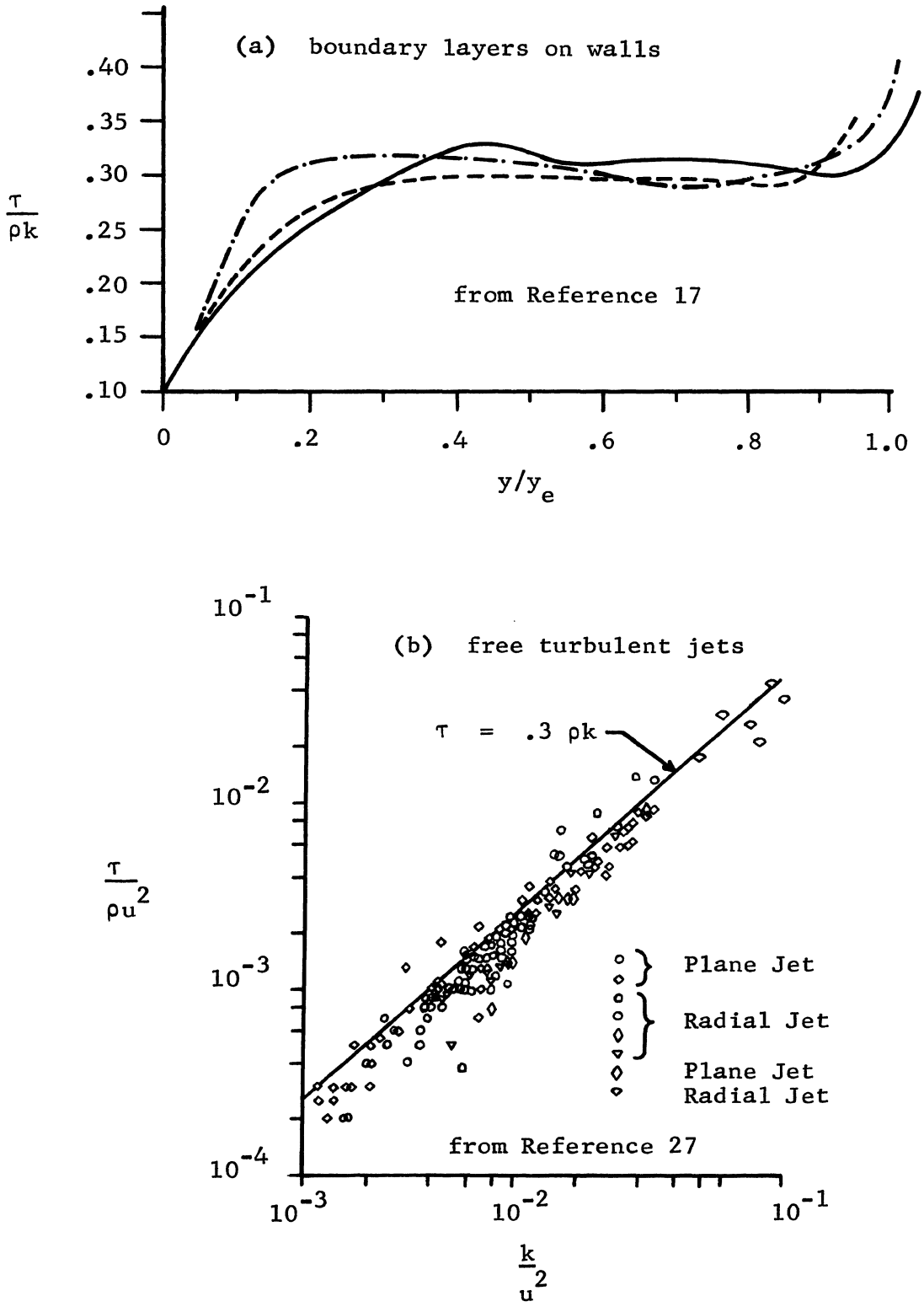

Figure 3. Correlation Between Shear Stress and Turbulent Kinetic Energy

was to modify the above relationship near the axis of symmetry where the shear goes to zero while the turbulence kinetic energy does not. Between the axis of symmetry and the point of maximum shear they change the relation to,

$$\tau = .3\rho k \frac{\left(\frac{\partial u}{\partial y}\right)_1}{\left(\frac{\partial u}{\partial y}\right)_{\tau m}} \tag{34}$$

where $\left(\frac{\partial u}{\partial y}\right)_1$ = the local mean velocity gradient

$\left(\frac{\partial u}{\partial y}\right)_{\tau m}$ = the mean velocity gradient at the point of maximum shear.

A similar approach was attempted with wall boundary layers in this study. The relation was modified to the form

$$\tau = .3\rho k \, (\partial u/\partial y)_{yi}/(\partial u/\partial y)_1 \quad \text{(i.e., } (\partial u/\partial y)_{yi}\text{)} \tag{35}$$

where $(\partial u/\partial y)_{yi}$ is the velocity gradient at the location of maximum shear stress if it did not occur at the wall or at some arbitrary non-dimensional location if the maximum shear stress occurred at the wall. This approach was successful in the case of Klebanoff's zero pressure gradient case but could not be made to work with cases in which a pressure gradient was present. The success or failure of the predictions was found to be very sensitive to the location at which $(\partial u/\partial y)_{yi}$ was evaluated.

In the present analysis, equation 33 has been assumed valid over the entire boundary layer. This assumption implies that there must be a positive value of turbulence kinetic energy at the wall when there is shear stress at the wall. Experimental measurements of fluctuating velocities very near a wall indicate that the turbulence kinetic energy

approaches zero at the wall (see Figure 4). These measurements are in agreement with the physical reasoning that since there can be no slip between the fluid and the wall (i.e., the fluid next to the wall is at rest relative to the wall), there can be no fluctuating velocity at the wall. The approach then has been to use the measured values of turbulence kinetic energy in the boundary layer except in the region very near the wall (say $y/y1 < .1$) and to substitute a fictitious non-zero turbulence kinetic energy "slip" value at the wall. The "slip" value is determined based on equation 33 using the measured wall shear stress. This manipulation is justified since the goal in solving the turbulence kinetic energy equation is to provide a means for determining the shear stress throughout the boundary layer, not to determine the turbulence kinetic energy profile. In other words, modification of the turbulence kinetic energy equation is justifiable if it leads to acceptable results for the remaining dependent variable profiles and hence a better understanding of the structure of the turbulent boundary layer.

The dissipation term of the turbulence kinetic energy equation was represented as,

$$Dk = a_2 \rho k^{3/2} / y_1 \tag{36}$$

In the case of profiles with a shear peak located at a distance of $y/y_1 > 0.25$, a_2 was computed from

$$\begin{aligned} a_2 &= 1.8 && y > y_{\tau m} \\ a_2 &= 1.8\ y_{\tau m}/y && y \leq y_{\tau m} \end{aligned} \tag{37}$$

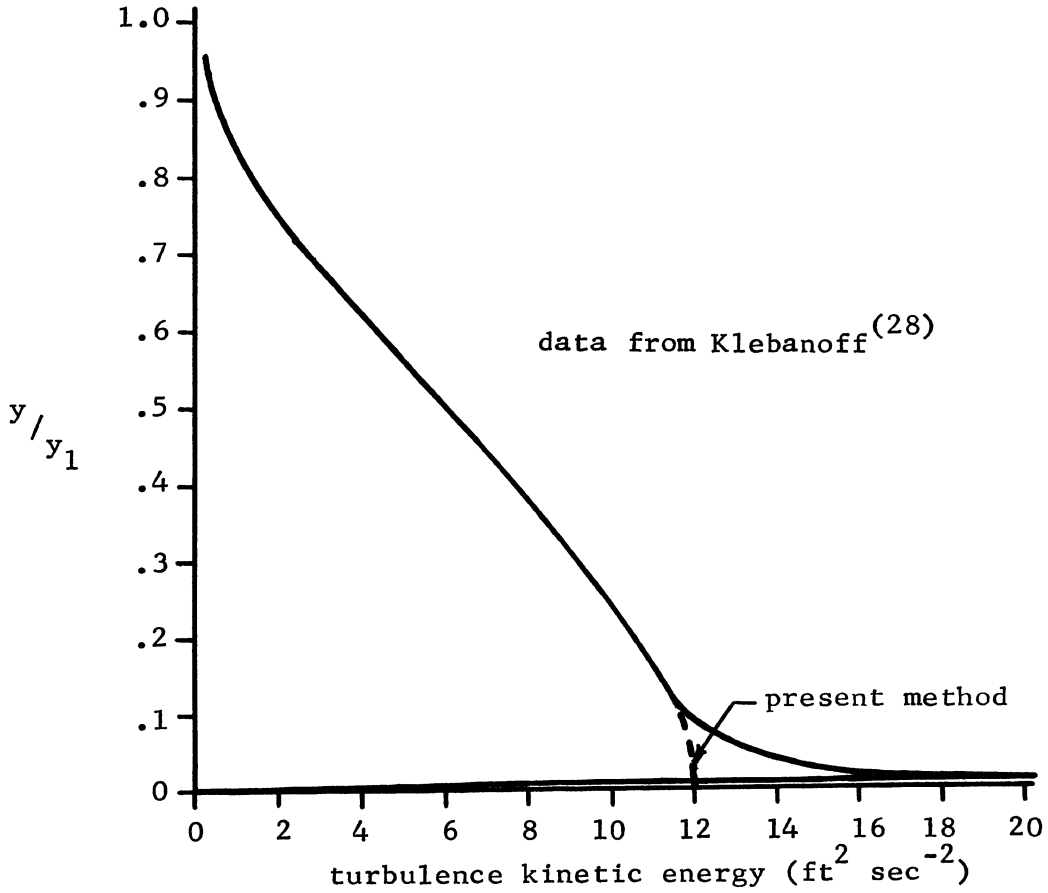

Figure 4. The Distribution of Turbulence Kinetic Energy throughout a Typical Turbulent Boundary Layer

where $y_{\tau m}$ is the location of the maximum shear point. When no shear peak occurred at a distance of $y/y1 \geq 0.25$, a_2 was computed from,

$$\begin{aligned} a_2 &= 1.8 && y > y1/4 \\ a_2 &= 1.8\ y1/4y && y \leq y1/4 \end{aligned} \tag{38}$$

The value 1.8 was determined by numerical experiments with the solution procedure and agrees well with the values of 1.5 to 1.7 determined by Lee and Harsha as being reasonable for cases of free turbulent mixing. This model is plotted along with Bradshaw's model in Figure 5 for comparison. As can be seen, the amount of empiricism has been reduced. It is not claimed that the present model is more accurate than that of Bradshaw. However, the outer part of the boundary layer is very similar to a wake flow and the demonstrated success of a constant value of a_2 in free mixing studies of Lee and Harsha seems to justify the present model.

The diffusion coefficient of the turbulence kinetic energy equation (ϵ/σ_k) was taken as the effective viscosity divided by 0.7 (i.e., $\sigma_k = .7$). The physical reason for a simple model of this kind is that when one observes turbulent flow, the most prominent change from laminar flow is the movement of "clumps" of fluid from one streamline to another. These clumps carry momentum, total enthalpy, turbulent kinetic energy, etc. with them. Therefore, since the diffusion mechanism is the same, it is reasonable to expect the diffusion coefficients to be linearly related. It was found that the solutions were relatively insensitive to the value of σ_k indicating that diffusion of turbulence kinetic energy did not play a major role in the boundary layers investigated. σ_k plays

as applied to the
data of Klebanoff

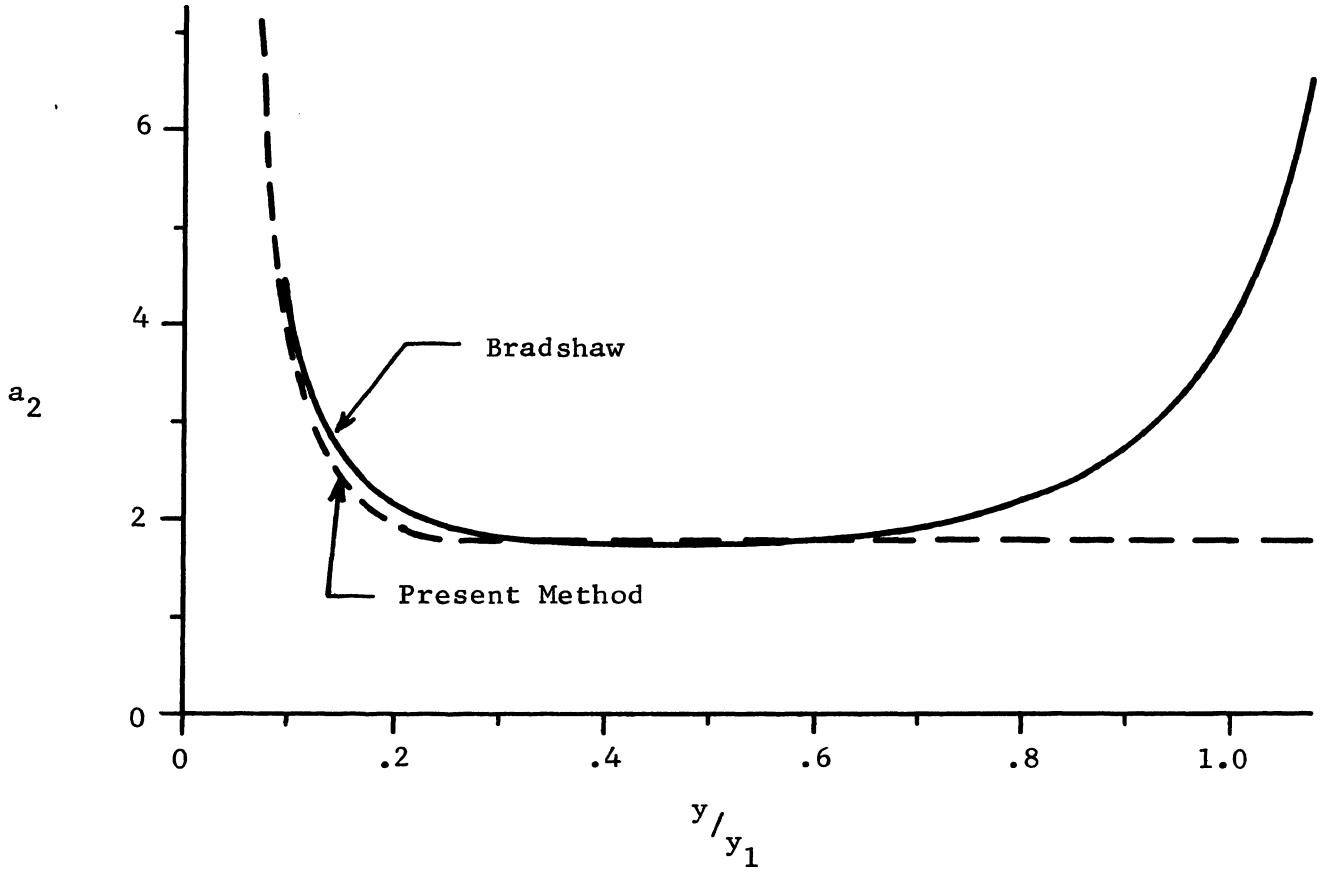

Figure 5. A Model for the Dissipation of Turbulence Kinetic Energy

the same role in the turbulence kinetic energy equation that Prandtl Number does in the energy equation.

D. Boundary Conditions

The initial profiles and the boundary conditions in the direction the solution is to proceed must be known in order to fully define the problem. In the case of the longitudinal momentum equation, this means that the initial velocity profile and the free stream velocity as a function of downstream location must be known. The longitudinal velocity at the wall is assumed to be zero since the fluid does not slide over the wall. The free stream velocity distribution is determined by the inviscid flow field and may be expressed as a longitudinal pressure gradient through the Euler equation.

In the case of the turbulence kinetic energy equation, the initial turbulence kinetic energy profile must be known or estimated. The free stream turbulence kinetic energy is assumed to be small. Physically, the turbulence kinetic energy becomes zero at the wall since the fluid actually in contact with the wall sticks to the wall and must have zero velocity. However, as discussed previously in the section concerned with the empirical closure equations, the turbulence kinetic energy equation has been modified so that equation 33 is valid all the way to the wall. Therefore, if the wall shear stress is known, the turbulence kinetic energy wall boundary condition may be computed from equation 33. Figure 4 presents a comparison between the measured values of turbulence kinetic energy and those derived from the measured shear stress by means of equation 33 for the data of Klebanoff[28]. The extent of the modification is quite clear. The computed and measured values of turbulence

kinetic energy agree very well as close to the wall as $y/y_1 = .09$. Closer to the wall however, the measured turbulence kinetic energy climbs to a high value and then decays rapidly to zero at the wall. Extrapolation to the wall of the computed turbulence kinetic energy profile from $y/y_1 > .09$ gives good agreement with the computed turbulence kinetic energy based on measured shear at the wall, however.

One of the quantities a boundary layer prediction scheme should predict is the wall shear since this is often one of the primary reasons for the analysis. The paradox here is that it is also required as a boundary condition for the turbulence kinetic energy equation. This has been resolved in the present study by predicting the shear at the wall from the mean velocity profile in the vicinity of the wall using a "Law of the Wall" equation of the form,

$$\frac{u}{u^*} = \frac{1}{k}\left\{\ln \frac{\rho y u^*}{\mu} + c\right\} \tag{39}$$

where $u^* = \sqrt{\tau_w/\rho}$ wall shear velocity

$k = .41$

$$c = 1.85 - .0075 \frac{dp}{dx} + 200 \frac{m_I}{\rho_I u_\infty}$$

An assumption used in forming the finite-difference equations by the miniature integral approach is that the variation of the dependent variable between grid points in the cross stream direction is linear. This assumption is valid everywhere except near the wall. Near the wall, gradients may become very steep in which case the assumption of a linear variation of the dependent variable between the first node away from the wall and the wall value would be a poor approximation (consider the

velocity profile for instance). Therefore, a "slip" value of the dependent variable (φ) is used very near the wall so that the φ vs. ω line passing through this value gives a better approximation for this region. To determine a suitable "slip velocity" at the wall for instance, it is assumed that in this region the velocity profile is of the power-law type:

$$u \alpha (y - y_w)^{\beta} \tag{40}$$

The definition of ω leads to,

$$u \alpha (\omega - \omega_w)^{\beta/(1 + \beta)} \tag{41}$$

By matching the slope at a point half way between the wall and the first node away from the wall and the velocity at the first node away from the wall, the "slip velocity" may be computed from

$$u_s = \frac{1}{1 + 2\beta} u_1 \tag{42}$$

where u_1 = the velocity at the first mode.

Very near the wall, the advection term $\rho u \frac{\partial \varphi}{\partial x}$ becomes comparatively small and may be neglected. In this case the equations become ordinary differential equations. These equations have been solved numerically by Patankar and Spalding[18] with parametric variations on the various constants (dp/dx in the longitudinal momentum equation). The results have then been combined into algebraic expressions for β.

In the case of the turbulence kinetic energy equation this approach has not been applied because of the modification of the turbulence

kinetic energy equation as justified previously. The k vs. ω variation has been assumed linear in this region.

E. Solution of the Finite Difference Equations

The following is a brief introduction to the solution scheme used. It is included here for the sake of continuity. A much more detailed description is given by Patankar and Spalding in reference 18 which should be consulted if the reader wishes more than a cursory knowledge of the technique.

As shown in subsection "B" above, the governing equations can be reduced to the common form,

$$\frac{\partial \varphi}{\partial x} + (a + b\omega) \frac{\partial \varphi}{\partial \omega} = \frac{\partial}{\partial \omega} \left(c \frac{\partial \varphi}{\partial \omega}\right) + d \qquad (43)$$

This equation is solved by a "marching" forward integration procedure with the equation simulated by a finite difference element subdivision of the boundary layer. Therefore, at each step in the integration the values of φ will be computed at discrete values of ω for chosen steps in the longitudinal direction. The discrete values of ω and the integration steps in the x direction form a rectangular mesh which serves as a basis for the finite difference approximation of equation 43. The nomenclature for the approximation scheme is shown in Figure 6.

Rather than use the popular Crank-Nicholson scheme[29], a fully implicit scheme based on a miniature integral has been employed to remove the necessity for equal spacing of node points in the ω direction. It is assumed that in the ω direction, φ varies linearly with ω between mesh points. The variation in the x direction is considered

to be stepwise evaluated over the interval at the downstream location. To linearize the equations, the coefficients a, b and c of Equation 43 are evaluated at the upstream mesh points.

In Figure 6, the u subscripts indicate the upstream location while the D subscripts indicate downstream locations. The + subscripts indicate nodes where the value of ω is larger while - subscripts indicate nodes where the value of ω is smaller. Double letter subscripts indicate midpoint locations in the ω direction. For instance, φ_{vv} is half way between φ_u and φ_{u+} while all three are at the same upstream x location. The shaded area represents the projection of the surface of interest (i.e., φ_{vv-}, φ_u, φ_{vv+}, φ_{DD+}, φ_D, φ_{DD-}, φ_{vv-}) on the x, ω plane. Frequent reference to this figure will help in an understanding of the finite difference scheme described below.

The convection terms of Equation 43 are expressed as,

$$\partial\varphi/\partial x \approx \left\{ \int_{x_u}^{x_D} \int_{\omega_{DD-}}^{\omega_{DD+}} (\partial\varphi/\partial x)\, d\omega dx \right\} / \left\{ (x_D - x_u)(\omega_{DD+} - \omega_{DD-}) \right\} \tag{44}$$

$$(a + b\omega)\ (\partial\varphi/\partial\omega) \approx \left\{ \int_{\omega_{DD-}}^{\omega_{DD+}} (a + b\omega)\ (\partial\varphi/\partial\omega)_{x=x_D}\, d\omega \right\} / (\omega_{DD+} - \omega_{DD-}) \tag{45}$$

i.e., $(a + b\omega)$

Remembering the assumed linear variation of φ between ω points leads to the approximations

$$\frac{\partial\varphi}{\partial x} \approx P_1\ (\varphi_{D+} - \varphi_{u+}) + P_2(\varphi_D - \varphi_u) + P_3\ (\varphi_{D-} - \varphi_{u-}) \tag{46}$$

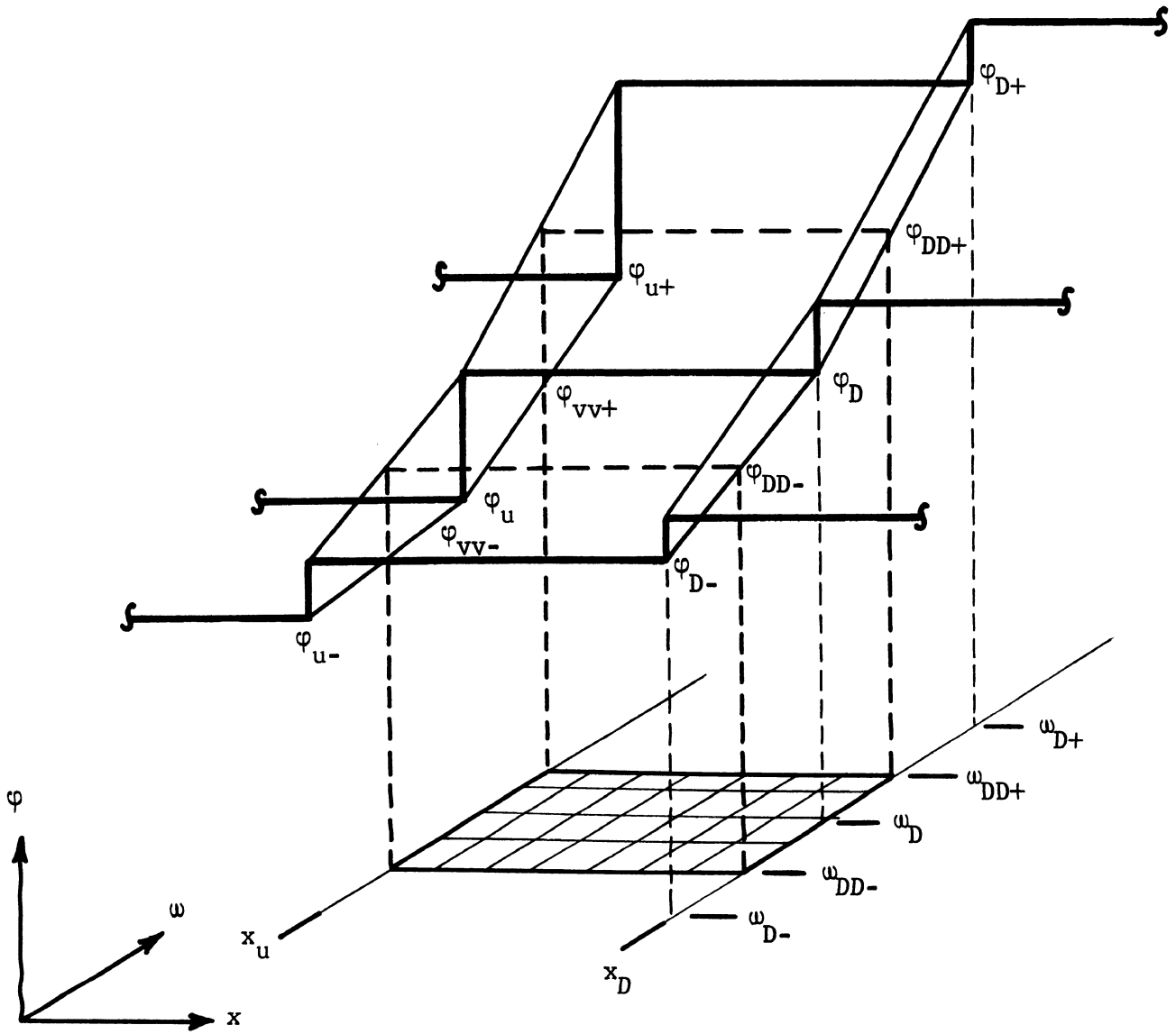

Figure 6. Miniature Integral Model for the Finite Difference Scheme

where

$$P_1 \equiv \frac{\omega_{D+} - \omega_D}{4(x_D - x_u)(\omega_{D+} - \omega_{D-})}$$

$$P_2 \equiv \frac{3}{4(x_D - x_u)}$$

$$P_3 \equiv \frac{\omega_D - \omega_{D-}}{4(x_D - x_u)(\omega_{D+} - \omega_{D-})}$$

$$a \frac{\partial \varphi}{\partial \omega} \approx Q \, (\varphi_{D+} - \varphi_{D-}) \tag{47}$$

where

$$Q \equiv \frac{a}{\omega_{D+} - \omega_{D-}}$$

$$b\omega \frac{\partial \varphi}{\partial \omega} \approx R_1 \varphi_{D+} + R_2 \varphi_D + R_3 \varphi_{D-} \tag{48}$$

where

$$R_1 \equiv \frac{b}{4} \frac{\omega_{D+} + 3\omega_D}{\omega_{D+} - \omega_{D-}}$$

$$R_2 \equiv - b/4$$

$$R_3 \equiv - \frac{b}{4} \frac{\omega_{D-} + 3\omega_D}{\omega_{D+} - \omega_{D-}}$$

The complete convection term can be expressed as,

$$\frac{\partial \varphi}{\partial x} + (a + b\omega) \frac{\partial \varphi}{\partial \omega} = g_1 \varphi_{D+} + g_2 \varphi_D + g_3 \varphi_{D-} + g_4 \tag{49}$$

where

$$g_1 \equiv P_1 + Q + R_1$$

$$g_2 \equiv P_2 + R_2$$

$$g_3 \equiv P_3 - Q + R_3$$

$$g_4 \equiv -P_1 \varphi_{u+} - P_2 \varphi_u - P_3 \varphi_{u-}$$

Note that all g's are expressed in terms of known quantities.

The diffusion term of Equation 43 may be expressed as,

$$\frac{\partial}{\partial\omega}\left(C \frac{\partial\varphi}{\partial\omega}\right) \approx \frac{2}{\omega_{D+} - \omega_{D-}} \left\{ C_{uu+} \frac{\varphi_{D+} - \varphi_{D-}}{\omega_{D+} - \omega_D} - C_{uu-} \frac{\varphi_D - \varphi_{D-}}{\omega_D - \omega_{D-}} \right\} \tag{50}$$

By defining

$$g_5 \equiv \frac{2C_{uu+}}{(\omega_{D+} - \omega_{D-})(\omega_{D+} - \omega_D)}$$

$$g_6 \equiv \frac{2C_{uu-}}{(\omega_{D+} - \omega_{D-})(\omega_D - \omega_{D-})}$$

the diffusion term may be written as,

$$\frac{\partial}{\partial\omega}\left(C \frac{\partial\varphi}{\partial\omega}\right) \approx g_5 (\varphi_{D+} - \varphi_D) - g_6 (\varphi_D - \varphi_{D-}) \tag{51}$$

As previously discussed in subsection B of this section (see also Equation 32), the longitudinal momentum equation has been linearized by evaluating the "C" of Equation 51 at the upstream location. The method may be plainly seen by reference to the C_{uu+} and C_{uu-} terms in Equation 50.

The source term "d" of Equation 43 is assumed uniform throughout the area of integration and equal to the value at the downstream mesh

line. "d" may not be linear in φ but it is evaluated from the linearized formula,

$$d_D = d_u + \frac{\partial d}{\partial \varphi} (\varphi_D - \varphi_u) \tag{52}$$

The source term for the momentum equation is evaluated from

$$d \approx \frac{\int_{\omega_{DD-}}^{\omega_{DD+}} (d)_D \, d\omega}{(\omega_{DD+} - \omega_{DD-})} \tag{53}$$

since the velocity is assumed to vary linearly with ω between mesh points. The source term for the momentum equation may be written then as,

$$d = S_1 U_D + S_2 U_D + S_3 U_{D-} + S_4 \tag{54}$$

where

$$S_1 = \frac{P_1}{P_{u+} U^2_{u+}} \frac{dp}{dx} (x_D - x_u)$$

$$S_2 = \frac{P_2}{P_u U^2_u} \frac{dp}{dx} (x_D - x_u)$$

$$S_3 = \frac{P_3}{P_{u-} U^2_{u-}} \frac{dp}{dx} (x_D - x_u)$$

$$S_4 = -2 \frac{dp}{dx} (x_D - x_u) \left\{ \frac{P_1}{\rho_{u+} U_{u+}} + \frac{P_2}{\rho_u U_u} + \frac{P_3}{\rho_{u-} U_{u-}} \right\}$$

By grouping all of the finite difference terms goether, the equation may be written for each node point in implicit form in terms of the dependent variables at the downstream location of the node of interest and the two nearest nodes. In this manner the nodes of the boundary layer form a set of simultaneous linear algebraic equations of the form,

$$\begin{bmatrix} B_1 & C_1 & & & & & \\ A_2 & B_2 & C_2 & & & & \\ & A_3 & B_3 & C_3 & & & \\ & & A_4 & B_4 & \cdots & C_4 & \\ & & & & & & \\ & & & & A_n & B_n \end{bmatrix} \cdot \begin{bmatrix} \varphi_1 \\ \varphi_2 \\ \varphi_3 \\ \varphi_4 \\ \\ \varphi_n \end{bmatrix} = \begin{bmatrix} D_1 \\ D_2 \\ D_3 \\ D_4 \\ \\ D_n \end{bmatrix}$$

(55)

The transfer matrix for this set of equations is tri-diagonal in form and is easily solved by back substitution.

IV. DISCUSSION OF PREDICTIONS

A logical progression of increasingly complex turbulent boundary layers was used in developing the mathematical models described in the previous section. A wide range of boundary conditions were investigated since the prediction scheme being sought was to have as broad a range of application as possible. The empirical information needed to define a prospective model was established by forcing the model to provide adequate predictions for the simplest cases. As the model was applied to more complex cases, minor modifications were made to the model in an attempt to obtain adequate predictions without invalidating the previous predictions with the model. It is necessary to evaluate models in this manner since it is possible to develop a model which will adequately predict a narrow range of complex turbulent boundary layers but provide erroneous predictions in other cases. The mathematical models finally selected are those which provided the best predictions with accelerated, neutral, and decelerated boundary layers and with positive, zero and negative mass addition at the wall.

The first case each model was tested against was flow along an impermeable flat plate in zero pressure gradient. The test case used was the experimental results of Klebanoff[28]. This was a particularly good starting point because Klebanoff measured the mean velocity profile, and enough fluctuating velocity information so that the turbulent kinetic energy and shear stress profiles could be determined for this

the simplest of all equilibrium boundary layers.* All empirical information for the models being tested was then arranged to maintain the non-dimensional velocity boundary layer and a reasonable shear profile for forty initial boundary layer thicknesses downstream. Assuming this condition could be met, the models were then tested against an initially disturbed, relaxing boundary layer on an impermeable flat plate in zero pressure gradient. Some data of Levitch[30] were used for this purpose. These data appear to be somewhat in question because of the discontinuity in the shear stress profile at the wall. However, a valid model should predict the correct trend in this case. Next, the models were tested against two equilibrium boundary layer cases with adverse pressure gradient (decelerating flow). Experimental information for these two cases was that of Bradshaw.[24] Finally, the models were tested against several cases of favorable pressure gradient (accelerating flow) along an impermeable wall and along a permeable wall with blowing and suction at the wall. The data of Julien[31] and Thielbahr, et al[32] were used for these cases. Unfortunately, no shear or turbulence kinetic energy measurements were made in these cases. In these cases, the initial turbulence kinetic energy profiles had to be assumed and the accuracy of the downstream kinetic energy profiles could be tested only indirectly by the resulting shape of the downstream velocity profiles and the predicted wall shear stress. A matrix of test cases is given in Table I to describe the range of conditions covered and give the reader an easy cross reference to use if he should like to

---

*For purposes of this study, equilibrium boundary layers have been defined as those where the non-dimensionalized mean velocity profile remains constant.

TABLE I. MATRIX OF TEST CASES

Case	Ref.	$\partial p/\partial x$ ($lb_f ft^{-2} ft^{-1}$)	F
1	28	0	0
2	30	0	0
3	24	.491	0
4	24	.602	0
5	31	0	0
6	32	-.635	0
7	32	-.787	0
8	32	-.787	.001
9	32	-.787	.004
10	32	-.787	-.001
11	32	-.787	-.002

$$F = \frac{\rho_I v_I}{\rho_\infty u_\infty}$$

make comparisons other than those given below. The columns containing information about pressure gradient and wall mass transfer indicate relative order of magnitude. Case 1 is Klebanoff's[28] experiment, Case 2 is that of Levitch[30], and Cases 3 and 4 are the positive pressure gradient results of Bradshaw[24]. Cases 5 thru 11 are those of Julien[31] and Thielbahr, et al[32].

Figure 7a provides a comparison of the free stream velocity schedules among the cases investigated. Cases 1, 2 and 5 are zero pressure gradient cases of various free stream velocities. Cases 3 and 4 are cases of positive pressure gradient while the remainder are negative pressure gradient cases. A comparison between the experimental and analytical wall shear velocities (see Equation 39) is presented in Figure 7b. The comparison between the analytical and experimental wall shear velocities indicates adequate prediction capability for wall shear stress.

A. The Impermeable Wall in Zero Pressure Gradient

Klebanoff (Case 1) made measurements in an equilibrium boundary layer. In an equilibrium boundary layer it is necessary to make measurements at only one streamwise location since the shape of the non-dimensional velocity profile is invarient if the cross stream distance is non-dimensionalized with respect to the boundary layer thickness and the velocity magnitude is non-dimensionalized with respect to the free stream velocity. The prediction method was started using the measured velocity profile and the measured turbulence kinetic energy profile modified close to the wall as discussed previously. The analysis was carried out to a downstream distance of forty initial boundary layer thicknesses. The

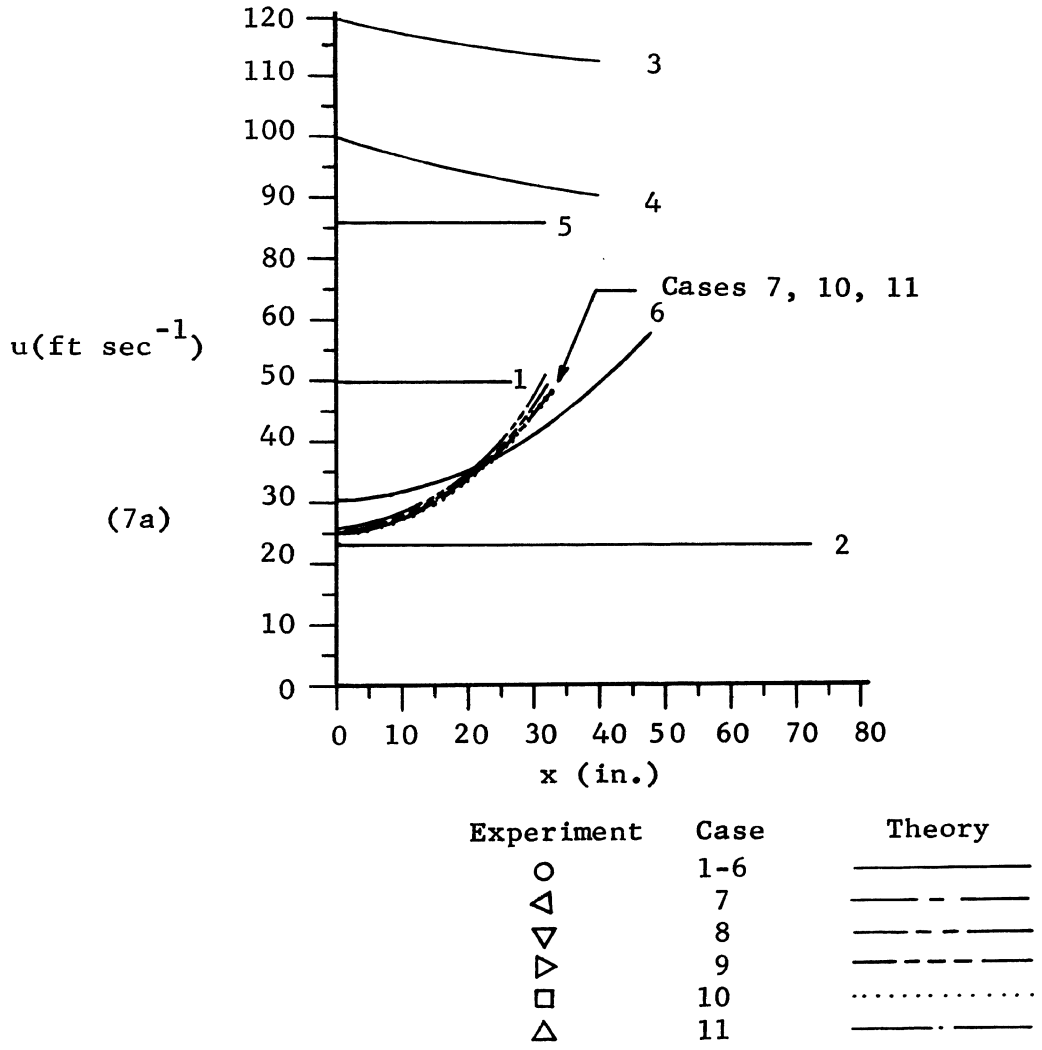

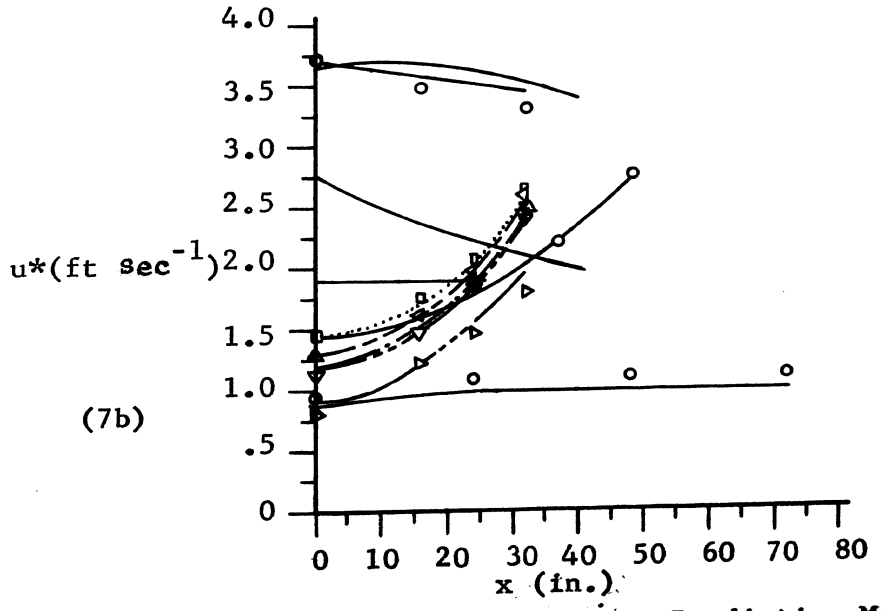

Figure 7. The Range of Cases to which the Prediction Method has been Applied

resultant shear and velocity profiles for Klebanoff's case are presented in Figure 8. The non-dimensionalized velocity profiles throughout were virtually the same. The shear stress profile while maintaining the same shape decreased slightly in magnitude in keeping with the expected reduction in wall friction coefficient for boundary layers of this type. It is evident from these results that the chosen mathematical models and prediction technique provide excellent predictions for this case.

Julien's experiment (Case 5) is similar to the experiment of Case 1 and was carried out on the same apparatus used for Cases 6 through 11. No hot-wire anemometry data is available for Cases 5 through 11. Therefore, a method had to be found to generate the initial turbulence kinetic energy profiles. These profiles were generated by using profiles of the same shape as the data of Klebanoff and stretching it to fit the width of the boundary layer of interest and matching the wall value of turbulence kinetic energy with the measured wall shear stress through Equation 33. This analysis then was conducted for two reasons: (1) to determine how the assumption of an initial turbulence kinetic energy profile would affect the solution, and (2) to determine the feasibility of using the data from this apparatus. The assumption is that if the profile shapes can be satisfied and if the downstream wall shear stresses are adequately predicted then items (1) and (2) above are satisfactory. Figure 9 presents the measured and predicted velocity and shear stress profiles for the initial profile and two others, the last of which is some 35 initial boundary layer thicknesses downstream. The agreement among the velocity profiles is excellent in terms of boundary layer growth and shape. The

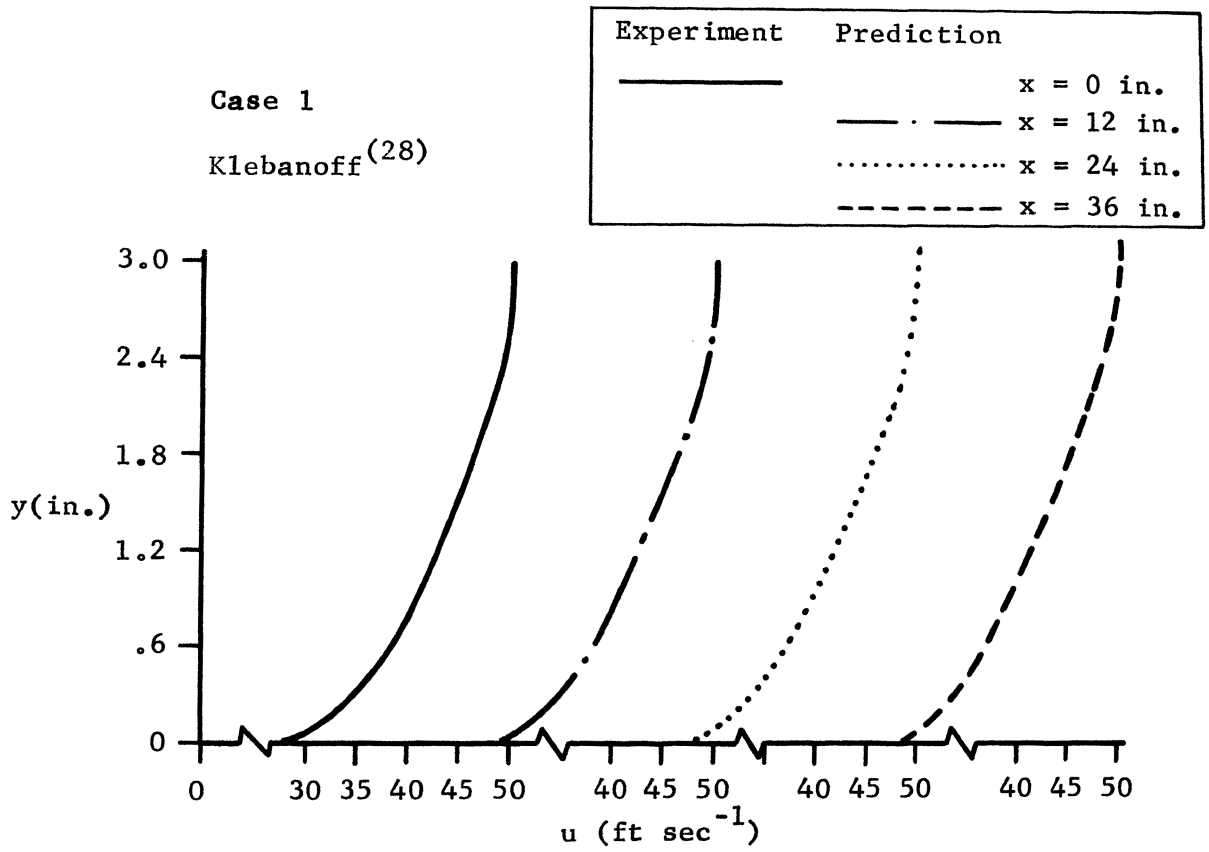

NOTE: The coordinate system is placed at the location of the initial profiles for all predicted results

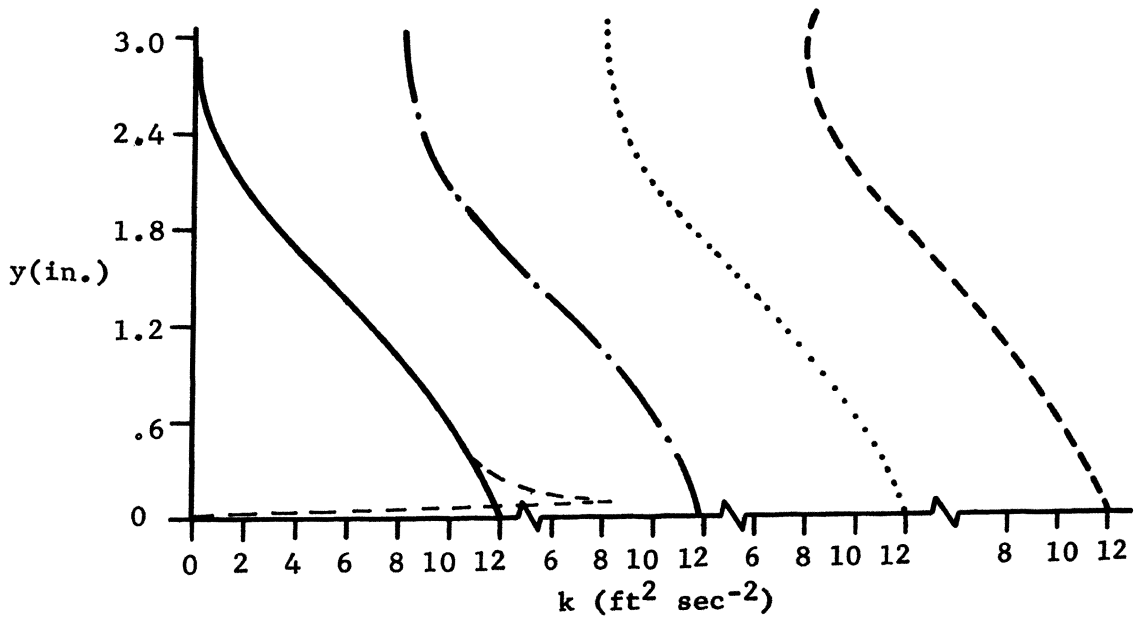

Figure 8. Prediction of the Simplest of Boundary Layers

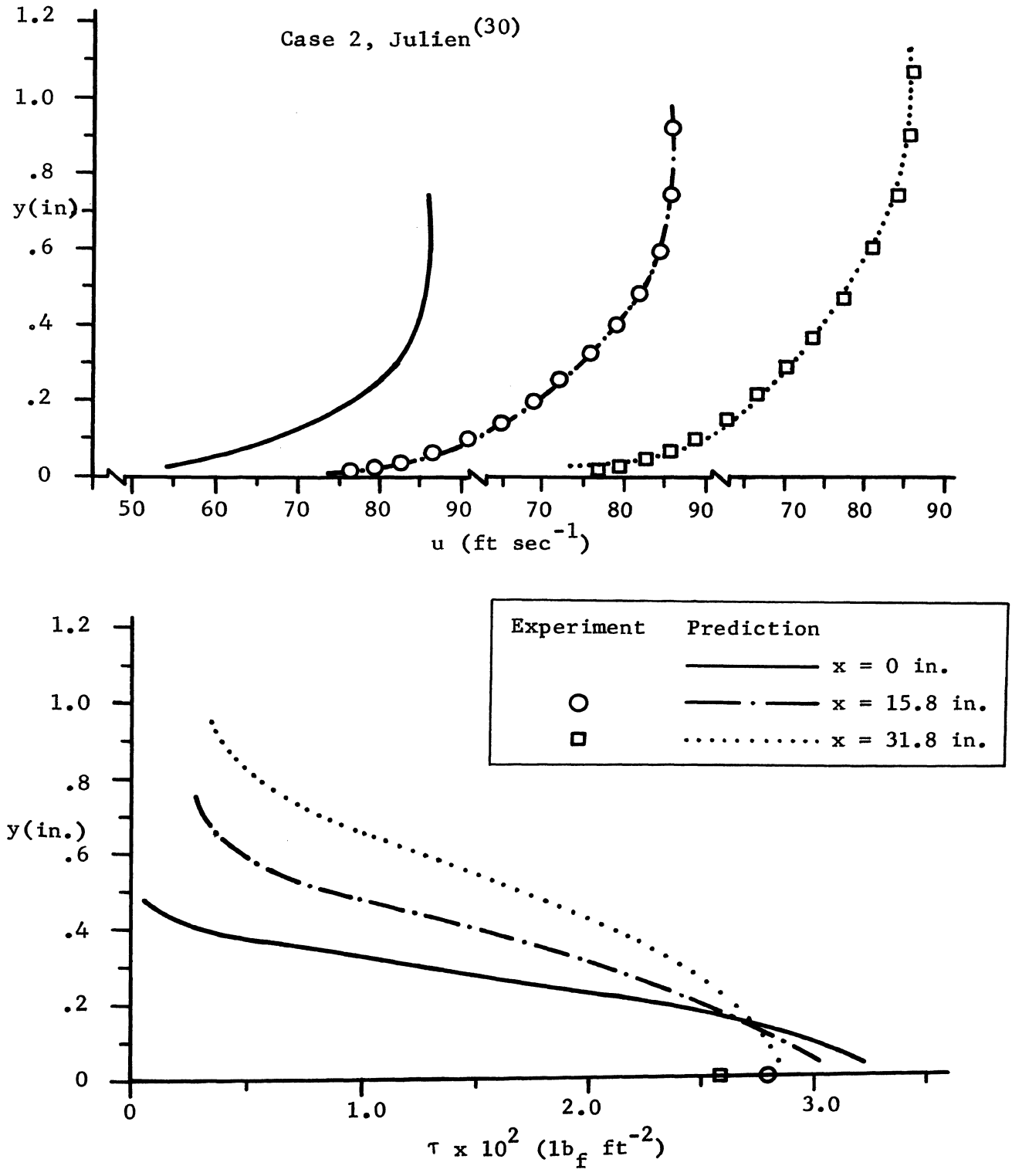

Figure 9. Prediction of the Simplest Boundary Layer with Increased Free Stream Velocity

shear stress profile maintains the same shape as the prediction progresses. The agreement between the measured and the predicted wall shear stress is good. The predicted variation of wall shear stress with distance downstream goes in the correct direction and is probably as good as the measured value since wall shear stress is a difficult quantity to measure.

Case 2 (Levitch) is an interesting non-equilibrium boundary layer. It was created by blowing into a turbulent boundary layer for some distance to perturb the normal velocity and shear stress profile shapes and then abruptly terminating the blowing and observing these profiles as the boundary layer "relaxed" toward an equilibrium condition. The velocity and shear profiles were measured with a hot-wire anemometer. The results of the predictions for this case are presented in Figure 10. The predicted wall shear stress proceeded in the correct direction but was 10 percent lower than the reported measured results. The velocity profiles are good except in the inner 20 percent of the boundary layer. When the experimental velocity profiles were carefully plotted, a definite inflection point occurred at the place where the predicted and experimental profiles begin to diverge. It is entirely possible that the measurement probe might have encountered a "wall effect" in this inner region. The agreement between the predicted and measured shear stress profiles is adequate. The "hook" in the predicted shear stress profile which develops in the first 24 inches is gradually damped out and good agreement is evident at the 72 inch station. This "hook" may be caused by inferior starting conditions for the turbulence kinetic energy profile. In any event, Case 2 which was the first and strongest non-equilibrium boundary layer examined exhibited reasonable agreement between measurement and theory.

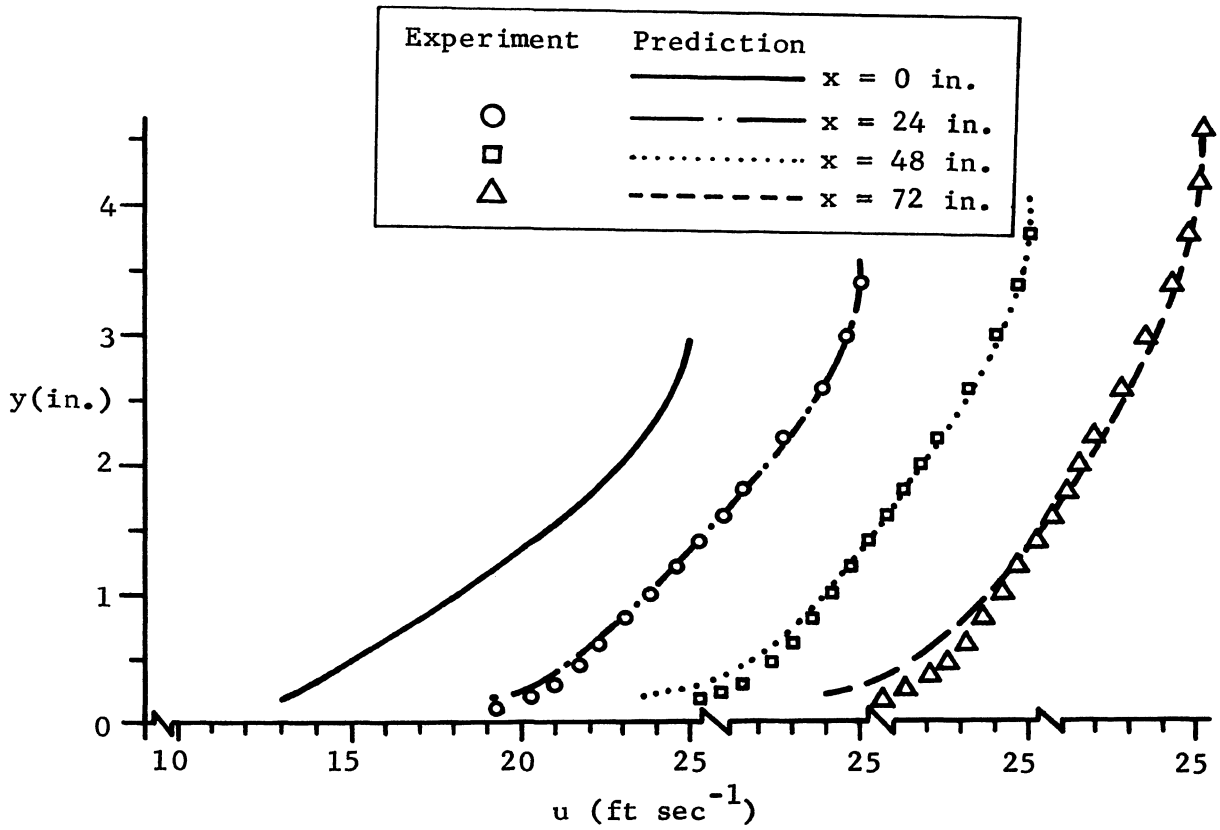

Case 5, Levitch[31]

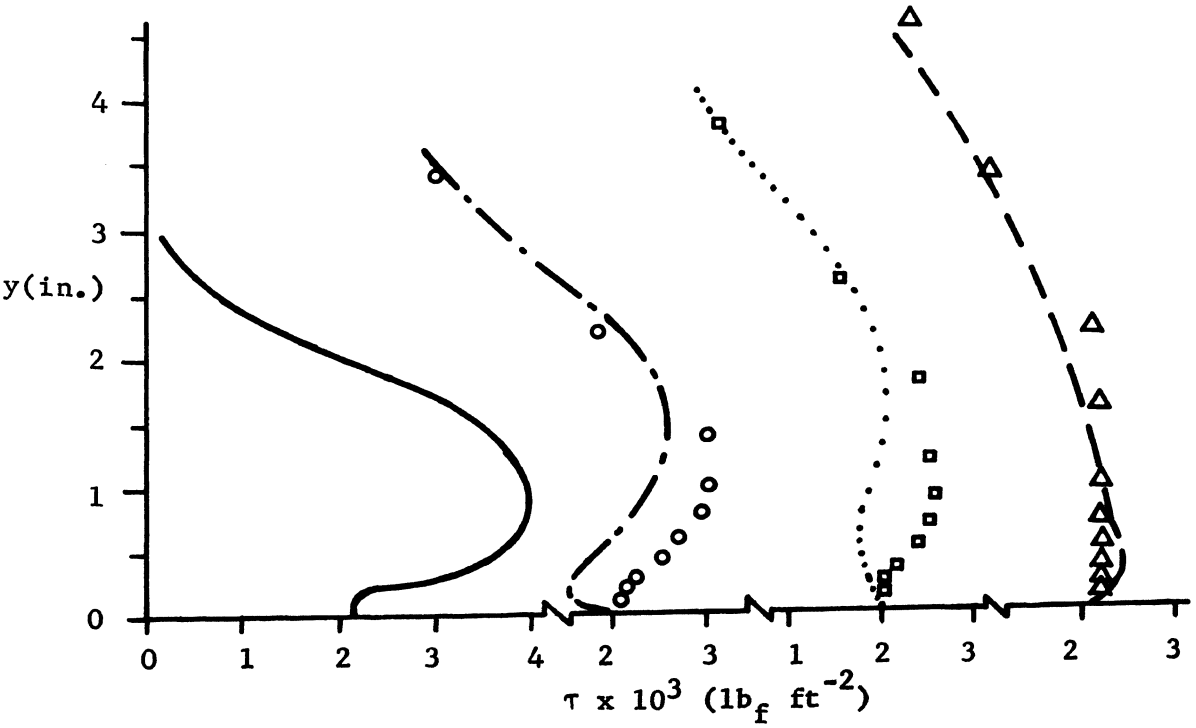

Figure 10. Prediction of a Perturbed Boundary Layer

Since the prediction scheme provided reasonable results for boundary layers without free stream pressure gradient, it was next applied to boundary layers in the presence of pressure gradients.

B. The Impermeable Wall in the Presence of a Pressure Gradient

Most real boundary layers develop in the presence of a pressure gradient in the flow direction. Flow conditions with a negative pressure gradient are normally referred to as favorable or accelerating conditions whereas flow conditions with a positive pressure gradient are referred to as unfavorable or decelerating conditions. Four cases with pressure gradient along an impermeable wall were examined in this study: two accelerating and two decelerating.

Bradshaw (24) performed experimental measurements of mean velocity and turbulent shear stress in two equilibrium boundary layers with adverse or decelerating pressure gradient. The experimental apparatus was adjusted so that the free stream velocity varied exponentially with distance as,

$$u_\infty \propto x^a$$

The two experiments reported were for a = -.15 and a = -.255. The non-dimensionalized velocity profiles at various stations were found to be coincident in each case. The predictions were started using the measured mean velocity profiles and initial turbulence kinetic energy profiles were derived from the measured shear profiles using Equation 33. The results of the predictions for a = -.15 (Case 3) are given in Figure 11. The non-dimensional velocity profile remained essentially unchanged for thirty boundary layer thicknesses. The shear stress profile shape

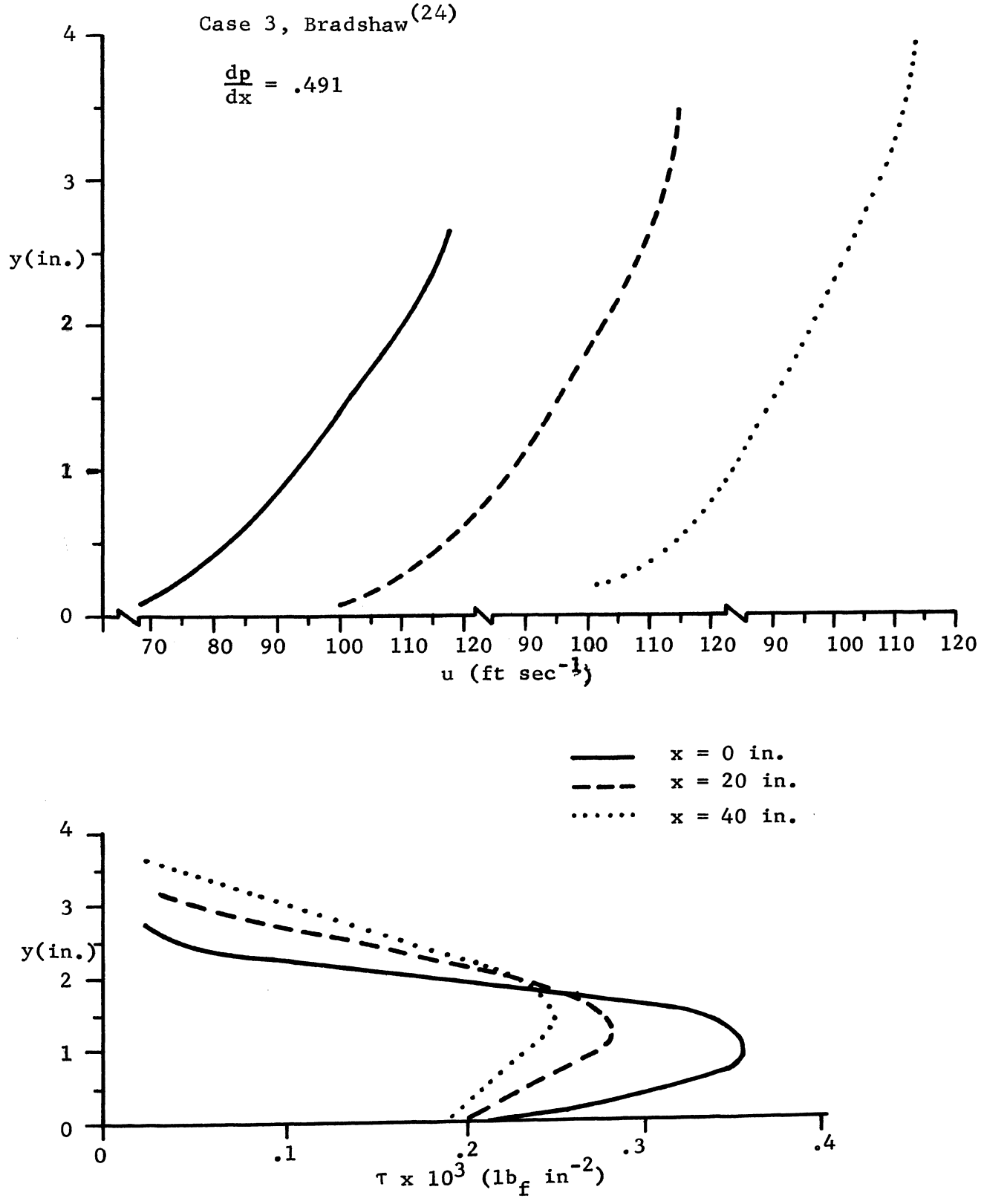

Figure 11. Prediction of a Boundary Layer with Slight Adverse Pressure Gradient

remained the same as the prediction advanced in the downstream direction. Figure 12 shows similar results for a = -.255 (Case 4). The predictions for both cases appear to be very good.

The two cases examined for the effects of an accelerating boundary layer (Cases 6 and 7) come from the results of Thielbahr et al[32]. Unfortunately, Thielbahr did not make hot-wire anemometer measurements and therefore no data is available on shear stress or turbulence kinetic energy. However, wall shear stresses are reported. In each case the pressure gradient was relatively low at the station of the initial profile. Therefore, the initial turbulence kinetic energy profile was assumed by making use of Klebanoff's measured turbulence kinetic energy profile and proceeding as indicated for Julien's data (see subchapter A of this chapter). Figure 13 presents a comparison between the experimental and predicted velocity profiles and the predicted shear stress profiles for a slightly accelerating boundary layer at various downstream locations as noted. The agreement between predicted and measured velocity profiles is excellent. The fact that the outer portion of the shear stress profiles are almost the same indicates that the assumption concerning the initial turbulence kinetic energy profile was adequate. Figure 14 presents similar results for a more rapidly accelerating boundary layer. Once again, the agreement between the experimental and predicted velocity profiles is excellent. The good agreement between the measured wall shear and the predicted shear profiles seems to indicate that the models are adequate for this case also.

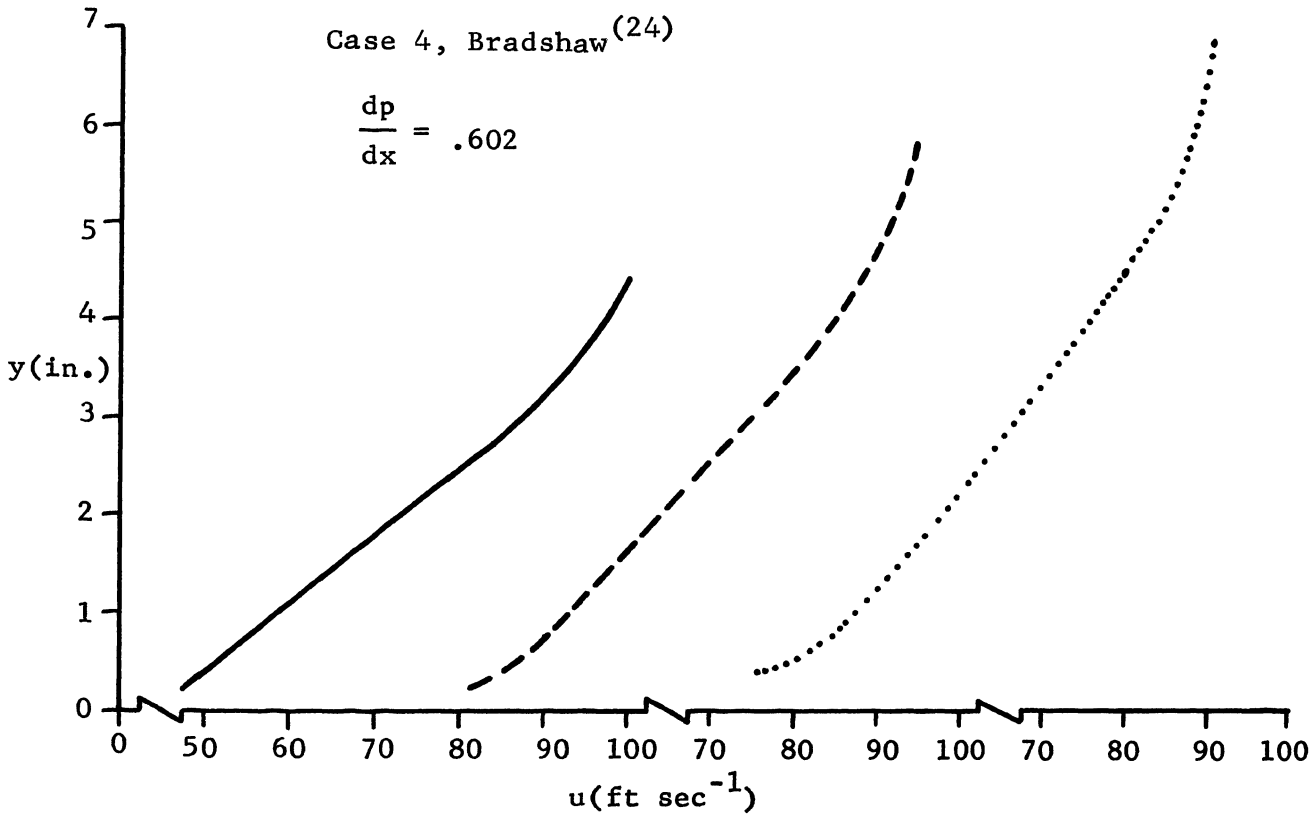

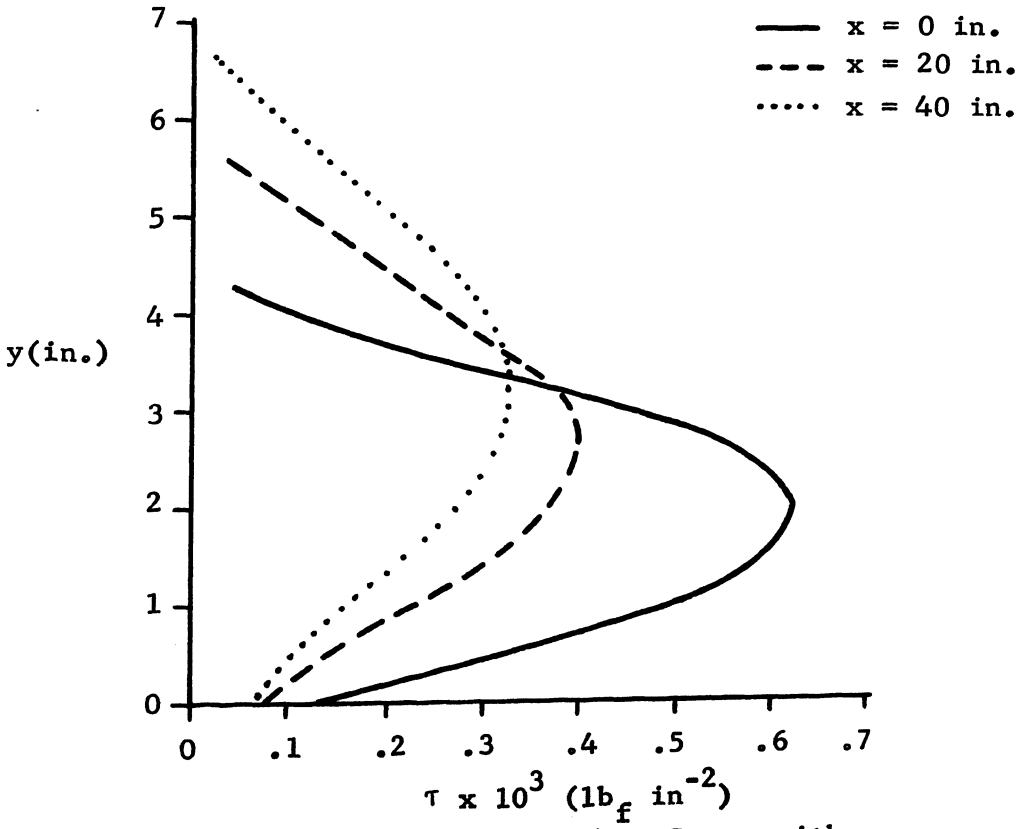

Figure 12. Prediction of a Boundary Layer with Moderate Adverse Pressure Gradient

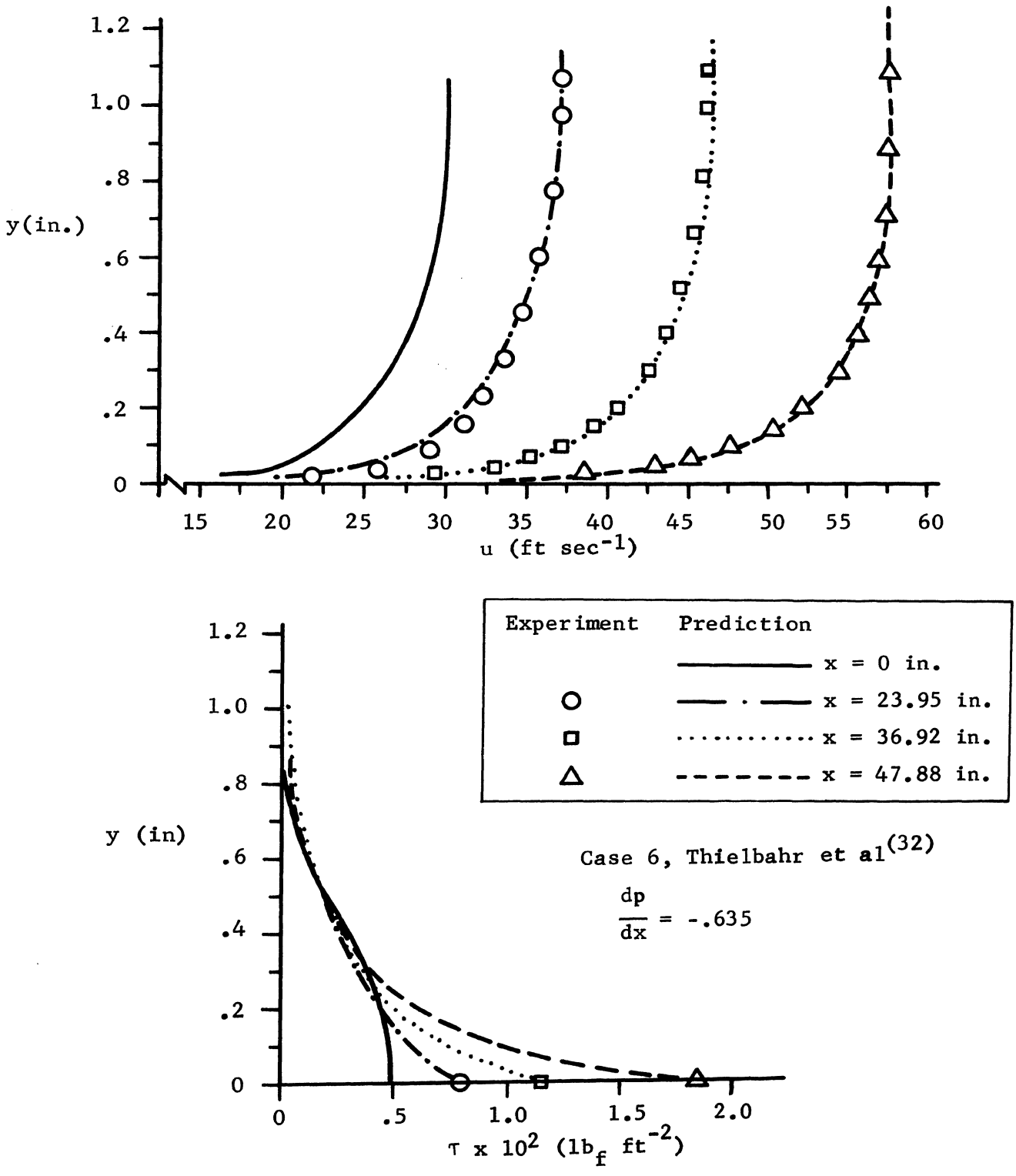

Figure 13. Prediction of a Boundary Layer with Slight Favorable Pressure Gradient

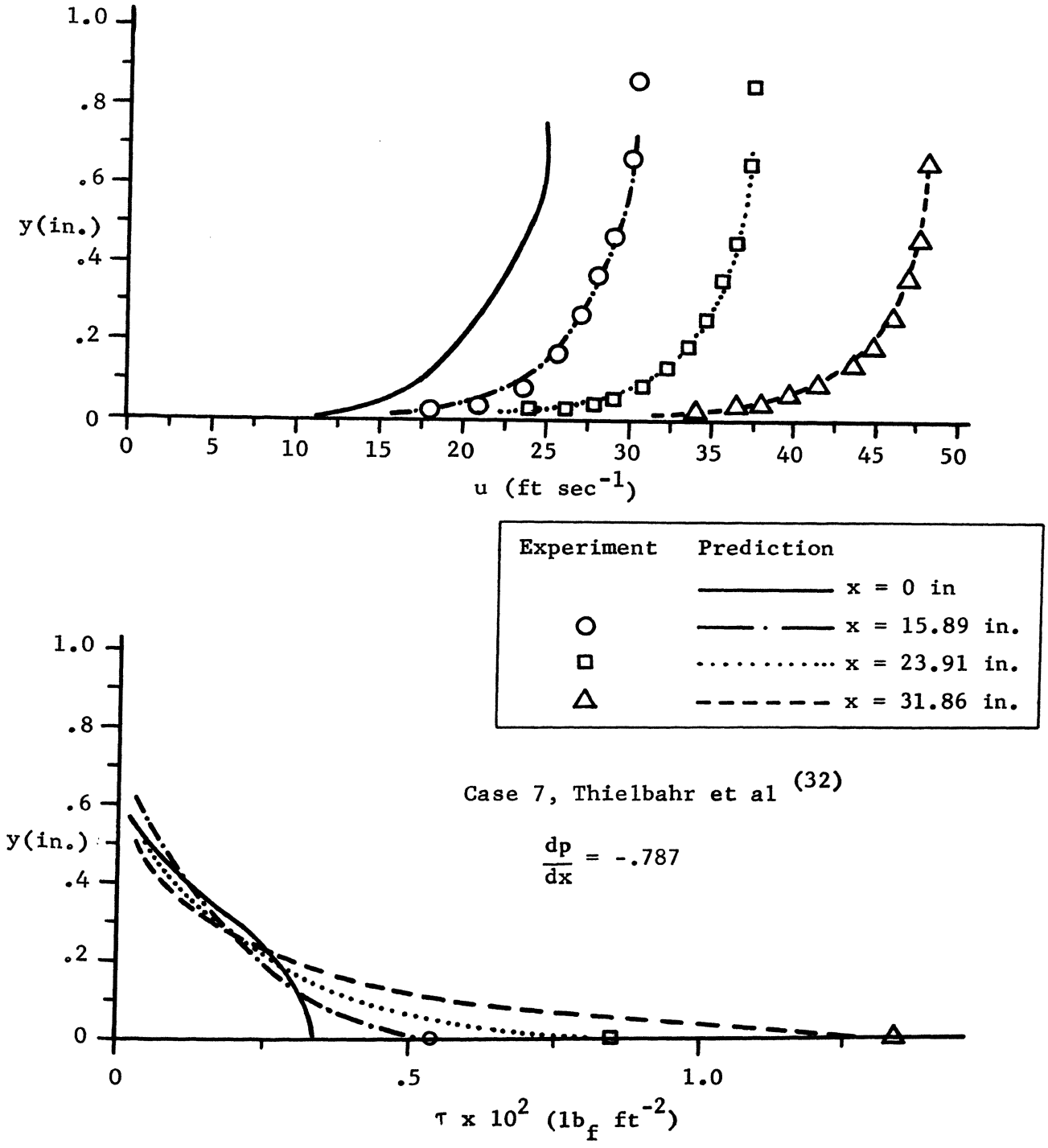

Figure 14. Prediction of a Boundary Layer with Stronger Favorable Pressure Gradient

In summary, it appears that the mathematical models used are quite adequate for flows along an impermeable wall with positive or negative pressure gradient at least throughout the range tested.

C. Accelerated Boundary Layers with Blowing or Suction

As mentioned in Section I, turbulent boundary layers are often controlled by mass transfer at the wall in engineering applications. A truly useful prediction method should then also have this capability. Four accelerated boundary layers with varying amounts of mass transfer at the wall have been investigated to demonstrate the capability of the present prediction method. A blowing parameter "F" has been defined as,

$$F = \frac{\rho_I \, v_I}{\rho_\infty \, u_\infty}$$

where the subscript "I" indicates conditions at the wall; thus, v_I is the gas transpiration velocity at the wall. The four values of F investigated were -.002, -.001, +.001, and +.002. The experimental data used was once again that of Thielbahr et al[32] and the initial conditions were established in the same manner as that used for Cases 5 through 7. It is unfortunate that no hot-wire anemometer data is available for these cases because the shape of the shear stress profile measured by Levitch just downstream of a blowing section indicated a maximum shear stress at some location away from the wall. Therefore, the use of the Klebanoff turbulence kinetic energy profile shape may not be realistic here. It was used however, for lack of better data. All of the Cases (8-11) investigated with mass transfer at the wall had the same free stream velocity schedule as did Case 7, the larger maximum pressure gradient case for the impermeable wall situation. The results for

Cases 8 through 11 are given in Figures 15 through 18. Cases 8 and 10, the lowest blowing and suction cases, respectively, predict very good velocity profiles. Cases 9 and 11 do not produce velocity profiles which are in as good agreement with the experimental data but the predictions are reasonable. Inadequacy of the initial turbulence kinetic energy profiles may account for these deviations. Suction Cases 10 and 11 produce what appear to be reasonable velocity profile and wall shear stress predictions. However, the shear stress profiles change rapidly from the initial shear stress profiles indicating that the initial profiles which were assumed were of the wrong shape. The shear stress predictions of blowing Cases 8 and 9 develop definite "hooks" in the profiles near the wall. These hooks are consistent with the experimental results of Levitch and are to be expected with blowing since this will force the location of maximum shear stress away from the wall. It is impossible to say quantitatively at the present time just how accurate the predictions are for cases with mass addition at the wall. The urgent need for experimental hot-wire anemometer data is obvious.

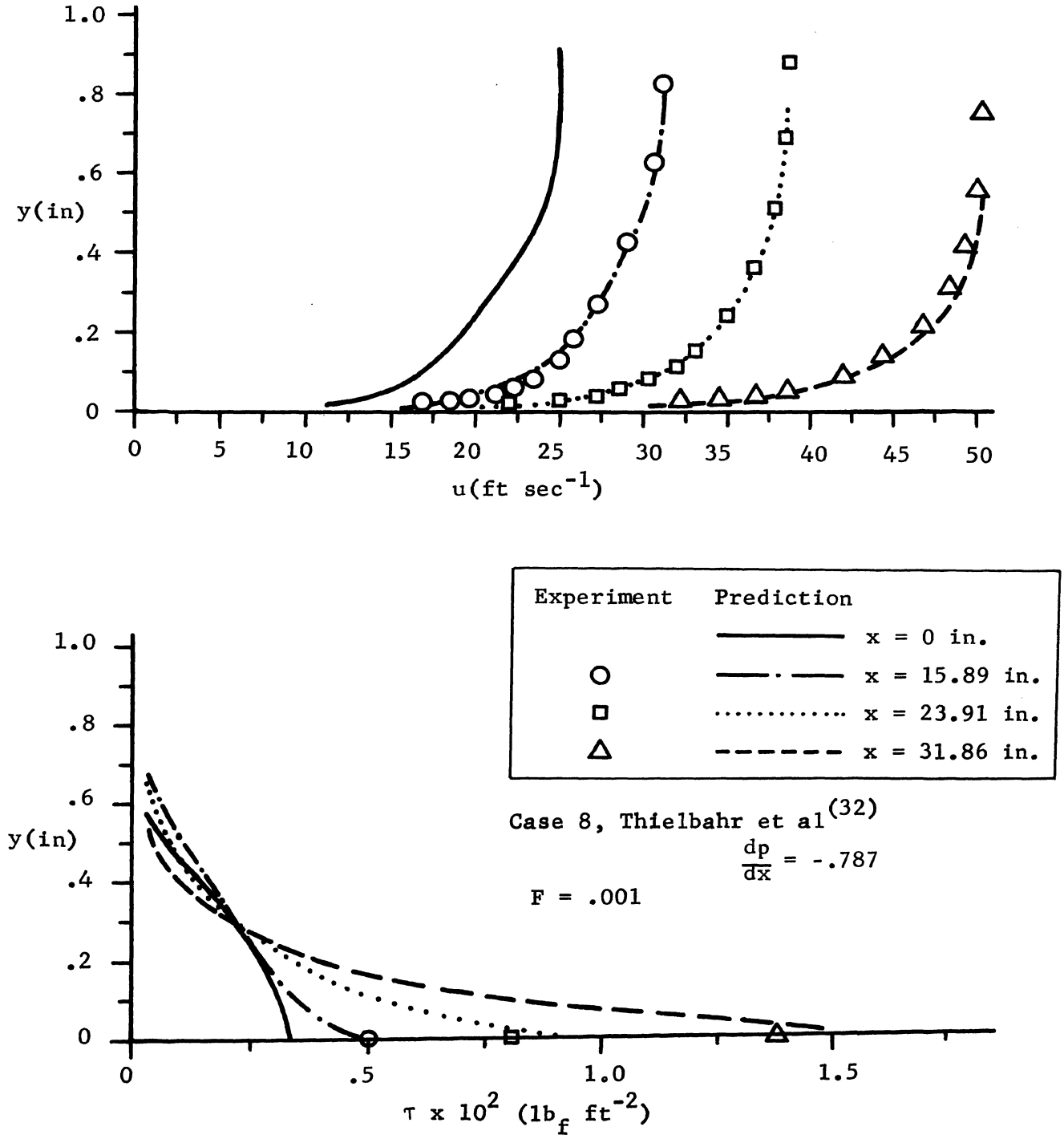

Figure 15. Prediction of an Accelerated Boundary Layer with Slight Injection

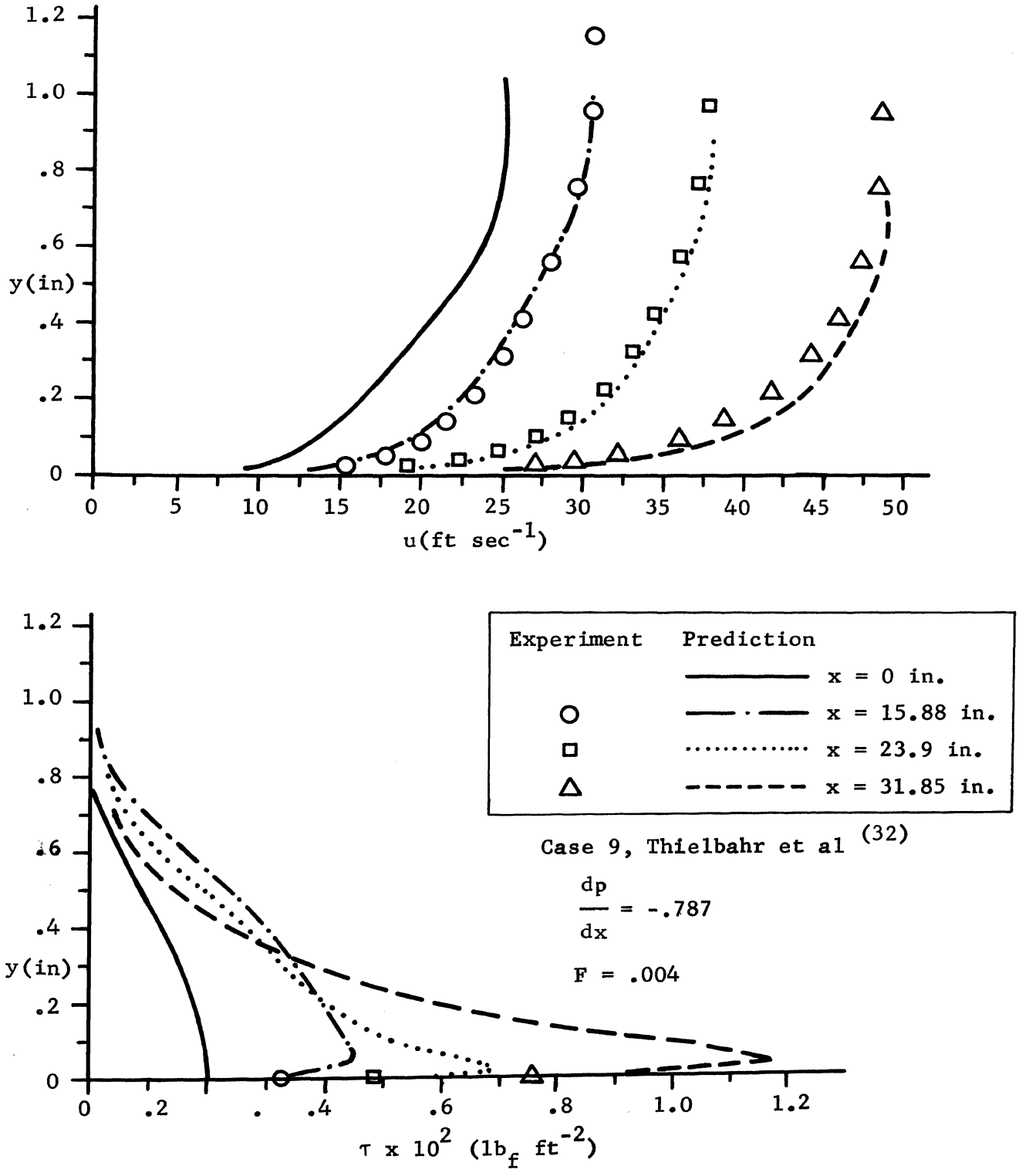

Figure 16. Prediction of an Accelerated Boundary Layer with Stronger Injection

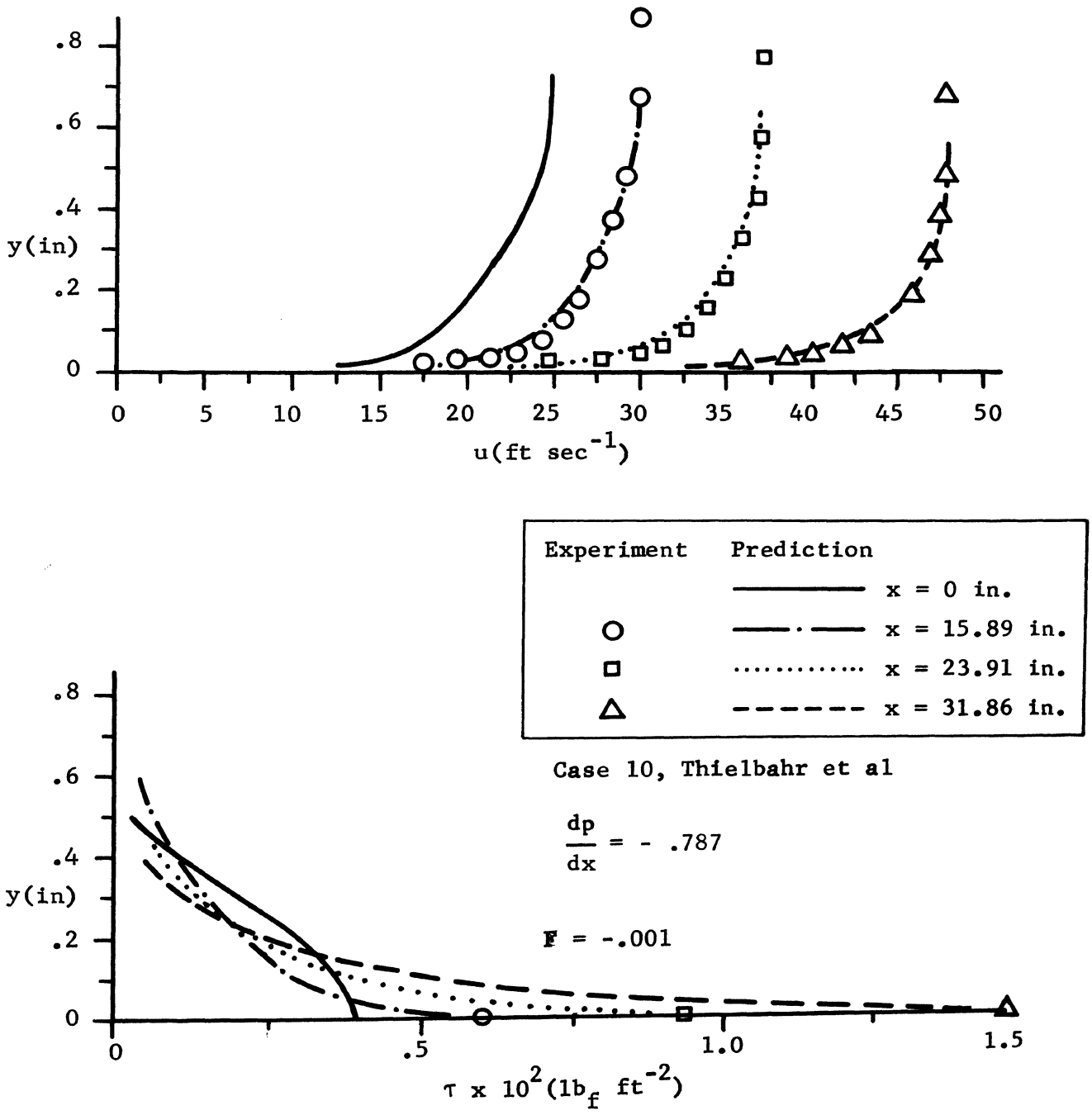

Figure 17. Prediction of an Accelerated Boundary Layer with Slight Suction

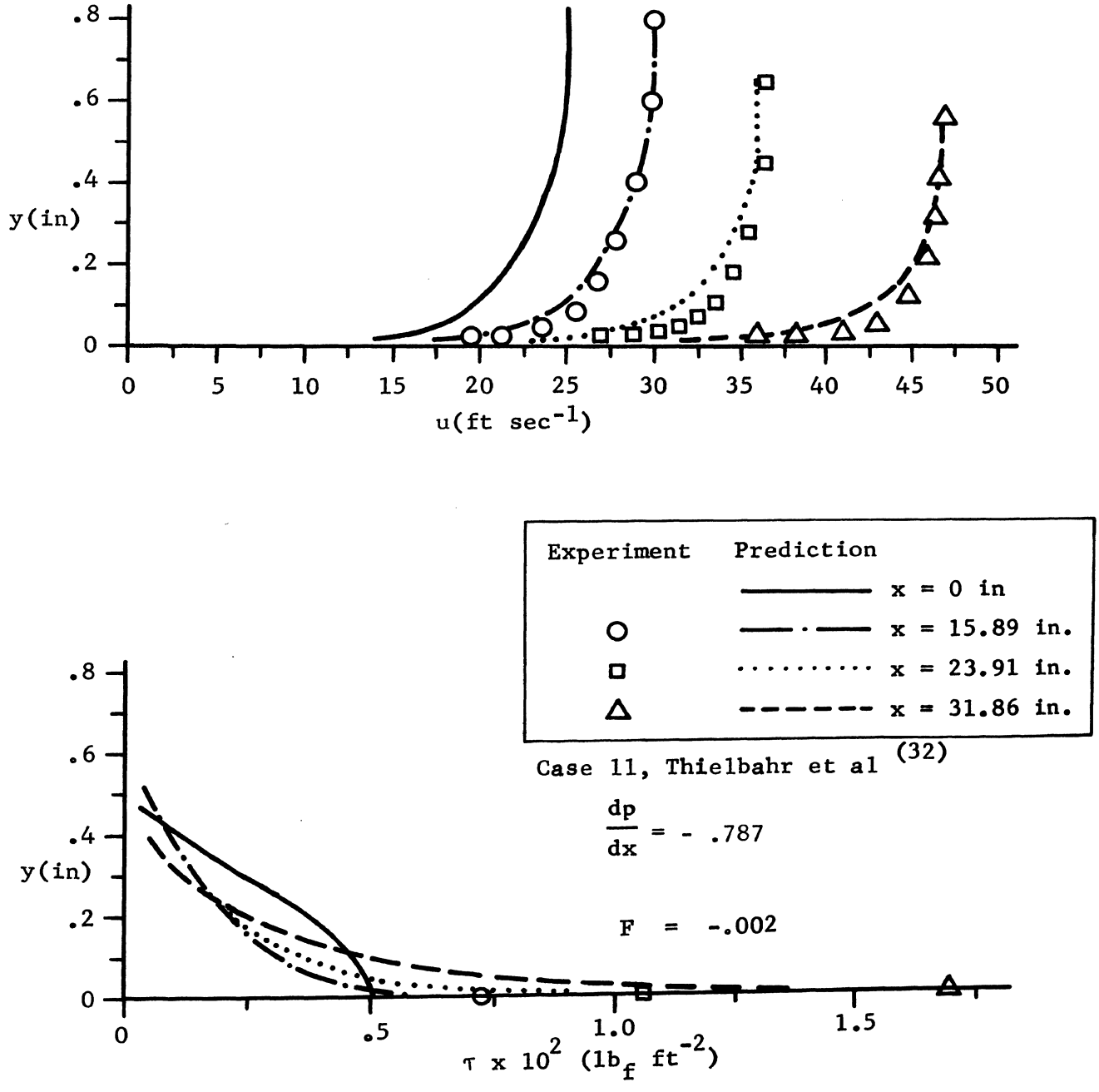

Figure 18. Prediction of an Accelerated Boundary Layer with Stronger Suction

V. CONCLUSIONS AND RECOMMENDATIONS

The feasibility of using the turbulence kinetic energy equation as an aid in predicting the behavior of several classes of turbulent boundary layers has been investigated. Since turbulence kinetic energy must be conserved in turbulent boundary layers, the proper addition of a conservation of turbulence kinetic energy equation to the more generally applied conservation equations of momentum and mass allows more of the physics of the flow to be considered. The following conclusions have been reached based on the successful prediction of the wide variety of turbulent boundary layers analyzed in this investigation:

1. It has been shown that a single computation method can be used to predict the behavior of accelerated, decelerated, or neutral (negative, positive or zero pressure gradient) turbulent boundary layers along an impermeable wall.

2. It has also been shown that the same computational method can be used to predict the behavior of turbulent boundary layers with blowing or suction.

3. Four empirical models (three for the turbulence kinetic energy equation and one for the momentum equation) are needed to close the system of governing equations when the conservation equations of turbulence kinetic energy, momentum and mass are employed. These models are for:

a. Production of turbulence kinetic energy.

b. Dissipation of turbulence kinetic energy.

c. Diffusion of turbulence kinetic energy.

d. Diffusion of momentum.

Sufficient experimental data exist for adequate definition of two of these models (a and d), whereas the remaining two are not so well defined.

4. Adequate empirical models can be defined for the outer (nearer the free stream) 80 percent of the turbulent boundary layer flow field.

5. A "law of the wall" expression has been developed which can be applied to the flow field behavior very near the wall. Consistent results of accuracy suitable for engineering application can be obtained with this model.

6. The computer program modified for this research is an effective tool for solving simultaneous parabolic equations of the boundary layer type and testing the validity of proposed empirical relations.

Based on the demonstrated correlations between predictions and experiments for the wide variety of cases, it is felt that this approach should be extended to boundary layers of increased complexity. It is recommended that the approach be extended to the following engineering applications:

1. Turbulent boundary layers with significant thermal gradients should be attacked. It has been demonstrated in Section II above that the

energy equation may be added to the group of governing equations. Some of the data of Thielbahr et al[32] can be used for this purpose. If the wall boundary condition can be successfully modeled, the method could be extended to cover many heat transfer applications of engineering importance.

2. The method should be applied to the analysis of meteorological phenomena such as reactions caused by the air-sea interface and air pollution. The big problem in this application is obtaining sufficient data on the air mass involved. If a typical situation could be scaled down sufficiently to conduct tests in a wind tunnel, measurements could be relatively easily made. Assuming that mathematical models could be found which produced correlations between experiment and theory as good as those in Section IV, full scale experiments could be justified which would lead to possible control of these phenomena.

3. This prediction method should be considered for use in prediction of the effects of thermal and particulate waste diffusion in flowing streams. In this case the flow field is not really a boundary layer as such but actually a free mixing process. Understanding of the diffusion mechanism of the wastes could lead to less effect on the stream ecology or more efficient location of inlet and outlet points for waste disposal systems.

4. A final recommendation which must be made concerns the philosophy of approach to the understanding of turbulent boundary layers. Research in both experimental and analytical investigations into the nature of turbulence should be more clearly related. During the course of this research, numerous situations were encountered in which turbulent boundary layers had been carefully experimentally constructed and measured. However, no hot-wire anemometer measurements had been made. Without these measurements, only secondary comparisons can then be made between experiments and theory. On the other side, an equal number of situations can be sighted where analytical schemes are proposed in which experimental verification of the models used is very difficult if not impossible. If research into the nature of turbulence is to be successful, a conscientious effort must be made to consider experiment and analysis when conducting either.

VI. APPENDICES

Three appendices have been added to this thesis to guide those readers interested in more than a cursory observation of this research.

Appendix A provides the philosophy for arriving at the governing equations for the type of turbulent boundary layer analyzed here. Appendix B describes the transformation of the governing equations used to perform efficient numerical calculation. Appendix C is a FORTRAN listing of the computer program used in the predictions described in the body of the thesis. Copies of the program deck can be made available to those interested in serious application of the prediction method.

APPENDIX A

GOVERNING EQUATIONS OF THE TURBULENT BOUNDARY LAYER

This appendix contains the derivation of the governing equations of a turbulent boundary layer. The finite element used in the derivation of these equations is shown in Figure A-1. The flow is assumed to be "steady" so that there is no variation of a mean fluid property with time.

A. Continuity

The fluid in the turbulent boundary layer is governed by the conservation of mass. Since mass is neither created or destroyed in the boundary layer, an account of the rate of mass entering and leaving an elemental volume can be made.

The rate of mass entering the left face of the element in Figure A-1 is,

$$\rho(2\pi r dy)u \tag{A-1}$$

while the rate of mass entering the inner face of the element is,

$$\rho(2\pi r dx)v \tag{A-2}$$

The rate of mass leaving the element through the right face is,

$$\rho(2\pi r dy)u + \frac{\partial}{\partial x}\left\{\rho(2\pi r dy)u\right\} dx \tag{A-3}$$

while the rate of mass leaving through the outer face is,

$$\rho(2\pi r dx)v + \frac{\partial}{\partial y}\left\{\rho(2\pi r dx)v\right\} dy. \tag{A-4}$$

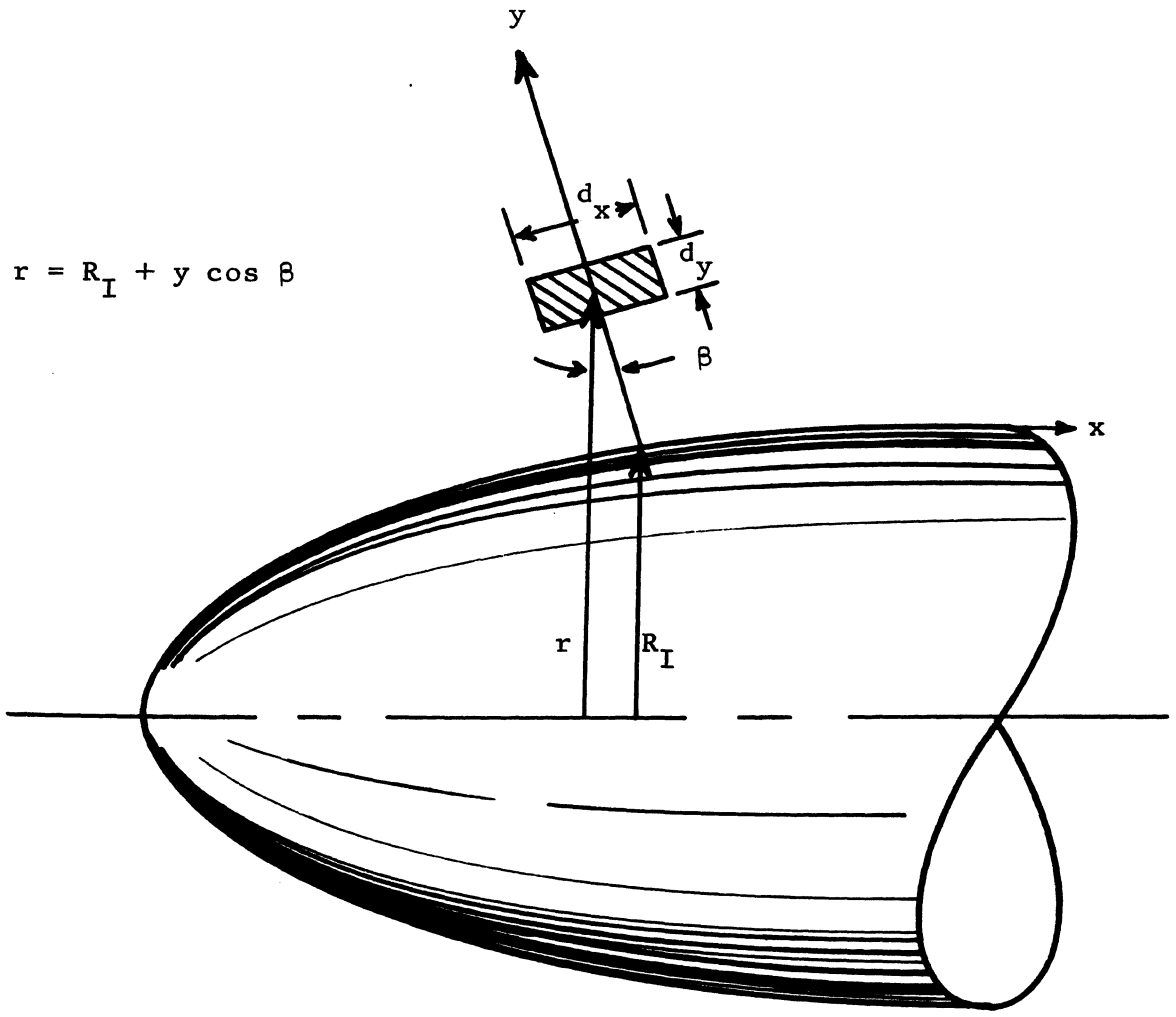

Figure A-1. The Element of Integration

Therefore, the net rate of fluid leaving the element must be zero and,

$$\frac{\partial}{\partial x}(\rho u r) + \frac{\partial}{\partial y}(\rho v r) = 0 \qquad \text{(A-5)}$$

after obvious algebraic manipulation.

The case of planar flow may be thought of as flow over a body of revolution with a very large body radius compared to the boundary layer thickness. In this case,

$$\frac{\partial r}{\partial x} = \frac{\partial r}{\partial y} = 0$$

so that equation A-5 may be reduced to the form

$$\frac{\partial}{\partial x}(\rho u) + \frac{\partial}{\partial y}(\rho v) = 0 \qquad \text{(A-6)}$$

By making use of a "keying" integer α, equations A-5 and A-6 may be handled in the common form,

$$\frac{\partial}{\partial x}\left\{\rho u r^{\alpha}\right\} + \frac{\partial}{\partial y}\left\{\rho v r^{\alpha}\right\} = 0 \qquad \text{(A-7)}$$

where $\alpha = 0$ in the case of planar flows and $\alpha = 1$ in the case of axi-symmetric flows.

B. Longitudinal Momentum

Another governing equation can be obtained by applying Newton's Second Law of Motion in the longitudinal direction. There are pressure, momentum, and shear forces acting in the boundary layer which must be balanced if "steady" motion is to be maintained.

The pressure force on the left face is

$$p2\pi r dy \tag{A-8}$$

while the pressure force on the right face is

$$p2\pi r dy + \frac{\partial}{\partial x}\left\{p2\pi r dy\right\}\ dx \tag{A-9}$$

The longitudinal momentum force at the left face is,

$$\rho u(2\pi r dy)u \tag{A-10}$$

while the longitudinal momentum force at the inner face is,

$$\rho v(2\pi r dx)u \tag{A-11}$$

The longitudinal momentum force at the right face is,

$$\rho u(2\pi r dy)u + \frac{\partial}{\partial x}\left\{\rho u(2\pi r dy)u\right\}\ dx \tag{A-12}$$

while the longitudinal momentum force at the outer face is,

$$\rho v(2\pi r dx)u + \frac{\partial}{\partial y}\left\{\rho v(2\pi r dx)u\right\}\ dy \tag{A-13}$$

The shear force at the inner surface is

$$\tau(2\pi r dx) \tag{A-14}$$

while the shear force at the outer surface is

$$\tau(2\pi r dx) + \frac{\partial}{\partial y}\left\{\tau(2\pi r dx)\right\}\ dy \tag{A-15}$$

The shear forces due to fluid dilation have been assumed to be relatively negligible.

If the flow is "steady", summation of forces in the longitudinal direction must be zero. Therefore, summing Equations A-8 through A-15 and dividing through by 2π dx dy produces,

$$\frac{\partial}{\partial x}\left\{r\rho uu\right\} + \frac{\partial}{\partial y}\left\{r\rho uv\right\} = \frac{\partial}{\partial y}\left\{r\tau\right\} - \frac{\partial}{\partial x}\left(rp\right) \tag{A-16}$$

or,

$$r\rho u \frac{\partial u}{\partial x} + r\rho v \frac{\partial u}{\partial y} + u\left\{\frac{\partial}{\partial x}\left(r\rho u\right) + \frac{\partial}{\partial y}\left(r\rho v\right)\right\} =$$

$$\frac{\partial}{\partial y}\left\{r\tau\right\} - r\frac{dp}{dx} - p\frac{\partial r}{\partial x} \tag{A-17}$$

The last term on the left hand side of Equation A-17 is equal to zero because of the continuity equation. From Figure A-1,

$$r = R_I + y\cos\beta \tag{A-18}$$

Therefore,

$$\frac{\partial r}{\partial x} = \frac{\partial R_I}{\partial x} + y\frac{\partial}{\partial x}\left(\cos\beta\right) \tag{A-19}$$

Assuming that R_I and cos β vary relatively slowly in the longitudinal direction, then $\partial r/\partial x \approx 0$. Equation A-17 may then be written as,

$$\rho u \frac{\partial u}{\partial x} + \rho v \frac{\partial u}{\partial y} = r^{-\alpha}\frac{\partial}{\partial y}\left(r^{\alpha}\tau\right) - \frac{dp}{dx} \tag{A-20}$$

Assuming that the pressure does not vary across the boundary layer and that the shear may be described by an effective viscosity ϵ, the longitudinal momentum Equation A-20 becomes,

$$\rho u \frac{\partial u}{\partial x} + \rho v \frac{\partial u}{\partial y} = r^{-\alpha} \frac{\partial}{\partial y} \left(r^{\alpha} \epsilon \frac{\partial u}{\partial y}\right) - \frac{dp}{dx} \qquad \text{(A-21)}$$

C. Conservation of Energy

When boundary layers with significant temperature gradients are analyzed, conservation of energy produces an additional governing equation. In the following derivation, diffusion of energy in the cross stream direction is assumed to be much larger than diffusion in the streamwise direction.

The total enthalpy of the fluid is assumed to be composed of four parts: (1) the static enthalpy due to temperature, (2) the kinetic energy due to the mean velocity, (3) the kinetic energy due to the fluctuating velocity, and (4) chemical energy released during chemical reaction.

$$\bar{h} = h + \frac{u^2}{2} + k + \sum_{j=1}^{n} h_j c_j \qquad \text{(A-22)}$$

where:

$\bar{h}$ = Stagnation enthalpy

h = Static enthalpy

u = Mean velocity

k = Turbulence kinetic energy

h_j = Enthalpy of reaction for species j

c_j = Concentration of species j

The net energy convected out of the differential element by the mean flow velocity is,

$$2\pi \, dx \, dy \left\{ \frac{\partial}{\partial x} (r\rho u\bar{h}) + \frac{\partial}{\partial y} (r\rho v\bar{h}) \right\} \tag{A-23}$$

By applying the continuity equation, Equation A-23 may be reduced to,

$$2\pi \, dx \, dy \left\{ r\rho u \frac{\partial \bar{h}}{\partial x} + r\rho v \frac{\partial \bar{h}}{\partial y} \right\} \tag{A-24}$$

The net diffusion of energy out of the differential element due to a static enthalpy gradient may be written as,

$$-2\pi \, dx \, dy \frac{\partial}{\partial y} \left\{ \frac{\epsilon}{\sigma_h} r \frac{\partial h}{\partial y} \right\} \tag{A-25}$$

where ϵ/σ_h is defined as the exchange coefficient of heat flux. σ_h may be thought of as an effective Prandtl number. Equation A-25 may be expanded using Equation A-22 to,

$$-2\pi \, dx \, dy \frac{\partial}{\partial y} \left\{ \frac{\epsilon}{\sigma_h} r \left(\frac{\partial \bar{h}}{\partial y} - \frac{\partial (u^2/2)}{\partial y} - \frac{\partial k}{\partial y} - \sum_{j=1}^{n} h_j \frac{\partial C_j}{dy} \right) \right\} \tag{A-26}$$

The net diffusion of energy out of the differential element due to the turbulence kinetic energy gradient may be written as,

$$-2\pi \, dx \, dy \frac{\partial}{\partial y} \left\{ \frac{\epsilon}{\sigma_k} r \frac{\partial k}{\partial y} \right\} \tag{A-27}$$

where ϵ/σ_k is defined as the exchange coefficient of the turbulence kinetic energy flux.

The net diffusion of energy out of the differential element due to the reacting species gradient may be written as,

$$-2\pi\, dx\, dy \frac{\partial}{\partial y} \left\{ \sum_{j=1}^{n} \frac{\epsilon}{\sigma_{c_j}} r h_j \frac{\partial c_j}{dy} \right\} \qquad \text{(A-28)}$$

where ϵ/σ_{c_j} is defined as the exchange coefficient of the reacting species flux. σ_{c_j} may be thought of as an effective Lewis number for the reacting species.

By setting the sum of Equations A-24 through A-28 equal to zero in order to satisfy the first law of thermodynamics, the energy equation may be written as,

$$\rho u \frac{\partial \bar{h}}{\partial x} + \rho v \frac{\partial \bar{h}}{\partial y} = r^{-\alpha} \frac{\partial}{\partial y} \left\{ \frac{r^{\alpha} \epsilon}{\sigma_h} \left(\frac{\partial \bar{h}}{\partial y} + \left[\frac{\sigma_h}{\sigma_k} - 1 \right] \frac{\partial k}{\partial y} \right. \right.$$

$$\left. \left. + \sum_{j=1}^{n} \left[\frac{\sigma_h}{\sigma_{c_j}} - 1 \right] \frac{\partial c_j}{\partial y} + \left[\sigma_h - 1 \right] \frac{\partial (u^2/2)}{\partial y} \right) \right\} \qquad \text{(A-29)}$$

D. Turbulence Kinetic Energy

The turbulence kinetic energy equation is normally obtained by multiplying each momentum equation by the velocity in that direction, time averaging and then summing the modified momentum equations together. A different approach will be used here. In applying the turbulence kinetic energy to boundary layer prediction the assumption is made that turbulence kinetic energy is a dependent variable quantity of the flow which must be conserved. It may be convected, diffused, generated, and dissipated but it must be accounted for so that the net amount in evidence at any point in the boundary layer can be determined.

The net amount of turbulence kinetic energy convected out of the control volume is, (see Figure A-1 for coordinate system and Equation 22 for definition of k)

$$2\pi \, dx \, dy \, \frac{\partial}{\partial x} (\rho urk) + 2\pi \, dx \, dy \, \frac{\partial}{\partial y} (\rho vrk)$$

or

$$2\pi \, dx \, dy \left\{ \rho ur \, \frac{\partial k}{\partial x} + \rho vr \, \frac{\partial k}{\partial y} + k \left[\frac{\partial}{\partial x} (\rho ur) + \frac{\partial}{\partial y} (\rho vr) \right] \right\}$$

which on application of the continuity equation becomes,

$$2\pi r \, dx \, dy \left\{ \rho u \, \frac{\partial k}{\partial x} + \rho v \, \frac{\partial k}{\partial y} \right\} \qquad \text{(A-30)}$$

The net amount of turbulence kinetic energy diffused from the control volume is

$$2\pi \, dx \, dy \, \frac{\partial}{\partial y} (r \, J_k)$$

where J_k is the diffusional flux of turbulence kinetic energy in the y direction. Assuming that the diffusional flux can be represented by a diffusion coefficient and the turbulence kinetic energy gradient in that direction, i.e.

$$J_k = - \frac{\epsilon}{\sigma_k} \frac{\partial k}{\partial y}$$

then, the net diffusion of turbulence kinetic energy out of the control volume may be written as

$$-2\pi \, dx \, dy \, \frac{\partial}{\partial y} \left(r \, \frac{\epsilon}{\sigma_k} \, \frac{\partial k}{\partial y} \right) \qquad \text{(A-31)}$$

Describing the dissipation of turbulence kinetic energy in terms of a rate per unit volume per unit time, the dissipation of turbulence kinetic energy within the control volume may be written as

$$2\pi r \, dx \, dy \, D_k \tag{A-32}$$

Turbulence kinetic energy is generated by the mean velocity gradient of the flow. If G_k is defined as the rate of generation of turbulence kinetic energy per unit volume, per unit of time, per unit of velocity gradient, the generation within the control volume may be written as

$$2\pi r \, dx \, dy \, G_k \left(\frac{\partial u}{\partial x} + \frac{\partial v}{\partial y} + \frac{\partial u}{\partial y} + \frac{\partial v}{\partial x}\right)$$

but $\frac{\partial u}{\partial y}$ is much larger than the other three gradients so that the generation term becomes,

$$2\pi r \, dx \, dy \, G_k \frac{\partial u}{\partial y} \, . \tag{A-33}$$

Summation of Equations A-30 through A-33 then creates the conservation of turbulence kinetic energy equation as

$$\rho u \frac{\partial k}{\partial x} + \rho v \frac{\partial k}{\partial y} = \frac{1}{r} \frac{\partial}{\partial y} \left(r \frac{\epsilon}{\sigma_k} \frac{\partial k}{\partial y}\right) - D_k + G_k \frac{\partial u}{\partial y} \, .$$

However, $G_k = \frac{\partial u}{\partial y}$ consistent with the formulation of ϵ in the streamwise momentum equation. Therefore,

$$\rho u \frac{\partial k}{\partial x} + \rho v \frac{\partial k}{\partial y} = \frac{1}{r} \frac{\partial}{\partial y} \left(r \frac{\epsilon}{\sigma_k} \frac{\partial k}{\partial y}\right) + \epsilon \left(\frac{\partial u}{\partial y}\right)^2 - D_k \tag{A-34}$$

APPENDIX B

TRANSFORMATION OF THE GOVERNING EQUATIONS

This appendix explains the coordinate transformations used to simplify the governing equations. A general equation, typical in form to each of the governing equations is carried through two transformations to the final form.

A. The Von Mises Transformation

All of the governing equations with the exception of the continuity equation may be written in the general form (see Appendix A):

$$\rho u \frac{\partial \varphi}{\partial x} + \rho v \frac{\partial \varphi}{\partial y} = r^{\alpha} \frac{\partial}{\partial y} \left(r^{\alpha} D_c \frac{\partial \varphi}{\partial y} \right) + R_c \qquad \text{(B-1)}$$

where φ represents the dependent variable of interest, D_c represents the diffusion coefficient for this equation and R_e represents the remaining terms of the equation.

The first transformation is a stretching of the y coordinate used to incorporate the solution of the continuity equation with each dependent variable equation. The continuity equation is:

$$\frac{\partial}{\partial x} (\rho u r^{\alpha}) + \frac{\partial}{\partial y} (\rho v r^{\alpha}) = 0 \qquad \text{(B-2)}$$

Let a stream function Ψ be defined such that,

$$\frac{\partial \Psi}{\partial x} = -\rho v r^{\alpha} \qquad \text{and} \qquad \frac{\partial \Psi}{\partial y} = \rho u r^{\alpha} \qquad \text{(B-3)}$$

Substitution of B3 into B2 shows that this stream function will satisfy the continuity equation.

The general Equation B1 is then transformed from the x, y coordinate system to the x, Ψ coordinate system by stretching the y coordinate, thus -

$$\frac{\partial}{\partial x} = \frac{\partial}{\partial x}\frac{\partial x}{\partial x} + \frac{\partial}{\partial \Psi}\frac{\partial \Psi}{\partial x} = \frac{\partial}{\partial x} - \rho v r^{\alpha}\frac{\partial}{\partial \Psi}$$

$$\frac{\partial}{\partial y} = \frac{\partial}{\partial x}\frac{\partial x}{\partial y} + \frac{\partial}{\partial \Psi}\frac{\partial \Psi}{\partial y} = \rho u r^{\alpha}\frac{\partial}{\partial \Psi} \qquad \text{(B-4)}$$

Therefore, the transformation of B1 using B4 results in

$$\rho u\left\{\frac{\partial \varphi}{\partial x} - \rho v r^{\alpha}\frac{\partial \varphi}{\partial \Psi}\right\} + \rho v\left\{\rho u r^{\alpha}\frac{\partial \varphi}{\partial \Psi}\right\} = r^{-\alpha}\rho u r^{\alpha}\frac{\partial}{\partial \Psi}$$

$$\left\{r^{\alpha} D_c \rho u r^{\alpha}\frac{\partial \varphi}{\partial \Psi}\right\} + R_e \qquad \text{(B-5)}$$

or

$$\frac{\partial \varphi}{\partial x} = \frac{\partial}{\partial \Psi}\left\{D_c \rho u r^{2\alpha}\frac{\partial \varphi}{\partial \Psi}\right\} + \frac{R_e}{\rho u} \qquad \text{(B-6)}$$

B. The Nondimensional Stream Function Transformation

To make the computation as efficient as possible it is desirable that the computation net expand or contract with the physical boundary layer. This has been accomplished in this case by defining a nondimensional stream function ω as,

$$\omega = \frac{\Psi - \Psi_I}{\Psi_E - \Psi_I} \qquad \text{(B-7)}$$

where Ψ_E is the stream function at the outer edge of the boundary layer and Ψ_I is the stream function at the inner edge of the boundary layer. The effect then is to nondimensionalize the cross stream variable. Therefore,

$$\frac{\partial}{\partial x} = \frac{\partial}{\partial x}\frac{\partial x}{\partial x} + \frac{\partial}{\partial \omega}\frac{\partial \omega}{\partial x} = \frac{\partial}{\partial x} + \frac{\partial \omega}{\partial x}\frac{\partial}{\partial \omega}$$

$$\frac{\partial}{\partial \Psi} = \frac{\partial}{\partial x}\frac{\partial x}{\partial \Psi} + \frac{\partial}{\partial \omega}\frac{\partial \omega}{\partial \Psi} = \frac{\partial \omega}{\partial \Psi}\frac{\partial}{\partial \omega} \qquad \text{(B-8)}$$

but $$\frac{\partial \omega}{\partial \Psi} = \frac{1}{\Psi_E - \Psi_I} \qquad \text{(B-9)}$$

and $$\frac{\partial \omega}{\partial x} = \frac{(\Psi_E - \Psi_I)\ (-\partial \Psi_I/\partial x) - (\Psi - \Psi_I)\ (\frac{\partial \Psi_E}{\partial x} - \partial \Psi_I/\partial x)}{(\Psi_E - \Psi_I)^2}$$

or $$\frac{\partial \omega}{\partial x} = \frac{\rho_I v_I r_I^{\alpha} - \omega\ (\rho_I v_\rho r_I^{\alpha})}{\Psi_E - \Psi_I}$$

so that

$$\frac{\partial}{\partial x} = \frac{\partial}{\partial x} + \left\{\frac{\rho_I v_I r_I^{\alpha} - \omega\ (\rho_I v_I r_I^{\alpha} - \rho_E v_E r_E^{\alpha})}{\Psi_E - \Psi_I}\right\}\frac{\partial}{\partial \omega}$$

$$\frac{\partial}{\partial \Psi} = \frac{1}{\Psi_E - \Psi_I}\frac{\partial}{\partial \omega} \qquad \text{(B-10)}$$

Applying transformation equations B10 to equation B6 gives:

$$\frac{\partial \varphi}{\partial x} + \left\{\frac{\rho_I v_I r_I^{\alpha} - \omega(\rho_I v_I r_I^{\alpha} - \rho_E v_E r_E^{\alpha})}{\Psi_E - \Psi_I}\right\}\frac{\partial \varphi}{\partial \omega} =$$

$$\frac{1}{\Psi_E - \Psi_I}\frac{\partial}{\partial \omega}\left\{\frac{D_c \rho u r^{2\alpha}}{\Psi_E - \Psi_I}\frac{\partial \varphi}{\partial \omega}\right\} + \frac{R_e}{\rho u} \qquad \text{(B-11)}$$

and by defining $\dot{m} = \rho v$, equation B11 may be written in its final form as:

$$\frac{\partial \varphi}{\partial x} + \left\{\frac{r_I^{\alpha}\dot{m}_I - \omega\ (r_I^{\alpha}\dot{m}_I - r_E^{\alpha}\dot{m}_E)}{\Psi_E - \Psi_I}\right\}\frac{\partial \varphi}{\partial \omega} =$$

$$\frac{\partial}{\partial \omega}\left\{\frac{D_c \rho u r^{2\alpha}}{(\Psi_E - \Psi_I)^2}\frac{\partial \varphi}{\partial \omega}\right\} + \frac{R_e}{\rho u} \qquad \text{(B-12)}$$

APPENDIX C

COMPUTER PROGRAM FOR SOLUTION OF THE PARABOLIC BOUNDARY LAYER EQUATIONS

```
      COMMON /MXFER/BLOW
      COMMON/DUDYF/DUDY25,ISLO,DUDY50,ISLO5
      COMMON /GEN/PEI,AMI,AME,DPDX,PREF(3),PR(3),P(3),DEN,
     1AMU,XU,XD,XP,XL,DX,INTG,CSALFA,XPCG
     1/I/N,NP1,NP2,NP3,NEQ,NPH,KEX,KIN,KASE,KRAD,KPRAN
     1/B/BETA,GAMA(3),TAUI,TAUE,AJI(3),AJE(3),INDI(3),
     1INDE(3)
     1/V/U(43),F(3,43),R(43),RHO(43),OM(43),Y(43)
     1/C/SC(43),AU(43),BU(43),CU(43),A(3,43),B(3,43),C(3,43)
     1/L1/YL,UMAX,UMIN,FR,YIP,YEM
      COMMON/PR/UGU,UGD
      COMMON /L/AK,ALMG
      COMMON/AUXP/TEMPE(43),TEMP(43),PO(43),AMACH(43)
      COMMON/BAR/GABAR(43),RBAR(43)
      COMMON/AUXY/YY(43),XXU,RR1
      COMMON  /SHEAR/ SHEAR(43),SCSH(43)
      COMMON /ASD/ ASD1,ASD2
      COMMON /IDIN/ INDIC
      COMMON/DUD/DUDOM(43), DUDY(43), ADUDY(43), ADUDYM
      COMMON/DCON/DXC
      COMMON /KE/ AKEM
      COMMON/STORE/OLDU(43)
      COMMON /FREE/FREVEL(35)
      COMMON /TAUW/CFW(35)
      COMMON /IJAN/TDUDY,MTKE
      COMMON/WRITE/OUT(7)
      INDIC=0
      READ (5,8000) NCASE
8000  FORMAT(2I5)
   16 CONTINUE
      INDIC=INDIC+1
      X = 0.0
      INTG=0
      AKEM=0.0
      YL=0.01
      IOUT=1
      CALL CONST
      CALL BEGIN
      UGU=U(NP3)
      UGD=UGU
      AMI=0.
      AME=0.
      GO TO 25
   15 CALL READY
   25 CONTINUE
      CALL CDUDOM(U,OM,DUDOM)
      INTG=INTG+1
      CALL LENGTH
```

```
      CALL SHEARS
      CALL ENTRN
C
C  CHOICE OF FORWARD STEP
      FRA=.05
      DXCN=.4+DXC
      DXA=DXCN*YL
      IF(AMI.EQ.0..AND.AME.EQ.0.) GO TO 1000
      DX=ABS(FRA   *PEI/(R(1)*AMI-R(NP3)*AME)
      IF(DX.GT.DXA) GO TO 1000
      IF (DX.LT.0.) GO TO 85
      GO TO 1001
 1000 DX=DXA
1001  XD=XU+DX
      IF(XD.LT.OUT(IOUT).OR.XU.EQ.OUT(IOUT)) GO TO 77
      XD=OUT(IOUT)
      DX=XD-XU
   77 CONTINUE
C
C     CALCULATES CHANGE IN FREE STREAM VELOCITY
      CALL FREEU(XU,XD,UGU,UGD)
      U(NP3)=UGD
      CALL PRE(XU,XD,DPDX)
      IF(KASE.EQ.2) GO TO 26
      IF(KIN.EQ.1)CALL MASS(XU,XD,AMI)
      IF(KEX.EQ.1)CALL MASS(XU,XD,AME)
      CALL WALL
   26 XXU=12.0*XU
      RR1=12.0*R(1)
      DO 90  I=1,NP3
      OLDU(I)=U(I)
   90 YY(I)=12.0*Y(I)
      CALL FUGA2(F,Y,DUDY,YL,NP1,TDUDY,MTKE)
      DUDY25=TDUDY
      ISLO=MTKE
C
      CALL COEFF
      IF(XU.LT.OUT(IOUT)) GO TO 555
      CALL OUTPUT
      IOUT=IOUT+1
  555 CONTINUE
      CALL SOLVE(AU,BU,CU,U,NP3)
C  SETTING UP VELOCITIES AT A SYMMETRY LINE
      IF(KIN.NE.3) GO TO 71
      U(1)=U(2)
      IF(KRAD.EQ.0)U(1)=.75*U(2)+.25*U(3)
   71 IF(KEX.EQ.3)U(NP3)=.75*U(NP2)+.25*U(NP1)
   72 CONTINUE
```

```
      IF(NEQ.EQ.1) GO TO 30
      DO 45 J=1,NPH
      IF(J.EQ.1)CALL TKEW(XD,U(NP3),F(1,1))
      DO 46 I=2,NP2
      AU(I)=A(J,I)
      BU(I)=B(J,I)
   46 CU(I)=C(J,I)
      DO 47 I=1,NP3
   47 SC(I)=F(J,I)
      CALL SOLVE(AU,BU,CU,SC,NP3)
      IF(J.NE.1) GO TO 1002
      DO 1003 JJ=1,NP3
1003  IF(SC(JJ).LT.0.) SC(JJ)=0.
1002  CONTINUE
      DO 48 I=1,NP3
   48 F(J,I)=SC(I)
      IF(KASE.EQ.2) GO TO 81
C
C  SETTING UP WALL VALUES OF F
      IF(J.EQ.1) GO TO 50
      IF(KIN.EQ.1.AND.INDI(J).EQ.2)F(J,1)=((1.+BETA+GAMA(J))
     1*F(J,2)-(1.+BETA-GAMA(J))*F(J,3))*.5/GAMA(J)
      IF(KEX.EQ.1.AND.INDE(J).EQ.2)F(J,NP3)=((1.+BETA+
     1GAMA(J))*F(J,NP2)-(1.+BETA-GAMA(J))*F(J,NP1))*.5/
     2GAMA(J)
      GO TO 51
   50 CALL TKEW(XD,U(NP3),F(1,1))
   51 CONTINUE
C  SETTING UP SYMMETRY-LINE VALUES OF F
   81 IF(KIN.NE.3) GO TO 82
      F(J,1)=F(J,2)
      IF(KRAD.EQ.0)F(J,1)=.75*F(J,2)+.25*F(J,3)
   82 IF(KEX.EQ.3)F(J,NP3)=.75*F(J,NP2)+.25*F(J,NP1)
   45 CONTINUE
   30 XP=XU
      XU=XD
      UGU=UGD
C
C     CALCULATION OF AUXILLARY PARAMETERS
      CALL DENSTY
      PEI=PEI+DX*(R(1)*AMI-R(NP3)*AME)
C  THE TERMINATION CONDITION
      IF(OUT(IOUT).EQ.0..AND.XP.NE.0.) GO TO 85
      IF(IOUT.EQ.8) GO TO 85
      IF(XU.LT.XL)GO TO 15
      IF(XU.GE.XL)GO TO 85
      GO TO 16
   85 CONTINUE
```

```
      IF (INDIC.NE.NCASE) GO TO 16
      CALL EXIT
      END
      SUBROUTINE BEGIN
      COMMON /MXFER/BLOW
      COMMON/WRITE/OUT(7)
      COMMON /L1/YL,UMAX,UMIN,FR,YIP,YEM
      COMMON /FREE/FREVEL(35)
      COMMON /GEN/PEI,AMI,AME,DPDX,PREF(3),PR(3),P(3),DEN,
     1AMU,XU,XD,XP,XL,DX,INTG,CSALFA,XPCG
     1/I/N,NP1,NP2,NP3,NEQ,NPH,KEX,KIN,KASE,KRAD,KPRAN
     1/B/BETA,GAMA(3),TAUI,TAUE,AJI(3),AJE(3),INDI(3),
     1INDE(3)
     1/V/U(43),F(3,43),R(43),RHO(43),OM(43),Y(43)
      COMMON/AUXP/TEMPE(43),TEMP(43),PO(43),AMACH(43)
      COMMON/BAR/GABAR(43),RBAR(43)
      COMMON /XPLOT/NPLOT
      COMMON /ASD/ ASD1,ASD2
      COMMON /L/AK,ALMG
      COMMON  /SHEAR/ SHEAR(43),SCSH(43)
      COMMON/DCON/DXC
      COMMON /COM/COMT(80)
      COMMON /TAUW/CFW(35)
C   PROBLEM SPECIFICATION
      READ(5,8001)(COMT(I),I=1,80)
8001  FORMAT(20A4)
      READ (5,42) KRAD,KIN,KEX,NEQ,N,INTKE,KPRAN,KSST,KSEV
   42 FORMAT (9I5)
      READ (5,43) XL,XPCG,ASD1,ASD2,ALMG,PREF(1),PREF(2),
     1PREF(3),DXC,SHS,BLOW
   43 FORMAT (11E5.0)
   44 FORMAT (2E10.0)
      KASE=2
      IF(KIN.EQ.1.OR.KEX.EQ.1)KASE=1
      XU=0.
      NPH=NEQ-1
      NP1=N+1
      NP2=N+2
      NP3=N+3
C   INITIAL VELOCITY PROFILE
      READ (5,444) Y(1), (Y(I), I=3,NP1), Y(NP3)
      READ (5,444) U(1), (U(I), I=3,NP1), U(NP3)
      IF(INTKE.EQ.0) READ(5,444)(F(1,I),I=1,21)
      IF(INTKE.NE.0)READ(5,444)F(1,1),(F(1,I),I=3,NP1),
     1F(1,NP3)
      IF(NEQ.GE.3)READ(5,444)F(2,1),(F(2,I),I=3,NP1),
     1F(2,NP3)
C     F(2,I) ARE STAGNATION TEMPERATURES IN RANKINE
```

```
      IF(NEQ.LT.3) GO TO 113
      DO 112 I=1,NP3
  112 F(2,I)=F(2,I)*6000.
113   CONTINUE
  444 FORMAT (7F10.5)
      Y(  1)=Y(  1)/12.
      DO 111 I=3,NP1
      Y(I)=Y(I)/12.
  111 CONTINUE
      Y(NP3)=Y(NP3)/12.
      READ(5,444)FREVEL,CFW
      READ(5,444) OUT
      DO 302 KK=1,7
  302 OUT(KK)=OUT(KK)/12.
      CALL LENGTH
      IF(INTKE.NE.0) GO TO 446
      CALL TKEW(XU,U(NP3),F(1,1))
      CALL GOTKE(U,Y,YL,NP1,F)
  446 CONTINUE
C  CALCULATION OF SLIP VELOCITIES AND DISTANCES
      BETA=.143
      GO TO (71,72,73),KIN
   71 U(2)=U(3)/(1.+2.*BETA)
      Y(2)=Y(3)*BETA/(2.+BETA)
      GO TO 74
   72 U11=U(1)*U(1)
      U13=U(1)*U(3)
      U33=U(3)*U(3)
      SQ=84.*U11-12.*U13+9.*U33
      U(2)=(16.*U11-4.*U13+U33)/(2.*(U(1)+U(3))+SQRT(SQ))
      Y(2)=Y(3)*(U(2)+U(3)-2.*U(1))*.5/(U(2)+U(3)+U(1))
      GO TO 74
   73 IF(KRAD.NE.0) GO TO 89
      U(2)=(4.*U(1)-U(3))/3.
      Y(2)=0.
      GO TO 74
   89 U(2)=U(1)
      Y(2)=Y(3)/3.
   74 GO TO (75,76,77),KEX
   75 U(NP2)=U(NP1)/(1.+2.*BETA)
      Y(NP2)=Y(NP3)-(Y(NP3)-Y(NP1))*BETA/(2.+BETA)
      GO TO 78
   76 U(NP2)=U(NP3)
      Y(NP2)=Y(NP3)-(Y(NP3)-Y(NP1))*(U(NP2)+U(NP1)-2.*U(NP3)
     1)*.5/(U(NP2)+U(NP1)+U(NP3))
      GO TO 78
   77 U(NP2)=(4.*U(NP3)-U(NPI))/3.
      Y(NP2)=Y(NP3)
```

```
   78 CONTINUE
      IF(NEQ.EQ.1) GO TO 45
C     CALCULATION OF OTHER DEPENDENT VARIABLE SLIP VALUES
      DO 88 J=1,NPH
      GAMA(J)=.143
C*********
C     LINEAR VARIATION OF TKE AND Y NEAR THE WALL
      IF(J.EQ.1) GAMA(J)=1.
C*********
      GO TO (81,82,83),KIN
   81 F(J,2)=F(J,1)+(F(J,3)-F(J,1))*(1.+BETA-GAMA(J))/(1.+
     1BETA+GAMA(J))
      GO TO 84
   82 G=(U(2)+U(3)-8.*U(1))/(5.*(U(2)+U(3))+8.*U(1))
      GF=(1.-PREF(J))/(1.+PREF(J))
      GF=(G+GF)/(1.+G*GF)
      F(J,2)=F(J,3)*GF+(1.-GF)*F(J,1)
      GO TO 84
   83 F(J,2)=F(J,1)
      IF(KRAD.EQ.0)F(J,2)=(4.*F(J,1)-F(J,3))/3.
   84 GO TO (85,86,87),KEX
   85 F(J,NP2)=F(J,NP3)+(F(J,NP1)-F(J,NP3))*(1.+BETA-GAMA(J)
     1)/(1.+BETA-GAMA(J))
      GO TO 88
   86 G=(U(NP2)+U(NP1)-8.*U(NP3))/(5.*(U(NP2)+U(NP1))+8.*
     1U(NP3))
      GF=(1.-PREF(J))/(1.+PREF(J))
      GF=(G+GF)/(1.+G*GF)
      F(J,NP2)=F(J,NP1)*GF+(1.-GF)*F(J,NP3)
      GO TO 88
   87                 F(J,NP2)=(4.*F(J,NP3)-F(J,NP1))/3.
   88 CONTINUE
   45 CONTINUE
      CALL DENSTY
C  CALCULATION OF RADII
      CALL RAD(XU,R(1),CSALFA)
      IF(CSALFA.EQ.0..OR.KRAD.EQ.0) GO TO 27
      DO 28 I=2,NP3
   28 R(I)=R(1)+Y(I)*CSALFA
      GO TO 29
   27 DO 30 I=2,NP3
   30 R(I)=R(1)
   29 CONTINUE
C  CALCULATION OF OMEGA VALUES
      OM(1)=0.
      OM(2)=0.
      DO 49 I=3,NP2
   49 OM(I)=OM(I-1)+.5*(RHO(I)*U(I)*R(I)+RHO(I-1)*U(I-1)*
```

```
     1R(I-1))*(Y(I)-Y(I-1))
      PEI=OM(NP2)
      DO 59 I=3,NP1
   59 OM(I)=OM(I)/PEI
      OM(NP2)=1.0
      OM(NP3)=1.
      IF(NEQ.EQ.1)RETURN
      DO 69 J=1,NPH
      IF(KEX.EQ.1)INDE(J)=1
      IF(KIN.EQ.1) INDI(J)=1
   69 CONTINUE
      DO 1 J=1,NPH
1     P(J) = 3.68*(PR(J)/PREF(J)-1.0)*((PR(J)/PREF(J))**
     1(-.25))
      RETURN
      END
      SUBROUTINE CDUDOM(U,OM,DUDOM)
      REAL U(43),OM(43),DUDOM(43)
      COMMON/I/N,NP1,NP2,NP3,NEQ,NPH,KEX,KIN,KASE,KRAD,KPRAN
C     COMPUTES THE VELOCITY GRADIENT IN NON-DIMENSIONAL
C     STREAM FUNCTION COORDINATE FROM A SECOND ORDER FIT OF
C     THE NEAREST THREE POINTS.
      DO 1 I=3,NP1
      A2=((U(I+1)-U(I-1))/(OM(I+1)-OM(I-1))-(U(I)-U(I-1))/
     1(OM(I)-OM(I-1)))/(OM(I+1)-OM(I))
      A1=-(OM(I)+OM(I-1))*A2+(U(I)-U(I-1))/(OM(I)-OM(I-1))
    1 DUDOM(I)=A1+2.*A2*OM(I)
      DUDOM(2)=(U(1)-U(3))/(OM(1)-OM(3))
      GO TO (2,3,3),KIN
    2 DUDOM(1)=DUDOM(2)
      GO TO 4
    3 DUDOM(1)=0.
    4 DUDOM(NP2)=(U(NP1)-U(NP3))/(OM(NP1)-OM(NP3))
      DUDOM(NP3)=0.
      RETURN
      END
      SUBROUTINE COEFF
      COMMON /GEN/PEI,AMI,AME,DPDX,PREF(3),PR(3),P(3),DEN,
     1AMU,XU,XD,XP,XL,DX,INTG,CSALFA,XPCG
     1/I/N,NP1,NP2,NP3,NEQ,NPH,KEX,KIN,KASE,KRAD,KPRAN
     1/B/BETA,GAMA(3),TAUI,TAUE,AJI(3),AJE(3),INDI(3),
     1INDE(3)
     1/V/U(43),F(3,43),R(43),RHO(43),OM(43),Y(43)
     1/C/SC(43),AU(43),BU(43),CU(43),A(3,43),B(3,43),C(3,43)
      COMMON /L/AK,ALMG
      COMMON/MXMN/RHUMX,RHUMN,RHU(43),AL
      COMMON  /SHEAR/ SHEAR(43),SCSH(43)
      COMMON/DUD/DUDOM(43), DUDY(43), ADUDY(43), ADUDYM
```

```
      COMMON /RUH/ RAAUH(43)
      COMMON/DUDYF/DUDY25,ISLO,DUDY50,ISLO5
      DIMENSION G1(43),G2(43),G3(43),D(3,43),S1(43),S2(43),
     1S3(43)
C   CALCULATION OF SMALL C 'S
      DO 99 I=2,NP1
      RA=.5*(R(I+1)+R(I))
      RH=.5*(RHO(I+1)+RHO(I))
      UM=.5*(U(I+1)+U(I))
      CALL VEFF(I,I+1,EMU)
   99 SC(I)=RA*RA*RH*UM*EMU/PEI/PEI
C   THE CONVECTION TERM
      SA=R(1)*AMI/PEI
      SB=(R(NP3)*AME-R(1)*AMI)/PEI
      DX=XD-XU
      DO 71 I=3,NP1
      OMD=OM(I+1)-OM(I-1)
      P2=.25/DX
      P3=P2/OMD
      P1=(OM(I+1)-OM(I))*P3
      P3=(OM(I)-OM(I-1))*P3
      P2=3.*P2
      Q=SA/OMD
      R2=-SB*.25
      R3=R2/OMD
      R1=-(OM(I+1)+3.*OM(I))*R3
      R3=(OM(I-1)+3.*OM(I))*R3
      G1(I)=P1+Q+R1
      G2(I)=P2+R2
      G3(I)=P3-Q+R3
      CU(I)=-P1*U(I+1)-P2*U(I)-P3*U(I-1)
C   THE DIFFUSION TERM
      AU(I)=2./OMD
      BU(I)=SC(I-1)*AU(I)/(OM(I)-OM(I-1))
      AU(I)=SC(I)*AU(I)/(OM(I+1)-OM(I))
      IF(NEQ.EQ.1) GO TO 33
      DO 34 J=1,NPH
      C(J,I)=-P1*F(J,I+1)-P2*F(J,I)-P3*F(J,I-1)
      CALL SOURCE(J,I,CS,D(J,I))
      C(J,I)=-C(J,I)+CS-F(J,I)*D(J,I)
      A(J,I)=AU(I)/PREF(J)
      B(J,I)=BU(I)/PREF(J)
   34 CONTINUE
C   SOURCE TERM FOR VELOCITY EQUATION
   33 PHI = 0.0
      S1(I) = (DPDX + PHI)*DX
      S2(I)=P2*S1(I)/(RHO(I)*U(I))
      S3(I)=P3*S1(I)/(RHO(I-1)*U(I-1))
```

```
      S1(I)=P1*S1(I)/(RHO(I+1)*U(I+1))
      CU(I)=-CU(I)-2.*(S1(I)+S2(I)+S3(I))
      S1(I)=S1(I)/U(I+1)
      S2(I)=S2(I)/U(I)
      S3(I)=S3(I)/U(I-1)
   71 CONTINUE
C  COEFFICIENTS IN THE FINAL FORM
      DO 91 I=3,NP1
      RL=1./(G2(I)+AU(I)+BU(I)-S2(I))
      AU(I)=(AU(I)+S1(I)-G1(I))*RL
      BU(I)=(BU(I)+S3(I)-G3(I))*RL
   91 CU(I)=CU(I)*RL
      IF(NEQ.EQ.1) GO TO 76
      DO 92 J=1,NPH
      DO 92 I=3,NP1
      RL=1./(G2(I)+A(J,I)+B(J,I)-D(J,I))
      A(J,I)=(A(J,I)-G1(I))*RL
      B(J,I)=(B(J,I)-G3(I))*RL
   92 C(J,I)=C(J,I)*RL
   76 CALL SLIP
      RETURN
      END
      SUBROUTINE CONST
      COMMON /GEN/PEI,AMI,AME,DPDX,PREF(3),PR(3),P(3),DEN,
     1AMU,XU,XD,XP,XL,DX,INTG,CSALFA,XPCG
      COMMON /L/AK,ALMG
     1/I/N,NP1,NP2,NP3,NEQ,NPH,KEX,KIN,KASE,KRAD,KPRAN
     1/L1/YL,UMAX,UMIN,FR,YIP,YEM
      COMMON /ASD/ASD1,ASD2
      AK=.4
      AK=.435
      FR=.01
      PR(1)=.7
      PR(1)=1.
      PR(2)=.7
      PR(3) = 0.35
      AMU = 0.000012
      RETURN
      END
      SUBROUTINE DENSTY
      COMMON /GEN/PEI,AMI,AME,DPDX,PREF(3),PR(3),P(3),DEN,
     1AMU,XU,XD,XP,XL,DX,INTG,CSALFA,XPCG
     1/V/U(43),F(3,43),R(43),RHO(43),OM(43),Y(43)
     1/I/N,NP1,NP2,NP3,NEQ,NPH,KEX,KIN,KASE,KRAD,KPRAN
      COMMON/AUXP/TEMPE(43),TEMP(43),PO(43),AMACH(43)
      COMMON/BAR/GABAR(43),RBAR(43)
      COMMON/TEM/TEMPT(43)
      PINF=14.7*144.
```

```
      CP1=3.42
      CP2=0.24
      DO 45 I=1,NP3
      IF (NPH.LT.3) GO TO 46
      CPF=CP1*F(3,I)+CP2*(1.-F(3,I))
      CPF=CPF*25000.0
      GABAR(I)=1.28*F(3,I)+1.40*(1.-F(3,I))
      RBAR(I)=766.6*F(3,I)+53.35*(1.-F(3,I))
      GO TO 44
   46 CPF=.24*25000.
      F(3,I)=1.
      GABAR(I)=1.4
      RBAR(I)=53.35
      IF(NPH.LT.2)  F(2,I)=CPF*520.
   44 TEMP(I)=(F(2,I)-.5*U(I)*U(I))/CPF
      RHO(I)=PINF/(TEMP(I)*RBAR(I))
      TEMPT(I)=F(2,I)
   45 CONTINUE
      RETURN
      END
      SUBROUTINE ENTRN
      COMMON /GEN/PEI,AMI,AME,DPDX,PREF(3),PR(3),P(3),DEN,
     1AMU,XU,XD,XP,XL,DX,INTG,CSALFA,XPCG
      COMMON /L/AK,ALMG
     1/V/U(43),F(3,43),R(43),RHO(43),OM(43),Y(43)
     1/I/N,NP1,NP2,NP3,NEQ,NPH,KEX,KIN,KASE,KRAD,KPRAN
     1/L1/YL,UMAX,UMIN,FR,YIP,YEM
      COMMON  /SHEAR/ SHEAR(43),SCSH(43)
      COMMON/DUD/DUDOM(43)
      COMMON /ASD/ ASD1,ASD2
      GO TO (71,72,73),KIN
   71 CONTINUE
      GO TO 74
   72 IF (KPRAN.NE.0.OR.NEQ.EQ.1) GO TO 722
      AMI= ABS((SHEAR(  2)+SHEAR(  3)-2.*SHEAR(  1))/
     1     (U(2)+U(3)-2.*U(1)))
      GO TO 74
  722 AMI=8.*RHO(1)*((ALMG*YL)/(Y(2)+Y(3)))**2*ABS(U(2)+U(3)
     1-2.*U(1))
      GO TO 74
   73 AMI=0.
   74 GO TO (81,82,83),KEX
   81 RETURN
   82  AME=-8.*RHO(NP3)*((ALMG*YL)/(Y(NP1)+Y(NP2)-2.*Y(NP3)))
     1**2*ABS(U(NP1)+U(NP2)-2.*U(NP3))
       RETURN
   83 AME=0.
      RETURN
```

```
      END
      SUBROUTINE FBC(X,J,IND,AJFS)
      COMMON /GEN/PEI,AMI,AME,DPDX,PREF(3),PR(3),P(3),DEN,
     1AMU,XU,XD,XP,XL,DX,INTG,CSALFA,XPCG
     1/V/U(43),F(3,43),R(43),RHO(43),OM(43),Y(43)
      COMMON /KE/ AKEM
      IF(J.NE.2) GO TO 2
      IND=1
C     H MUST HAVE UNITS FT.FT/SEC.SEC
      AJFS=.341712E+7
      GO TO 3
2     CONTINUE
      IND = 1
      AJFS=F(1,1)
 3    CONTINUE
      RETURN
      END
      SUBROUTINE FREEU(XU,XD,UGU,UGD)
C    DETERMINES THE DOWNSTREAM VELOCITY FROM FREVEL ARRAY
C      WHICH IS INPUT AT 3 INCH INTERVALS IN BEGIN.
      COMMON/FREE/FREVEL(35)
      IF(FREVEL(1).EQ.0.) GO TO 1
      XDIN=XD*12.
      IX=XDIN/3.+1
      XS=(IX-1)*3.
      DELX=XDIN-XS
      UGD=FREVEL(IX)+(FREVEL(IX+1)-FREVEL(IX))*DELX/3.
      RETURN
C     APPLICABLE TO ZERO PRESSURE GRADIENT CASE.
1     UGD=UGU
      RETURN
      END
      SUBROUTINE FUGA2(F,Y,DUDY,YL,NP1,TDUDY,MTKE)
      REAL F(3,43),DUDY(43),Y(43)
      MTKE=0
      TKEM=F(1,3)
      DO 1 I=4,NP1
      IF(F(1,I).LT.TKEM) GO TO 1
      TKEM=F(1,I)
      MTKE=I
    1 CONTINUE
      DO 3 I=3,NP1
      YR=Y(I)/YL
      IF(YR.GT..25) GO TO 4
    3 CONTINUE
    4 CONTINUE
      IF(I.GE.MTKE) GO TO 5
      TDUDY=DUDY(MTKE)
```

```
      RETURN
    5 DELVG=DUDY(I)-DUDY(I-1)
      DELYR=(Y(I)-Y(I-1))/YL
      YY=YR-.25
      MTKE=I
      TDUDY=-YY/DELYR*DELVG+DUDY(I)
      RETURN
      END
      SUBROUTINE LENGTH
      COMMON /VELBDY/Y995
     1/I/N,NP1,NP2,NP3,NEQ,NPH,KEX,KIN,KASE,KRAD,KPRAN
     1/V/U(43),F(3,43),R(43),RHO(43),OM(43),Y(43)
     1/L1/YL,UMAX,UMIN,FR,YIP,YEM
C     THIS IS AN ABREVIATED VERSION TO BE USED WITH THE
C     BRADSHAW DISSIPATION MODEL. IT ASSUMES THE I BOUNDARY
C     IS A WALL AND SEARCHES THE OUTER VELOCITY PROFILE TO
C     FIND Y WHERE U=.995*UFREE                (Y995)
C     PROFILE TO FIND Y WHERE U=.995*UFREE       (Y995)
      ULOC=.995*U(NP3)
      DO 1 I=2,NP3
      II=NP3-I
      IF(U(II).LT.ULOC) GO TO 2
    1 CONTINUE
    2 IF(II.EQ.NP1) GO TO 3
      Y995=Y(II)+(Y(II+1)-Y(II))*(ULOC-U(II))/(U(II+1)-
     1U(II))
      YL=Y995
      RETURN
    3 Y995=Y(NP1)+(Y(NP3)-Y(NP1))*(ULOC-U(NP1))/(U(NP3)-
     1U(NP1))
      YL=Y995
      RETURN
      END
      SUBROUTINE MASS(XU,XD,AM)
      COMMON /V/U(43),F(3,43),R(43),RHO(43),OM(43),Y(43)
     1/I/N,NP1,NP2,NP3,NEQ,NPH,KEX,KIN,KASE,KRAD,KPRAN
     2/MXFER/BLOW
      AM=BLOW*RHO(1)*U(NP3)
      RETURN
      END
      SUBROUTINE OUTPUT
      COMMON /GEN/PEI,AMI,AME,DPDX,PREF(3),PR(3),P(3),DEN,
     1AMU,XU,XD,XP,XL,DX,INTG,CSALFA,XPCG
     1/V/U(43),F(3,43),R(43),RHO(43),OM(43),Y(43)
     1/C/SC(43),AU(43),BU(43),CU(43),A(3,43),B(3,43),C(3,43)
     1/MXFER/BLOW
      COMMON /L/AK,ALMG
     1/L1/YL,UMAX,UMIN,FR,YIP,YEM
```

```
      1/I/N,NP1,NP2,NP3,NEQ,NPH,KEX,KIN,KASE,KRAD,KPRAN
      1/B/BETA,GAMA(3),TAUI,TAUE,AJI(3),AJE(3),INDI(3),
      1INDE(3)
       COMMON/AUXP/TEMPE(43),TEMP(43),PO(43),AMACH(43)
       COMMON/AUXY/YY(43),XXU,RR1
       COMMON /XPLOT/NPLOT
       COMMON  /SHEAR/ SHEAR(43),SCSH(43)
       COMMON /IDIN/ INDIC
       COMMON/MXMN/RHUMX,RHUMN,RHU(43),AL
       COMMON/DUD/DUDOM(43), DUDY(43), ADUDY(43), ADUDYM
       COMMON  /ASD/  ASD1,ASD2
       COMMON/TEM/TEMPT(43)
       COMMON/UMUM/UMUZ(43),        YMU
       COMMON /COM/COMT(80)
       COMMON/ATKE/GEN(43),DIS(43),DERIV(43)
       DIMENSION URATIO(43),YRATIO(43)
       DIMENSION YYYY(45)
       DIMENSION                    DIF(43),DIF1(43)
       IF(INTG.NE.1) GO TO 15
       WRITE(6,8000)
8000   FORMAT('1')
       WRITE(6,8001)(COMT(I),I=1,80)
8001   FORMAT(20A4)
       WRITE(6,49)(OM(I),I=1,NP3)
   49  FORMAT(' THE VALUES OF OMEGA ARE '/(11F10.4))
   15  CONTINUE
       UOUT=.995*U(NP3)
       DO 60  I=1,NP3
       URATIO(I)=U(I)/UOUT
       YRATIO(I)=Y(I)/YL
   60  CONTINUE
       WRITE(6,51) XXU,RR1,YL,PEI
   51  FORMAT('1    XU=  ',2PE11.2,'   RI =  ',2PE11.2,' IN',
      1'    YL=  '
      2,2PE11.2,'   PEI=   ',2PE11.2)
       WRITE(6,54)
       CF1=2.*ASD1*F(1,1)/U(NP3)/U(NP3)
       WRITE(6,55)ASD1,ASD2,PREF(1),PREF(2),PREF(3),U(NP3),
      1CF1
   55  FORMAT(' ASD1=',F3.2,'  ASD2=',F5.3,'  PREF1=',F4.2,
      1'  PREF2=',
      2F4.2,'  PREF3=',F4.2,'  UFREE=',F7.3,'  CF=',F6.5)
       WRITE(6,56)GAMA(1),GAMA(2),GAMA(3),AMI,AME ,DPDX,BLOW
   56  FORMAT('0GAMA1=',E10.4,'  GAMA2=',E10.4,'  GAMA3=',
      1E10.4,'  AMI=',
      2E10.4,'  AME=',E10.4,'  DPDX=',E10.4,'  BLOW=',E10.4)
```

```
      WRITE(6,52)
   52 FORMAT(4X,'YRATIO',5X,'URATIO',6X,'DUDY',7X,'TKE',8X,
     1'GEN',8X,'DIS
     2',8X,' A2 ',9X,'H',10X,'C',8X,'RHO',8X,'  U ',8X,'Y')
   53 FORMAT(1X ,1P12E11.3)
   54 FORMAT(1HO  )
      DO 10  J1=1,NP3
      J2=NP2-J1+2
      YYYY(J2)=YY(J2)/YY(NP3)
   10 WRITE(6,53)YRATIO(J2),URATIO(J2),DUDY(J2),F(1,J2),
     1GEN(J2),DIS(J2),
     2DERIV(J2),F(2,J2),SHEAR(J2),RHO(J2),   U(J2),YY(J2)
      WRITE(6,8002) TAUI
8002  FORMAT(' PATANKAR SHEAR AT THE WALL =',E13.7)
       RETURN
      END
      SUBROUTINE PRE(XU,XD,DPDX)
      COMMON /PR/UGU,UGD
     1/V/U(43),F(3,43),R(43),RHO(43),OM(43),Y(43)
     1/I/N,NP1,NP2,NP3,NEQ,NPH,KEX,KIN,KASE,KRAD,KPRAN
C   HERE UGU AND UGD STAND FOR FREE-STREAM VELOCITIES AT XU
C     AND XD.
      DPDX=(UGU+UGD)*(UGU-UGD)*.5*RHO(NP3)/(XD-XU)
      RETURN
      END
      SUBROUTINE RAD(X,R1,CSALFB)
C     APPLICABLE TO AXISYMMETRIC MIXING LAYER AND JET
      COMMON /GEN/PEI,AMI,AME,DPDX,PREF(3),PR(3),P(3),DEN,
     1AMU,XU,XD,XP,XL,DX,INTG,CSALFA,XPCG
     1/V/U(43),F(3,43),R(43),RHO(43),OM(43),Y(43)
     1/I/N,NP1,NP2,NP3,NEQ,NPH,KEX,KIN,KASE,KRAD,KPRAN
      COMMON/UMUM/UMUZ(43),        YMU
      CSALFB=1.
      IF (KRAD.EQ.0) GO TO 18
      IF(KIN.EQ.3) GO TO 17
      IF(X.EQ.0.) GO TO 15
      R1=R(1)*(R(1)-2.*AMI*(X-XP)/(RHO(1)*U(1)))
      IF(R1.LT.0.)R1=0.
      R1=SQRT(R1)
      RETURN
   15 RO=.25/12.
      R1=RO-YMU
      RETURN
   17 R1=0.
      RETURN
   18 R1=1.
      RETURN
      END
```

```
      SUBROUTINE READY
      COMMON /GEN/PEI,AMI,AME,DPDX,PREF(3),PR(3),P(3),DEN,
     1AMU,XU,XD,XP,XL,DX,INTG,CSALFA,XPCG
     1/V/U(43),F(3,43),R(43),RHO(43),OM(43),Y(43)
     1/I/N,NP1,NP2,NP3,NEQ,NPH,KEX,KIN,KASE,KRAD,KPRAN
     1/B/BETA,GAMA(3),TAUI,TAUE,AJI(3),AJE(3),INDI(3),
     1INDE(3)
      CALL DENSTY
      CALL RAD(XU,R(1),CSALFA)
C   Y NEAR THE I BOUNDARY
      IF (R(1).EQ.0.) KIN=3
      GO TO (71,72,73),KIN
   71 Y(2)=(1.+BETA)*OM(3)*4./((3.*RHO(2)+RHO(3))*(U(2)+
     1U(3)))
      GO TO 74
   72 Y(2)=12.*OM(3)/((3.*RHO(2)+RHO(3))*(U(2)+U(3)+4.*U(1))
     1)
      GO TO 74
   73 Y(2)=.5*OM(3)/(RHO(1)*U(1))
   74 Y(3)=Y(2)+.25*OM(3)*(1./(RHO(3)*U(3))+2./(RHO(3)*U(3)+
     1RHO(2)*U(2)))
C   Y 'S FOR INTERMEDIATE GRID POINTS
      DO 50 I=4,NP1
   50 Y(I)=Y(I-1)+.5*(OM(I)-OM(I-1))*(1./(RHO(I)*U(I))+1./
     1(RHO(I-1)*U(I-1)))
C   Y NEAR THE E BOUNDARY
      Y(NP2)=Y(NP1)+.25*(OM(NP2)-OM(NP1))*(1./(RHO(NP1)*
     1U(NP1))+2./
     2(RHO(NP1)*U(NP1)+RHO(NP2)*U(NP2)))
   81 Y(NP3)=Y(NP2)+(1.+BETA)*(OM(NP2)-OM(NP1))*4./((
     1RHO(NP1)+3.*RHO(NP2)
     2 )*(U(NP1)+U(NP2)))
      GO TO 84
   82 Y(NP3)=Y(NP2)+12.*(OM(NP2)-OM(NP1))/((RHO(NP1)+3.*
     1RHO(NP2))*(U(NP2)
     2 +U(NP1)+4.*U(NP3)))
      GO TO 84
   83 Y(NP3)=Y(NP2)+.5*(OM(NP2)-OM(NP1))/(RHO(NP3)*U(NP3))
   84 IF(CSALFA.EQ.0..OR.KRAD.EQ.0) GO TO 51
      DO 52 I=2,NP3
   52 Y(I)=2.*Y(I)*PEI/(R(1)+SQRT(R(1)*R(1)+2.*Y(I)*PEI*
     1CSALFA))
      GO TO 56
   51 DO 54 I=2,NP3
   54 Y(I)=PEI*Y(I)/R(1)
   56 Y(2)=2.*Y(2)-Y(3)
      Y(NP2)=2.*Y(NP2)-Y(NP1)
C   CALCULATION OF RADII
```

```
      DO 57 I=2,NP3
      IF(KRAD.EQ.0)R(I)=R(1)
      IF(KRAD.NE.0)R(I)=R(1)+Y(I)*CSALFA
   57 CONTINUE
      RETURN
      END
      SUBROUTINE SHEARS
      COMMON /GEN/PEI,AMI,AME,DPDX,PREF(3),PR(3),P(3),DEN,
     1AMU,XU,XD,XP,XL,DX,INTG,CSALFA,XPCG
     1/I/N,NP1,NP2,NP3,NEQ,NPH,KEX,KIN,KASE,KRAD,KPRAN
     1/V/U(43),F(3,43),R(43),RHO(43),OM(43),Y(43)
     1/L1/YL,UMAX,UMIN,FR,YIP,YEM
      COMMON  /SHEAR/ SHEAR(43),SCSH(43)
      COMMON /ASD/ ASD1,ASD2
      COMMON/DUD/DUDOM(43), DUDY(43), ADUDY(43), ADUDYM
      COMMON /RUH/ RAAUH(43)
      COMMON/AVDU/AVDUY
      COMMON/KJU/KMU
      COMMON/DUDYF/DUDY25,ISLO,DUDY50,ISLO5
      DO 97 I=1,NP3
      RAAUH(I)=R(I)*RHO(I)*U(I)
      IF(U(I).EQ.0..AND.I.NE.NP3)RAAUH(I)=R(I)*RHO(I)*.5*
     1(U(I)+U(I+1))
      SCSH(I)=RAAUH(I)/PEI
      RAAUH(I)=RAAUH(I)*R(I)
      DUDY(I)=DUDOM(I)*SCSH(I)
   97 ADUDY(I)=ABS(DUDY(I))
      DUDY(2)=(U(3)-U(2))/(Y(3)-Y(2))
      ADUDY(2)=ABS(DUDY(2))
      DUDY(NP2)=(U(NP2)-U(NP1))/(Y(NP2)-Y(NP1))
      ADUDY(NP2)=ABS(DUDY(NP2))
      DO 96 I=1,NP1
      YRATIO=Y(I)/YL
      IF(YRATIO.GT..10) GO TO 98
   96 CONTINUE
   98 YRLOW=Y(I-1)/YL
      ISLO=I
      DELYR=YRATIO-YRLOW
      DELDU=DUDY(I)-DUDY(I-1)
      DUDY25=DUDY(I-1)+(.10-YRLOW)*DELDU/DELYR
      DO 70 I=ISLO,NP3
      YRATIO=Y(I)/YL
      IF(YRATIO.GT..5) GO TO 71
   70 CONTINUE
   71 YRLOW=Y(I-1)/YL
      ISLO5=I
      DELYR=YRATIO-YRLOW
      DELDU=DUDY(I)-DUDY(I-1)
```

```
      DUDY50=DUDY(I-1)+(.5-YRLOW)*DELDU*DELYR
      DO 101 J=2,NP2
      IF(KPRAN.NE.0..OR.NEQ.LT.2) GO TO 35
      DUM=ASD1*RHO(J)*F(1,J)
      SHEAR(J)=SIGN(DUM,DUDY(J))
      IF(NPH.GE.2) GO TO 100
      SHEAR(J)=SHEAR(J)+.000012*DUDY(J)
      GO TO 101
  100 SHEAR(J)=SHEAR(J)+VISCO(J)*DUDY(J)
      GO TO 101
   35 F(1,J)=0.
  101 CONTINUE
      GO TO (21,22,22),KIN
   21 CALL WALL
      GO TO 23
   22 SHEAR(1)=0.
   23 SHEAR(NP3)=0.
      RETURN
      END
      SUBROUTINE SLIP
      COMMON /GEN/PEI,AMI,AME,DPDX,PREF(3),PR(3),P(3),DEN,
     1AMU,XU,XD,XP,XL,DX,INTG,CSALFA,XPCG
     1/I/N,NP1,NP2,NP3,NEQ,NPH,KEX,KIN,KASE,KRAD,KPRAN
     1/B/BETA,GAMA(3),TAUI,TAUE,AJI(3),AJE(3),INDI(3),
     1INDE(3)
     1/V/U(43),F(3,43),R(43),RHO(43),OM(43),Y(43)
      COMMON /L/AK,ALMG
     1/C/SC(43),AU(43),BU(43),CU(43),A(3,43),B(3,43),C(3,43)
      COMMON /KE/ AKEM
C  SLIP COEFFICIENTS NEAR THE I BOUNDARY FOR VELOCITY
C      EQUATION.
      CU(2)=0.
      CU(NP2)=0.
      GO TO (71,72,73),KIN
   71 BU(2)=0.
      AU(2)=1./(1.+2.*BETA)
      GO TO 74
   72 SQ=84.*U(1)*U(1)-12.*U(1)*U(3)+9.*U(3)*U(3)
      BU(2)=8.*(2.*U(1)+U(3))/(2.*U(1)+7.*U(3)+SQRT(SQ))
      AU(2)=1.-BU(2)
      GO TO 74
   73 BU(2)=0.
      CALL VEFF(2,3,EMU)
      AK1=1./DX-DPDX/(RHO(1)*U(1)*U(1))
      AK2=-U(1)*AK1+DPDX/(RHO(1)*U(1))
      AJ=RHO(1)*U(1)*.25*(Y(2)+Y(3))**2/EMU
      IF(KRAD.EQ.0) GO TO 75
      AU(2)=2./(2.+AJ*AK1)
```

```
      CU(2)=-.5*AJ*AK2*AU(2)
      GO TO 74
   75 CU(2)=1./(2.+3.*AJ*AK1)
      AU(2)=CU(2)*(2.-AJ*AK1)
      CU(2)=-CU(2)*4.*AJ*AK2
C  SLIP COEFFICIENTS NEAR THE E BOUNDARY FOR VELOCITY
C     EQUATION.
   74 GO TO (81,82,83),KEX
   81 AU(NP2)=0.
      BU(NP2)=1./(1.+2.*BETA)
      GO TO 84
   82 SQ=84.*U(NP3)*U(NP3)-12.*U(NP3)*U(NP1)+9.*U(NP1)*
     1U(NP1)
      AU(NP2)=8.*(2.*U(NP3)+U(NP1))/(2.*U(NP3)+7.*U(NP1)+
     1SQRT(SQ))
      BU(NP2)=1.-AU(NP2)
      GO TO 84
   83 AU(NP2)=0.
      CALL VEFF(NP1,NP2,EMU)
      BK1=1./DX-DPDX/(RHO(NP3)*U(NP3)*U(NP3))
      BK2=-U(NP3)*BK1+DPDX/(RHO(NP3)*U(NP3))
      BJ=RHO(NP3)*U(NP3)*.25*(2.*Y(NP3)-Y(NP1)-Y(NP2))**2/
     1EMU
      CU(NP2)=1./(2.+3.*BJ*BK1)
      BU(NP2)=CU(NP2)*(2.-BJ*BK1)
      CU(NP2)=-CU(NP2)*4.*BJ*BK2
   84 IF(NEQ.EQ.1)RETURN
C  SLIP COEFFICIENTS NEAR THE I BOUNDARY FOR OTHER EQUATIONS
      DO 54 J=1,NPH
      C(J,2)=0.
      C(J,NP2)=0.
      GO TO (41,42,43),KIN
   41 CALL FBC(XD,J,INDI(J),QI)
      IF(INDI(J).EQ.1) GO TO 61
      AJI(J)=QI
      A(J,2)=1.
      B(J,2)=0.
      C(J,2)=8.*(1.+2.*BETA)*PREF(J)*AJI(J)/(AK*AK*BETA*(1.+
     1BETA)*(1.+
     2BETA)*(3.*RHO(2)+RHO(3))*U(3))
      GO TO 44
   61 F(J,1)=QI
      A(J,2)=(1.+BETA-GAMA(J))/(1.+BETA+GAMA(J))
      B(J,2)=1.-A(J,2)
      GO TO 44
   42 A(J,2)=(U(2)+U(3)-8.*U(1))/(5.*(U(2)+U(3))+8.*U(1))
      GF=(1.-PREF(J))/(1.+PREF(J))
      A(J,2)=(A(J,2)+GF)/(1.+A(J,2)*GF)
```

```
      B(J,2)=1.-A(J,2)
      GO TO 44
   43 B(J,2)=0.
      CS=0.
      DS=0.
      AK1=1./DX-DS
      AK2=-AK1*F(J,1)-CS
      AJF=AJ*PREF(J)
      IF(KRAD.EQ.0) GO TO 45
      A(J,2)=2./(2.+AJF*AK1)
      C(J,2)=-.5*AJF*AK2*A(J,2)
      GO TO 44
   45 C(J,2)=1./(2.+3.*AJF*AK1)
      A(J,2)=C(J,2)*(2.-AJF*AK1)
      C(J,2)=-C(J,2)*4.*AJF*AK2
C  SLIP COEFFICIENTS NEAR THE E BOUNDARY FOR OTHER EQUATIONS
   44 GO TO (51,52,53),KEX
   51 CALL FBC(XD,J,INDE(J),QE)
      IF(INDE(J).EQ.1) GO TO 31
      AJE(J)=QE
      B(J,NP2)=1.
      A(J,NP2)=0.
      C(J,NP2)=-8.*(1.+2.*BETA)*PREF(J)*AJE(J)/(AK*AK*BETA*
     1(1.+BETA)*
     2(1.+BETA)*(RHO(NP1)+3.*RHO(NP2))*U(NP1))
      GO TO 54
   31 F(J,NP3)=QE
      B(J,NP2)=(1.+BETA-GAMA(J))/(1.+BETA+GAMA(J))
      A(J,NP2)=1.-B(J,NP2)
      GO TO 54
   52 B(J,NP2)=(U(NP2)+U(NP1)-8.*U(NP3))/(5.*(U(NP2)+U(NP1))
     1+8.*U(NP3))
      GF=(1.-PREF(J))/(1.+PREF(J))
      B(J,NP2)=(B(J,NP2)+GF)/(1.+B(J,NP2)*GF)
      A(J,NP2)=1.-B(J,NP2)
      GO TO 54
   53 A(J,NP2)=0.
      CALL SOURCE(J,NP3,CS,DS)
      BK1=1./DX-DS
      BK2=-BK1*F(J,NP3)-CS
      BJF=BJ*PREF(J)
      C(J,NP2)=1./(2.+3.*BJF*BK1)
      B(J,NP2)=C(J,NP2)*(2.-BJF*BK1)
      C(J,NP2)=-C(J,NP2)*4.*BJF*BK2
   54 CONTINUE
      RETURN
      END
      SUBROUTINE SLOPE(I,U,OM,Z)
```

```
      REAL U(1),OM(1)
      A2=((U(I+1)-U(I-1))/(OM(I+1)-OM(I-1))-(U(I)-U(I-1))/
     1(OM(I)-OM(I-1)
     2))/(OM(I+1)-OM(I))
      A1=-(OM(I)+OM(I-1))*A2+(U(I)-U(I-1))/(OM(I)-OM(I-1))
      Z=A1+2.*A2*OM(I)
      RETURN
      END
      SUBROUTINE SOLVE(A,B,C,F,NP3)
C     THIS SOLVES EQUATIONS OF THE FORM
C     F(I) = A(I)*F(I+1) + B(I)*F(I-1) + C(I)
C     FOR I=2,NP2                                RO
      DIMENSION A(NP3),B(NP3),C(NP3),F(NP3)
      NP2=NP3-1
      B(2) = B(2)*F(1) + C(2)
      DO 48 I=3,NP2
      T = 1./(1.-B(I)*A(I-1))
      A(I) = A(I)*T
48    B(I) = (B(I)*B(I-1) + C(I))*T
      DO 50 I=2,NP2
      J=NP2-I+2
   50 F(J)=A(J)*F(J+1)+B(J)
      RETURN
      END
      SUBROUTINE SOURCE(J,I,CS,DS)
      COMMON /IJAN/TDUDY,MTKE
C  FOR CONSERVATION OF STAGNATION ENTHALPY
C  CAUTION- USE CONSISTENT UNITS
C     THE DOT PRODUCT OF E WITH J IS NEGLECTED
      COMMON /GEN/PEI,AMI,AME,DPDX,PREF(3),PR(3),P(3),DEN,
     1AMU,XU,XD,XP,XL,DX,INTG,CSALFA,XPCG
     1/V/U(43),F(3,43),R(43),RHO(43),OM(43),Y(43)
     1/I/N,NP1,NP2,NP3,NEQ,NPH,KEX,KIN,KASE,KRAD,KPRAN
     1/L1/YL,UMAX,UMIN,FR,YIP,YEM
     1/C/SC(43),AU(43),BU(43),CU(43),A(3,43),B(3,43),C(3,43)
      COMMON/ASD/ASD1,ASD2
      COMMON  /SHEAR/ SHEAR(43),SCSH(43)
      COMMON/DUD/DUDOM(43), DUDY(43), ADUDY(43), ADUDYM
      COMMON/AVDU/AVDUY
      COMMON/DUDYF/DUDY25,ISLO,DUDY50,ISLO5
      COMMON/RUH/RAAUH(43)
      COMMON/ATKE/GEN(43),DIS(43),DERIV(43)
      COMMON/STORE/OLDU(43)
      DIMENSION A2(43)
      IF (J.GT.3) GO TO 12
      GO TO (13,11,12),J
   11 CS=SC(I)*(U(I+1)*U(I+1)-U(I)*U(I))/(OM(I+1)-OM(I))
      CS=CS-SC(I-1)*(U(I)*U(I)-U(I-1)*U(I-1))/(OM(I)-OM(I-1)
```

```
     1)
      CS=(1.-1./PREF(J))*CS/(OM(I+1)-OM(I-1))
      CSKE=SC(I)*                              (F(1,I+1)-F(1,I))/
     1      (OM(I+1)-OM(I))
      CSKE=CSKE-SC(I-1)*(F(1,I)-F(1,I-1))/(OM(I)-OM(I-1))
      CS=CS+2.*(1./PREF(1)-1./PREF(J))*CSKE/(OM(I+1)-OM(I-1)
     1)
      CS=CS+CSKE
      DS=0.
      GO TO 3
   12 CONTINUE
      CS = 0.0
      DS = 0.0
      GO TO 3
   13 CS=ASD1*RHO(I)*F(1,I)*R(I)*R(I)*ABS(DUDOM(I))/PEI
      IF(INTG.LE.1) YLO=YL
C
      ASD2=1.8
      ASD2M=ASD2
      IF(I.LT.MTKE)ASD2M=ASD2M*Y(MTKE)/Y(I)
      DERIV(I)=ASD2M
      A2(I)=ASD2M
      DK=ASD2M*F(1,I)**1.5/YL
C
      DK=DK/OLDU(I)
      GEN(I)=CS
      DIS(I)=DK
      CS=CS-DK
      DS=0.
      IF(INTG.GT.1) DS=-1.5*A2(I)*SQRT(F(1,I))/YLO/OLDU(I)
      IF(I.EQ.NP1) YLO=YL
    3 CONTINUE
      RETURN
      END
      SUBROUTINE TKEW(X,UF,TKE)
      COMMON /TAUW/CFW(35)/ASD/ASD1,ASD2
      COMMON /V/U(43),F(3,43),R(43),RHO(43),OM(43),Y(43)
     1/L1/YL,UMAX,UMIN,FR,YIP,YEM/MXFER/BLOW
      COMMON/GEN/PEI,AMI,AME,DPDX,PREF(3),PR(3),P(3),DEN,AMU
     1,XU,XD,XP,XL,DX,INTG,CSALFA,XPCG
C
C     GET THE WALL SHEAR FROM LINEAR ITERATION USING THE
C     LOGARITHMIC LAW.
      IF(INTG.EQ.0) GO TO 6
      USTAR=SQRT(F(1,1))
      DO 1 I=1,42
      YR=Y(I)/YL
      IF(YR.GE..10) GO TO 2
```

```
    1 CONTINUE
    2 CONTINUE
      C=1.85-.0075*DPDX+200.*BLOW
      DO 3 J=1,10
    3 USTAR=U(I)/(2.44*(ALOG(Y(I)*USTAR/.00016)+C)      )
C     AVERAGE WITH THE NEXT CLOSEST NODE
      VSTAR=USTAR
      DO 5 J=1,10
      IF(VSTAR.GT.0.) GO TO 5
      VSTAR=USTAR
      GO TO 8
    5 VSTAR=U(I-1)/(2.44*(ALOG(Y(I-1)*VSTAR/.00016)+C)      )
    8 TKE=.5*(USTAR*USTAR+VSTAR*VSTAR)/ASD1
      RETURN
    6 CONTINUE
      TKE=CFW(1)*UF*UF/(2.*ASD1)
      RETURN
      END
      SUBROUTINE VEFF(I,IP1,EMU)
      COMMON/GEN/PEI,AMI,AME,DPDX,PREF(3),PR(3),P(3),DEN,AMU
     1,XU,XD,XP,XL,DX,INTG,CSALFA,XPCG
     1/V/U(43),F(3,43),R(43),RHO(43),OM(43),Y(43)
     1/I/N,NP1,NP2,NP3,NEQ,NPH,KEX,KIN,KASE,KRAD,KPRAN
     1/L1/YL,UMAX,UMIN,FR,YIP,YEM
      COMMON/SHEAR/SHEAR(43),SCSH(43)
      COMMON/MXMN/RHUMX,RHUMN,RHU(43),AL
     1/ASD/ASD1,ASD2
     2/DUD/DUDOM(43),DUDY(43),ADUDY(43),ADUDYM
     3/DUDYF/DUDY25,ISLO,DUDY50,ISLO5
      ASD1M=ASD1
      DUDYM=.5*(RHO(I)+RHO(IP1))*.5*(U(I)+U(IP1))/PEI*.5*
     1(R(I)+R(IP1))*(U(IP1)-U(I))/(OM(IP1)-OM(I))
      IF(DUDYM.EQ.0.) GO TO 68
      EMU=.5*(RHO(IP1)+RHO(I))*.5*(F(1,IP1)+F(1,I))*ASD1M/
     1DUDYM
      RETURN
   68 EMU=0.
      RETURN
      END
      SUBROUTINE WALL
      COMMON /GEN/PEI,AMI,AME,DPDX,PREF(3),PR(3),P(3),DEN,
     1AMU,XU,XD,XP,XL,DX,INTG,CSALFA,XPCG
     1/V/U(43),F(3,43),R(43),RHO(43),OM(43),Y(43)
     1/I/N,NP1,NP2,NP3,NEQ,NPH,KEX,KIN,KASE,KRAD,KPRAN
     1/B/BETA,GAMA(3),TAUI,TAUE,AJI(3),AJE(3),INDI(3),
     1INDE(3)
      COMMON  /SHEAR/ SHEAR(43),SCSH(43)
      COMMON/DUD/DUDOM(43), DUDY(43), ADUDY(43), ADUDYM
```

```
      COMMON /L/AK,ALMG
      COMMON /ASD/ ASD1,ASD2
C   CALCULATION OF BETA FOR THE E BOUNDARY
      IF(KEX.NE.1) GO TO 15
      YI=Y(NP3)-.5*(Y(NP1)+Y(NP2))
      UI=.5*(U(NP2)+U(NP1))
      RH=.25*(3.*RHO(NP2)+RHO(NP1))
      RE=RH*UI*YI/VISCO(NP3)
      FP=DPDX*YI/(RH*UI*UI)
      AM=AME/(RH*UI)
      CALL WF1(RE,FP,AM,S)
      BETA=SQRT(ABS(S+FP+AM))/AK
      TAUE=S*RH*UI*UI
      IF(NEQ.EQ.1) GO TO 36
C   CALCULATION OF GAMA 'S FOR THE E BOUNDARY
      DO 35 J=1,NPH
      CALL WF2(RE,FP,AM,PR(J),PREF(J),P(J),SF)
      GAMA(J)=(SF+AM)*PREF(J)/(AK*AK*BETA)
      IF(INDE(J).EQ.1)AJE(J)=SF*RH*UI*(F(J,NP2)+F(J,NP1)-2.*
     1F(J,NP3))*.5
   35 CONTINUE
   36 IF(KIN.NE.1)RETURN
C   CALCULATION OF BETA FOR THE I BOUNDARY
   15 YI=.5*(Y(2)+Y(3))
      UI=.5*(U(2)+U(3))
      RH=.25*(3.*RHO(2)+RHO(3))
      RE=RH*UI*YI/VISCO( 1 )
      FP=DPDX*YI/(RH*UI*UI)
      AM=AMI/(RH*UI)
      CALL WF1(RE,FP,AM,S)
      BETA=SQRT(ABS(S+FP+AM))/AK
      TAUI=S*RH*UI*UI
      IF(NEQ.EQ.1) RETURN
C   CALCULATION OF GAMA 'S FOR THE I BOUNDARY
C      NOTE CALCULATION ASSUMES H = 1.  SEE PAGE 64.
      DO 38 J=1,NPH
      CALL WF2(RE,FP,AM,PR(J),PREF(J),P(J),SF)
      GAMA(J)=(SF+AM)*PREF(J)/(AK*AK*BETA)
      IF(INDI(J).EQ.1)AJI(J)=SF*RH*UI*(2.*F(J,1)-F(J,2)-
     1F(J,3))*.5
C      LINEAR RELATION BETWEEN TKE AND Y
      IF(J.EQ.1) GAMA(J)=1.
   38 CONTINUE
      SHEAR(1)=ASD1*RHO(1)*F(1,1)*DUDY(1)/ABS(DUDY(1))
      RETURN
      END
      SUBROUTINE WF1(R,F,AM,S)
      COMMON /L/AK,ALMG
```

```
     1/WL/STO,AKS,RT,FT,AMT
      AKS=AK*AK
      RT=R*AKS
      ST=1./RT-.1561*RT**(-.45)+.08723*RT**(-.3)+.03713*RT**
     1(-.18)
      STO=ST
      IF(F.EQ.0.) GO TO 15
      FT=F/AKS
      FM=1.-4.*FT*RT/(585.+RT**2.5)**.4
      IF(FM.LT.0.)FM=0.
      ST=ST*FM**1.6
      GO TO 16
   15 IF(AM.EQ.0.) GO TO 16
      AMT=AM/AKS
      AMM=1.-AMT/(7.74*RT**(-1.17)+.956*RT**(-.25))
      ST=ST*AMM**4
   16 S=ST*AKS
      RETURN
      END
      SUBROUTINE WF2(R,F,AM,  PR ,PRT,P,S)
      COMMON /L/AK,ALMG
     1/WL/STO,AKS,RT,FT,AMT
      ST1=STO/(1.+P*SQRT(STO))
      IF(F.EQ.0.) GO TO 15
      SSEP=1.725*RT**(-.3333)*(P+6.8)**(-1.165)
      FD=.25*FT*RT/(1.+.0625*RT)
      ST1=ST1*(1.-FD)+FD*SSEP
   15 ST=ST1/PRT
      S=ST*AKS
      RETURN
      END
      FUNCTION VISCO(I)
      COMMON /GEN/PEI,AMI,AME,DPDX,PREF(3),PR(3),P(3),DEN,
     1AMU,XU,XD,XP,XL,DX,INTG,CSALFA,XPCG
     1/V/U(43),F(3,43),R(43),RHO(43),OM(43),Y(43)
     1/I/N,NP1,NP2,NP3,NEQ,NPH,KEX,KIN,KASE,KRAD,KPRAN
      COMMON/AUXP/TEMPE(43),TEMP(43),PO(43),AMACH(43)
      VISCO=AMU*(F(2,I)/F(2,NP3))**.76
      RETURN
      END
      FUNCTION SLOPE(A1,A2,A3,B1,B2,B3)
      C1=B1-B2
      C2=B1-B3
      C3=B1*B1-B2*B2
      CK=B2-B3
      IF(C1.EQ.0..OR.C2.EQ.0..OR.CK.EQ.0.) GO TO 1
      C4=A1-A2
      AA2=(C4*C2-C1*(A1-A3))/(C2*C3-C1*(B1*B1-B3*B3))
```

```
      AA1=(C4-AA2*C3)/C1
      SLOPE=AA1+2.*AA2*B3
      RETURN
    1 C1=A1-A2
      C2=A1-A3
      C3=A1*A1-A3*A3
      CK=A2-A3
      IF(C1.EQ.0..OR.C2.EQ.0..OR.CK.EQ.0.) GO TO 2
      C4=B1-B2
      AA2=(C4*C2-C1*(B1-B3))/(C2*C3-C1*(A1*A1-A3*A3))
      AA1=(C4-AA2*C3)/C1
      SLOPE=AA1+2.*AA2*A3
      IF(SLOPE.EQ.0.) GO TO 2
      SLOPE=1./SLOPE
      RETURN
    2 SLOPE=0.
      RETURN
      END
```

VII. BIBLIOGRAPHY

1. Karman, T. von, "Uber laminare und turbulente Reibung," Z. angew. Math. Mech., 1,223(1921).

2. Doenhoff, A. von and Tetervin, N., "Determination of General Relations for the Behavior of Turbulent Boundary Layers," NACA Report No. 772(1943).

3. Zwarts, F. J., "Turbulent Boundary Layer Predictions Using a Dissipation Integral Method," Proceedings of the Computation of Turbulent Boundary Layers - 1968 AFOSR-IFP-Stanford Conference, Vol. 1, 154-169.

4. Alber, I. E., "Application of an Exact Expression for the Equilibrium Dissipation Integral to the Calculation of Turbulent Nonequilibrium Flows," Proceedings of the Computation of Turbulent Boundary Layers - 1968 AFOSR-IFP-Stanford Conference, Vol. 1, 126-135, Thermosciences Division, Department of Mechanical Engineering, Stanford University (1969).

5. Rotta, J. C., "FORTRAN IV - Rechenprogramm Für Grenzschichten bei kompressiblen, ebenen und achsensymmetrischen Strömungen," AVA-Bericht 68 R 0 3.

6. Escudier, M. P. and Nicoll, W. B., "A Shear-Work-Integral Method for the Calculation of Turbulent Boundary-Layer Development," Proceedings of the Computation of Turbulent Boundary Layers - 1968 AFOSR-IFP-Stanford Conference, Vol. 1, 136-146, Thermosciences Division, Department of Mechanical Engineering, Stanford University (1969).

7. Head, M. R., "Entrainment in the Turbulent Boundary Layer," Aero. Res. Coun. R & M 3152 (1958).

8. Abbott, D. E. and Deiwert, G. S., "Application of the Method of Weighted Residuals to the Turbulent Boundary - Layer Equations. Part II. A Two Parameter Prediction Technique," Proceedings of the Computation of Turbulent Boundary Layers - 1968 AFOSR-IFP-Stanford Conference, Vol. 1, 46-53, Thermosciences Division, Department of Mechanical Engineering, Stanford University (1969).

9. Hirst, E. A. and Reynolds, W. C., "An Integral Prediction Method for Turbulent Boundary Layers Using the Turbulent Kinetic Energy Equation," Report MD-21, Department of Mechanical Engineering, Stanford University (1968).

10. Spalding, D. B., "Theories of the Turbulent Boundary Layer," Applied Mechanics Review 20, No. 8 (1967).

11. Boussinesq, T. V., "Theorie de l'ecoulement tourbillant," Mem. Pre. par. div. Sav., 23, 46 (1877).

12. Prandtl, L., "Ueber die ausgebildete Turbulenz." Z. angew, Math. Mech., 5, 136 (1925).

13. Prandtl, L. "Ueber ein neues Formelsystem fuer die ausgebildete Turbulenz," Nachr. d. Akad. D. Wiss. (Goettingen), 6 (1945).

14. Hinze, J. O., Turbulence, New York: McGraw-Hill Book Company, 1959.

15. Karman, T. von, "Mechanische Aehnlichkeit und Turbulenz," Nach. Gesell, Wiss. Goettingen, Math. Phys. Klasse, 5, 58 (1930).

16. Van Driest, E. R., "On Turbulent Flow Near a Wall," J. Aeronaut. Sci., Vol. 23, 1007 (1956).

17. Bradshaw, P., "The Turbulence Structure of Equilibrium Boundary Layers," J. of Fluid Mechanics, Vol. 29, Part 4, 625-645 (1967).

18. Patankar, S. V. and Spalding, D. B., Heat and Mass Transfer in Boundary Layers, Morgan - Grampian, London(1967).

19. Smith, A.M.O. and Cebaci, T., "Numerical Solution of the Turbulent Boundary - Layer Equations," Douglas Aircraft Div. Report DAC 33735 (1967).

20. Smith, A.M.O. and Cebaci, T., "Finite - Difference Solution of the Incompressible Turbulent Boundary - Layer Equations by an Eddy-Viscosity Concept," Proceedings of the Computation of Turbulent Boundary Layers - 1968 AFOSR-IFP-Stanford Conference, Vol. 1, 346-355, Thermosciences Div., Department of Mechanical Engineering, Stanford University (1969).

21. Nee, V. and Kovansznay, L., "A Phenomenological Theory of Quasi-Parallel Turbulent Shear Flows," Report No. 1, Dept. of Mechanics, The John Hopkins University.

22. Glushko, G. S., "Turbulent Boundary Layer on a Flat Plate in an Incompressible Fluid," NASA TT F-10, 080, Translation from Izvestiya Akademii Nank SSSR, Seriya Mekhanika, No. 4, 13-23 (1965).

23. Beckwith, I. E. and Bushnell, D. M., "Calculation of Mean and Fluctuating Properties of the Incompressible Turbulent Boundary Layer," Proceedings of the Computation of Turbulent Boundary Layers - 1968 AFOSR-IFD-Stanford Conference, Vol. 1, 275-299 Thermosciences Div., Department of Mechanical Engineering, Stanford University (1969).

24. Bradshaw, P., Ferriss, D. H., and Atwell, N. P., "Calculation of Boundary - Layer Development Using the Turbulent Kinetic Energy Equation," J. of Fluid Mechanics, Vol. 28, 3, 593-616 (1967).

25. Lee, S. C. and Harsha, P. T., "The Use of Turbulence Kinetic Energy in Free Mixing Studies," AIAA Journal, Vol. 8, 6, 1026-1032 (1970).

26. Goldstein, S., Modern Developments in Fluid Dynamics, 1, 128, Oxford, Clarendon Press.

27. Lee, S. C. and Auiler, J. E., "Theory of Two Dimensional Turbulent Wakes," AIAA Journal, Vol. 8, 10, 1876-1878 (1970).

28. Klebanoff, P. S., "Characteristics of Turbulence in a Boundary Layer with Zero Pressure Gradient", NACA Report 1247 (1955).

29. Smith, G. D., Numercial Solution of Partial Differential Equations, Oxford University Press, New York (1965).

30. Levitch, R. N., "The Effect of Discontinuation of Injection on the Transpired Turbulent Boundary-Layer", ScD Thesis, Massachusetts Institute of Technology (1966).

31. Julien, H. L., "The Turbulent Boundary Layer on a Porous Plate: Experimental Hydrodynamics of Favorable Pressure Gradient Flow", PhD Thesis, Stanford (1969).

32. Thielbahr, W. H., Kays, W. M. and Moffat, R. J., "The Turbulent Boundary Layer: Experimental Heat Transfer with Blowing, Suction and Favorable Pressure Gradient", Report No. HMT-5, Thermosciences Division, Department of Mechanical Engineering, Stanford University.

VIII. VITA

William Madison Byrne, Jr. was born on November 5, 1938 in Memphis, Tennessee. He received his primary education in Memphis, Tennessee and his secondary education in St. Louis, Missouri. He has received his college education from the Missouri School of Mines and Metallurgy, in Rolla, Missouri; the University of California at Los Angeles; and the University of Missouri - Rolla, in Rolla, Missouri. He received a Bachelor of Science degree in Mechanical Engineering from the Missouri School of Mines and Metallurgy, in Rolla, Missouri, in May 1960 and a Master of Science degree in Engineering from the University of California at Los Angeles, in Los Angeles, California, in September 1964.

Mr. Byrne has been enrolled in the Graduate School of the University of Missouri - Rolla since September 1967 and held a National Science Foundation Traineeship for the period September 1967 to September 1969. He also received a National Aeronautics and Space Administration grant for the period September 1969 to April 1970 and was a Mechanical and Aerospace Engineering Department teaching assistant from September 1969 to February 1970.

He married the former Miss Mary Constance Lamb of Glendale, Missouri on December 17, 1960. They have been blessed with two children, a daughter, Bonnie Sue Byrne, and a son, Paul William Byrne.